Stem Cells International

Musculoskeletal Stem/Progenitor Cells: from Basic Biology to Translational Medicine

Lead Guest Editor: Gehua Zhen
Guest Editors: Yi Zhang, Songfeng Chen, and Yusheng Li

Musculoskeletal Stem/Progenitor Cells: from Basic Biology to Translational Medicine

Stem Cells International

Musculoskeletal Stem/Progenitor Cells: from Basic Biology to Translational Medicine

Lead Guest Editor: Gehua Zhen
Guest Editors: Yi Zhang, Songfeng Chen, and Yusheng Li

Contents

Hindawi
Stem Cells International
Volume 2022, Article ID 1309684, 10 pages
https://doi.org/10.1155/2022/1309684

Research Article

Enhanced Repaired Enthesis Using Tenogenically Differentiated Adipose-Derived Stem Cells in a Murine Rotator Cuff Injury Model

Yang Chen,[1,2] **Yan Xu**,[1,2] **Guoyu Dai**,[1,2] **Qiang Shi**,[1,2,3] **and Chunyue Duan**[1,2]

[1]*Department of Spine Surgery and Orthopaedics, Xiangya Hospital, Central South University, Changsha, China 410008*
[2]*National Clinical Research Center for Geriatric Disorders, Xiangya Hospital, Central South University, Changsha, China 410008*
[3]*Department of Spine Surgery, The Affiliated Changsha Central Hospital, Hengyang Medical School, University of South China, Changsha, China 410004*

Correspondence should be addressed to Qiang Shi; shiqiang542@126.com and Chunyue Duan; docdcy@qq.com

Received 21 July 2021; Accepted 10 January 2022; Published 14 May 2022

Academic Editor: Antonio C. Campos de Carvalho

Rotator cuff tear (RCT) is among the most common shoulder injuries and is prone to rerupture after surgery. Selecting suitable subpopulations of stem cells as a new specific cell type of mesenchymal stem cells has been increasingly used as a potential therapeutic tool in regenerative medicine. In this study, murine adipose-derived SSEA-4+CD90+PDGFRA+ subpopulation cells were successfully sorted, extracted, and identified. These cells showed good proliferation and differentiation potential, especially in the direction of tendon differentiation, as evidenced by qRT-PCR and immunofluorescence. Subsequently, we established a murine rotator cuff injury model and repaired it with subpopulation cells. Our results showed that the subpopulation cells embedded in a fibrin sealant significantly improved the histological score, as well as the biomechanical strength of the repaired tendon enthesis at four weeks after surgery, compared with the other groups. Hence, these findings indicated that the subpopulation of cells could augment the repaired enthesis and lead to better outcomes, thereby reducing the retear rate after rotator cuff repair. Our study provides a potential therapeutic strategy for rotator cuff healing in the future.

1. Introduction

Rotator cuff tear (RCT) is a common clinical problem that often leads to shoulder pain and eventually disability, especially in youth sports participants and the elderly [1, 2]. Despite advances in surgical reattachment of the tendon to the bone, the failure rates of rotator cuff repair remain high [3, 4]. Moreover, instead of regenerating the specialized tendon enthesis, which can effectively disperse stress from the muscle, the fibrovascular scar tissue is prone to the formation with poor mechanical reinforcement after surgery [5, 6]. Hence, new repair strategies are required to enhance collagen organization and mechanical strength and prevent the formation of scar tissue.

Mesenchymal stem cells (MSCs) are pluripotent cells with capacities for self-renewal and multiple differentiations [7, 8]. In recent years, stem cell therapies have been proposed as a treatment option for rotator cuff tear by reducing muscle atrophy, fibrosis, and fatty degeneration [9, 10]. It is worth noting that adipose-derived mesenchymal stem cells (ADSCs) and bone marrow mesenchymal stem cells (BMSCs) are the most widely used in the musculoskeletal field [11, 12]. Furthermore, compared with BMSCs, ADSCs are easily harvested from the fat of most animals and humans [13]. However, optimal regeneration has not been achieved with these transplanted MSCs. Therefore, there is an urgent need to find a new subpopulation of stem progenitor cells to influence the regeneration of injured tendon enthesis.

Currently, based on the selection of antigenically defined subsets using fluorescence-activated cell sorting (FACS), the identification of selected subpopulation cells prone to tenogenic lineage differentiation is being performed [14]. Stage-specific embryonic antigen 4 (SSEA-4) is a specific marker

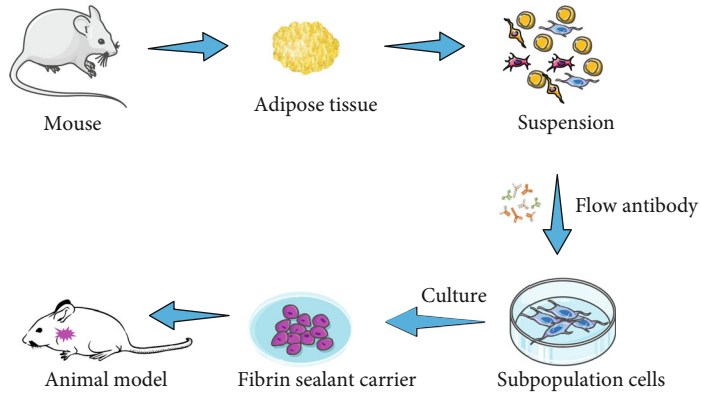

Figure 1: Schematic diagram showing the study design of adipose-derived subpopulation cells.

for pluripotent stem cells, which was first used to delineate changes during mouse embryonic development [15], and a subset of cells within the mouse adipose tissue expressing a SSEA-4 marker could be more likely to commit to desirable phenotypes. CD90 (Thy-1) was originally discovered as an antigen of T cells, thymocytes, neural cells, Kupffer's cells, and fibroblasts and could also be used as a marker for a variety of stem cells and for the axonal processes of mature neurons, which could be useful to identify and isolate ADSC subpopulations [16]. In addition, platelet-derived growth factor receptor alpha (PDGFRA) is thought to be essential for the derivation and maintenance of chondrocyte progenitor formation [17], which plays a crucial role in early embryonic mesenchymal stem cells and induces new tenocyte production for tendon regeneration and collagen organization [18]. To date, viable and homogenous subpopulation cells from human adipose tissue with superior differentiation have been successfully separated by the immunomagnetic sorting method [19, 20], serving as good candidates for biological augmentation of tissue repair. Therefore, it is valuable to explore the specific role and function of the tenogenic differentiation potential of mouse adipose-derived subpopulation cells, with positive markers SSEA-4+, CD90+, and PDGFRA+ and negative markers for hematopoietic antigens CD45-, Ter119-, CD31-, and 6C3-, on the repaired enthesis of the rotator cuff.

In this study, we aimed to identify a tenogenically differentiated subpopulation of stem cells from mouse adipose tissue for the first time. We then identified and evaluated the differentiation potential of the subpopulation cells. Furthermore, we evaluated the efficacy of adipose-derived subpopulation cells on tendon enthesis of the rotator cuff using a fibrin sealant carrier in a murine model.

2. Materials and Methods

2.1. Ethics Statement. The local animal ethics committee approved the experimental protocol for the use of mice in this study. All mice were housed under controlled conditions with free access to a normal chow diet and water. The number of mice required to evaluate rotator cuff repair was determined using a power analysis. All methods were performed according to relevant guidelines and regulations.

2.2. Study Design. First, three 12-week-old male pathogen-free wild-type C57Bl/6 mice (weight 24-26 g) were used for adipose tissue harvest to obtain ADSCs and the selected subpopulation cells. In addition, the subpopulation cells or ADSCs at passages 3-5 were used for in vitro differentiation, qPCR, immunofluorescence, picrosirius, and in vivo experiments. For the main study, a total of 56 animals were purchased and underwent acute unilateral detachment and transosseous repair of the supraspinatus (SS) tendon of the rotator cuff. After ADSCs and the selected subpopulation cells were collected and the fibrin sealant carrier was prepared, all mice were randomly assigned to one of the four groups with 14 mice per group: the control group without any treatment, fibrin sealant (FS) group with a fibrin carrier alone, ADSC group with 10^5 ADSCs in a fibrin sealant carrier at the tendon-bone repair site, and the subpopulation group with 10^5 subpopulation cells loaded with a fibrin sealant. Mice were humanely killed at four weeks to obtain supraspinatus tendon humeral complex specimens, followed by histological ($n = 6$ per group) and biomechanical analysis ($n = 8$ per group). The sample size from each group was determined before the in vivo experiments based on our power analysis and published studies in the murine rotator cuff injury model [21–23].

2.3. ADSC Harvest and Culture. The murine ADSCs were isolated from the subcutaneous adipose tissue in the abdomen of C57 mice according to the previous protocols [24]. In brief, subcutaneous fat from mice was dissected and carefully cleaned from adherent soft tissues. Then, fresh adipose tissue was washed with PBS solution, after which it was digested with 0.1% collagenase I solution to form chyle. Subsequently, the solution was added to complete medium at a volume ratio of 1 : 1 to stop digestion and then filtered with a 70 μm cell strainer (BD Falcon, USA). After centrifugation at 300 × g for 10 min, the cells were suspended in a complete medium containing 10% fetal bovine serum (FBS; Gibco), 1% glutamine (Thermo, USA), and 1% penicillin/streptomycin (HyClone) and seeded into 25 cm^2 culture flasks and

Table 1: Primer sequences used for qRT-PCR analysis.

Markers of tenogenic genes	Primer sequence (5′-3′)
EGR1	Forward TCGGCTCCTTTCCTCACTCA
	Reverse CTCATAGGGTTGTTCGCTCGG
SCX	Forward CTGGCCTCCAGCTACATTTCT
	Reverse GTCACGGTCTTTGCTCAACTT
TNMD	Forward ACACTTCTGGCCCGAGGTAT
	Reverse GACTTCCAATGTTTCATCAGTGC
GAPDH	Forward AGGTCGGTGTGAACGGATTTG
	Reverse TGTAGACCATGTAGTTGAGGTCA

cultured at 37°C in a humidified atmosphere containing 95% air and 5% CO_2. After reaching 70% to 80% confluence, the isolated cells were trypsinized, resuspended, and passaged.

2.4. Adipose-Derived Subpopulation Cell Sorting and Culture. The sorting and culture conditions of the subpopulation cells are depicted in Figure 1. Briefly, after the adipose tissue was digested into chyle and centrifuged at 4°C for 5 min at 1500 rpm, the supernatant was discarded, and the remaining precipitates were washed with FACS buffer. The related surface markers of the subpopulation cells were analyzed by flow cytometry analysis as follows: the precipitates (1×10^6 cells) were suspended in 100 μL phosphate-buffered saline (PBS) containing 10 μg/mL antibodies including Alexa Fluor® 700-conjugated CD31 (102444, BioLegend), Alexa Fluor® 700-conjugated CD45 (103128, BioLegend), Alexa Fluor® 700-conjugated Ter119 (116220, BioLegend), PerCP/Cyanine5.5-conjugated 6C3 (108316, BioLegend), PE-conjugated CD90 (555821, Biosciences, USA), PE/Cy7-conjugated PDGFRA (25-1401-80, eBioscience), and Alexa Fluor® 488-conjugated SSEA4 (330412, BioLegend). As an isotype control, nonspecific anti-mouse IgG coupled with Alexa Fluor® 700, PE, PE/Cy7, PerCP/Cyanine5.5, or Alexa Fluor® 700 (Becton Dickinson) was substituted for the primary antibody. After incubation for 30 min at 4°C, the cells were washed with PBS and resuspended in 500 μL of PBS for analysis. The subpopulation cells were sorted by flow cytometry using a Beckman Coulter XL System (Beckman, USA) and analyzed with FlowJo 10 software (Tree Star, USA).

The subpopulation cells were cultured in 3 mL primary medium containing 1% antibiotic-antimycotic (Gibco), DMEM/low glucose (Gibco), and 10% fetal bovine serum (FBS; Gibco). The cells were cultured in wells (1 mL/well) on a 12-well plate. The entire medium was replaced with medium every three days. The cells were subcultured when they reached 80%–90% confluence and used for further studies.

2.5. Colony-Forming Unit (CFU) Assay of Subpopulation Cells. In order to determine the optimal isolation cell seeding density of the subpopulation cells, nucleated cells were cultured in 6-well plates at 50, 500, and 5000 cells/cm^2 in the experiment; this procedure was repeated three times. On the 10th day of culture, after fixation with 4% paraformaldehyde, the cells were stained with 1% crystal violet (Solarbio, CHN) to quantify the colony formation. Distinguishable colonies larger than 2 mm in diameter were counted. Based on the maximum number of colonies obtained without contact inhibition, the optimal cell inoculation density was determined. The percentage of subpopulations was calculated by dividing the number of colonies under the optimum seeding density by the number of nucleated cells.

2.6. Cell Proliferation and Multidifferentiation Potential. The third passage subpopulation cells and ADSCs were collected; after counting and recording cells per mL, the cells were diluted to 75,000 per mL. Then, 100 μL of cells (7500 cells in total) and 100 μL medium were added to 5 wells and incubated overnight. At 1, 3, 5, 7, and 9 d, the cell counting kit-8 (CCK-8, Osaka, Japan) was used to assess the cell proliferation of the sample. The absorbance at 450 nm was measured using a microplate reader (Thermo Scientific).

The osteogenic, chondrogenic, and adipogenic differentiation potentials of the isolated cells were determined using Alizarin Red S staining (at day 14), Oil Red O staining (at day 21), and Alcian Blue staining (at day 28), respectively. In brief, cells were plated in 6-well plates at 5000 cells/cm^2 at 37°C and 5% CO_2 with complete medium. When the cell fusion reached 60%–70%, the osteogenic groups were treated with osteogenic differentiation medium (Cyagen, CHN), the adipogenic groups were induced with adipogenic differentiation medium (Cyagen, CHN), and the chondrogenic groups were induced with chondrogenic differentiation medium (Cyagen, CHN). At the end of differentiation, 1× PBS was used to wash the wells two times. After adding 2 mL 4% paraformaldehyde to each well to fix the contents for 30 min and washing with PBS, 1 mL Alizarin Red S, Oil Red O, and Alcian Blue solution were added to each well for 5 min. Images of stained cells were obtained using a fluorescence microscope and a light microscope.

2.7. Tenogenic Differentiation Test. Connective tissue growth factor (CTGF) is a growth factor that promotes the tenogenesis of cultured stem cells [25]. When the subpopulation cell or ADSC fusion reached 80%, the medium containing 25 ng/mL CTGF was refreshed in each well. The medium was replaced with fresh medium every three days.

After a 14-day culture, the expression of tenogenic lineage-specific genes (early growth response 1 (EGR1), scleraxis (SCX), and tenomodulin (TNMD)) was tested using qRT-PCR with appropriate primers (Table 1). Specifically, RNA was extracted using a RNeasy Kit (Qiagen, Hilden, Germany) according to the manufacturer's instructions. Complementary DNA was synthesized using a reverse transcriptase kit (Transgen, AT341, China), and quantitative PCR was performed using a qPCR kit (Promega, Wisconsin) and amplified on an ABI PRISM

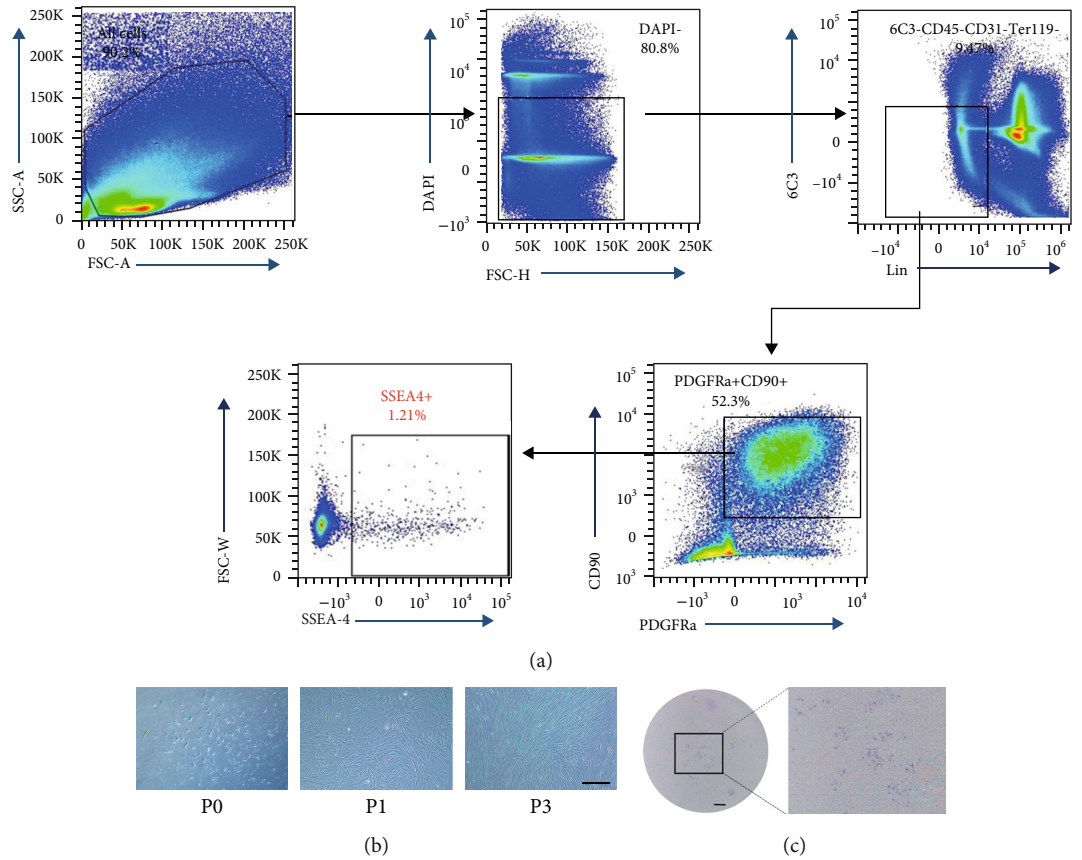

Figure 2: The characteristics of the subpopulation cells isolated from mouse adipose tissue. (a) Flow cytometry for the subpopulation cells. (b) Morphology of the subpopulation cells at different passages; scale bar = 200 μm. (c) Colony-forming unit assay of subpopulation cells after 10 days of culture; scale bar = 2 mm.

7900HT System (Applied Biosystems, Foster City). qRT-PCR conditions for each primer were performed as follows. First, total RNA (1000 ng) was reversely transcribed into first-strand cDNA in a 20 μL reaction with random primers using the TransScript All-in-One First-Strand cDNA Synthesis SuperMix Kit according to the manufacturer's instructions. PCR of 1 μL of diluted cDNA from each sample was carried out in 20 μL reactions containing Platinum SYBR Green qPCR SuperMix-UDG and appropriate primers in the ABI StepOne Plus System from Applied Biosystems. The PCR thermal cycle was set as follows: 10 min at 95°C for one cycle and 15 s at 95°C and 35 s at 60°C for 40 cycles. A melt curve analysis was performed at the end of each SYBR Green PCR. The efficiencies of all the primers were all over 90%. The relative gene expression was calculated using the $2 - \Delta\Delta$CT method and normalized to the levels of glyceraldehyde 3-phosphate dehydrogenase (GAPDH). Furthermore, immunofluorescence was used to assess the tenogenic differentiation. The cells were blocked with 1% bovine serum albumin and incubated with the primary antibody against tenomodulin antibody (TNMD, 1 : 200, Invitrogen, USA) at 4°C overnight. The corresponding secondary antibodies (goat anti-rabbit IgG H&L Alexa Fluor® 488, Abcam, USA) were then combined for 30 min before DAPI (H-1200, Vector Laboratories, Inc., CA, USA) was stained in the dark. The positive staining areas of the immunofluorescence of TNMD were measured by defining a region of interest (ROI) using ×10 magnification photomicrographs. Then, the positive area of the ROI was calculated with Image-Pro Plus software (version 6.0.0; Media Cybernetics Inc.).

In addition, the picrosirius red staining kit (Solarbio, CHN) was used to stain the cells to assess tenogenicity after a 21-day culture. After tenogenic differentiation was complete, 1× PBS was used to wash the wells two times. The cells in each well were fixed for 30 min with 2 mL 4% paraformaldehyde and then stained with 0.1% picrosirius red solution for 1 h at room temperature. After the staining solution was removed, the cells were thoroughly rinsed with 0.5% acetic acid. Images of stained cells were observed using a fluorescence microscope and a light microscope.

2.8. Animal Model. A mouse model of supraspinatus tendon enthesis healing was performed using the previously published techniques [23, 26]. Briefly, after anesthetization with an intraperitoneal injection of 0.3% pentobarbital sodium (0.6 mL/20 g; Sigma-Aldrich, St. Louis, MO), mice were placed in a right lateral decubitus position, incised, and bluntly separated to expose the deltoid under sterile conditions. After the deltoid was released with sharp dissecting scissors, the humerus was grasped to expose the enthesis of the SS tendon. Subsequently, the SS was transected with a

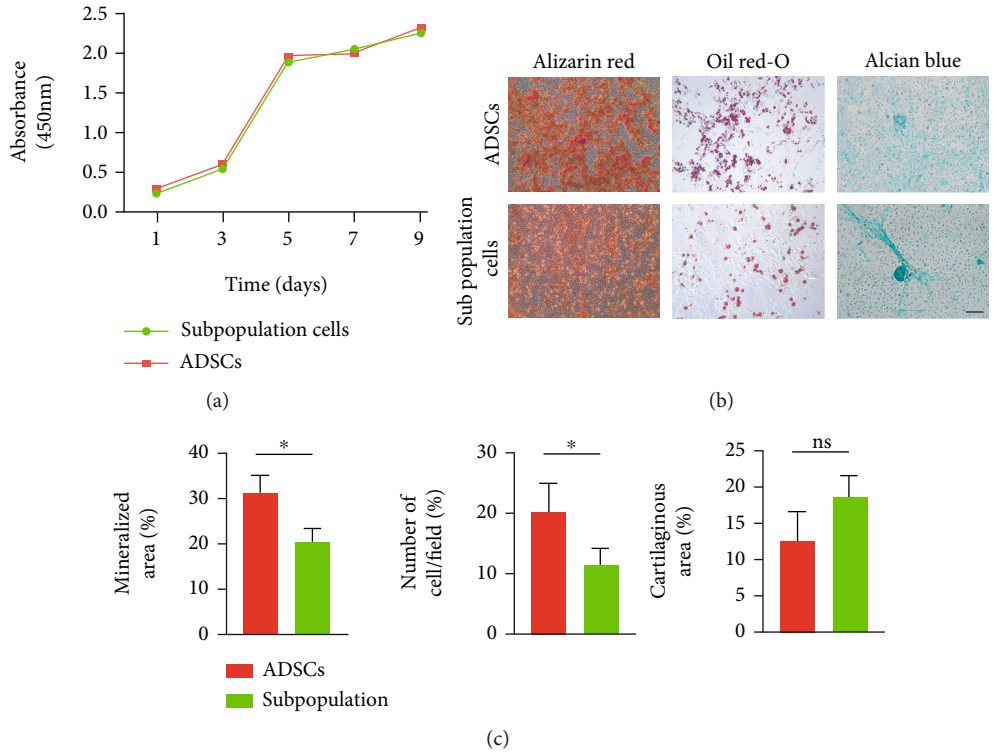

Figure 3: Proliferation and trilineage differentiation potential between ADSCs and the subpopulation cells. (a) Proliferation for both groups was determined using a CCK-8 assay. (b) Alizarin Red staining, Oil Red O staining, and Alcian Blue staining of the two groups after a 21-day culture. (c) Quantification of the extent of in vitro osteogenic, adipogenic, and chondrogenic differentiation between ADSCs and the subpopulation cells. Scale bar = 20 μm, $^*P < 0.05$. ns means no difference.

microscalpel, and a 6-0 PDS suture (Ethicon) was placed through the SS tendon in a figure-of-eight fashion. Next, the cartilage layer in the footprint on the greater tuberosity was completely removed with a no. 11 blade to expose the spongy bone. With the humerus stabilized, the suture was used to create a tunnel within the bone of the humeral head transversely from posterior to anterior, and the entrance of the bone tunnel was made from the supraspinatus footprint on the humeral head. For the control group, the suture was directly ligated to bring the tendon back down to its original insertion site. For the other groups, fibrinogen solution (Sigma-Aldrich) and thrombin solution (Sigma-Aldrich) were prepared and then mixed with normal saline (FS group), 10^5 subpopulation cells (subpopulation group), or ADSCs (ADSC group). The tendon was approximated by tying sutures over the original footprint. The wounds were closed using Ethicon sterile sutures. Buprenorphine (0.05 mg/kg) was administered with a subcutaneous injection for analgesic treatment, and penicillin G was administered for antibiotic treatment once a day for three days after surgery (0.05 mg/kg, subcutaneous injection).

2.9. Histological Experiments. Four weeks after the repair, the tendon enthesis specimens designated for histological analyses were fixed in 4% neutral buffered formalin for 24 h, decalcified in 10% ethylenediaminetetraacetate for two to three weeks, embedded in paraffin, and then sectioned at a 5 μm thickness. The slices were subsequently stained with hematoxylin and eosin (H&E) and toluidine blue-fast green (TB) to detect the healing characteristics of tendon enthesis. The stained sections were analyzed by two independent blinded observers using the previously established criteria of a modified tendon-to-bone maturing scoring system to evaluate the cellularity, vascularity, continuity, cell alignment of fibrocartilage, and tidemark from 0 to 4 points, respectively [27]. The difference between each group was compared using the total score of outcomes from the 10-fold magnification histology images. A higher score indicated better bone-tendon interface (BTI) healing, and a perfect score of 20 indicated healthy attachment with excellent maturation.

2.10. Biomechanical Testing. Biomechanical outcomes, such as failure load (N) and ultimate stress (MPa), were used as the ultimate indices to assess the healing quality of the bone-tendon interface, which was measured using a mechanical testing machine (MTS Systems Corp., USA). Before the test, the cross-sectional area (CSA) at the insertion of the SS tendon was measured and calculated using a caliper under a tension of 0.1 N. Subsequently, the tendon was gripped using a clamp with sandpaper, while the humerus was realigned in the bottom fixture. The specimens were loaded to failure at a rate of 0.03 mm/min after a preload of 0.1 N. Failure load (N) was obtained from the recorded load-displacement curve, and the ultimate stress

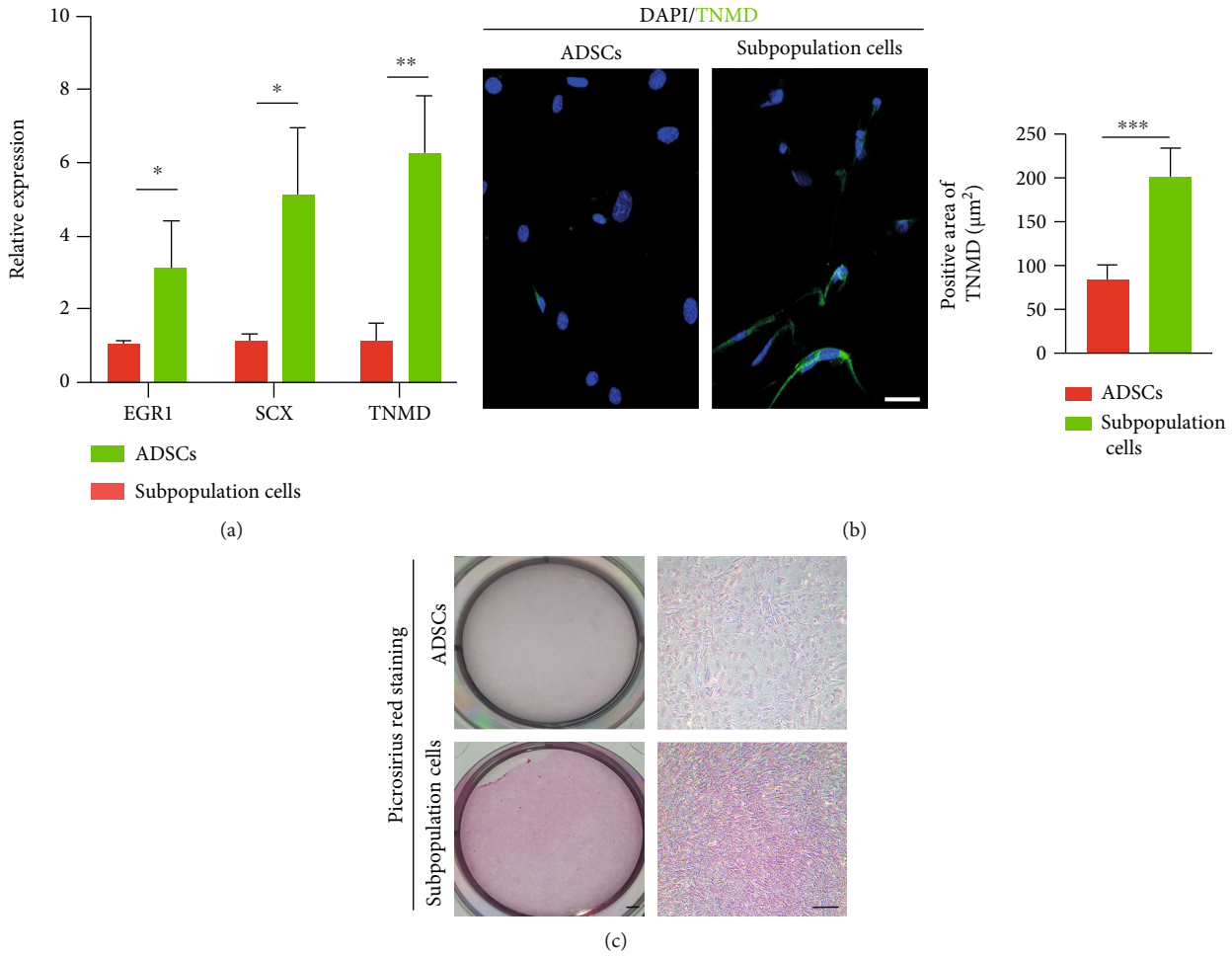

Figure 4: Tenogenic differentiation of ADSCs and subpopulation cells in vitro. (a) Tenogenic gene (EGR1, SCX, and TNMD) expression compared between ADSCs and the subpopulation cells. $^{*}P < 0.05$, $^{**}P < 0.01$. EGR1: early growth response1; Scx: scleraxis; Tnmd: tenomodulin. (b) Immunofluorescence for Tnmd expression of the two groups after 14 days of tenogenic induction and positive staining area of TNMD. Scale bar = 20 μm. (c) Picrosirius red staining for both groups. Scale bar on the left = 1 mm, scale bar on the right = 100 μm.

was calculated as the maximum load that the sample could withstand divided by the CSA. During testing, 0.9% saline was applied to prevent tissue dehydration.

2.11. Statistical Analysis. All quantitative data are presented as mean ± standard deviation (SD). A two-tailed unpaired Student's t-test was used to compare gene expression. Data on cell proliferation and biomechanical results were analyzed statistically using a one-way analysis of variance (ANOVA) with Tukey's post hoc test, while the histological scores among the groups were determined using the Mann-Whitney test. Statistical significance was set at $P < 0.05$. All data analyses were performed using SPSS software (version 17.0).

3. Results

3.1. Characteristics of the Mouse Adipose Tissue-Derived Subpopulation Cells. A specific subset of cells (>1%) was successfully isolated from mouse adipose tissue with positive markers SSEA-4, CD90, and PDGFRA but negative markers for hematopoietic antigens Ter119, CD31, 6C3, and CD45 (Figure 2(a)). These immunophenotypic profiles were in accordance with the criteria for defining MSCs proposed by the International Society for Cellular Therapy (ISCT) [28]. After the primary culture, adherent cells and spindle-shaped or rounder-shaped colonies were observed (Figure 2(b)). Specifically, most of the isolated cells exhibited spindle-shaped and fibroblast-like morphology; few of them still displayed a rounder shape at passage 1. With the passage of cells, the subpopulation cells exhibited a homogeneous spindle-shaped morphology. After 10 days of culture, the subpopulation cells at passage 4 formed adherent cell colonies (7.13 ± 1.22, Figure 2(c)).

3.2. Proliferation and Trilineage Differentiation Potential between Subpopulation Cells and ADSCs. CCK-8 analysis was used to measure cell proliferation. Our results indicated that passage 3 of the isolated subpopulations proliferated at a high rate within the first nine days, and no significant differences were observed between the subpopulations of cells and ADSCs (Figure 3(a)).

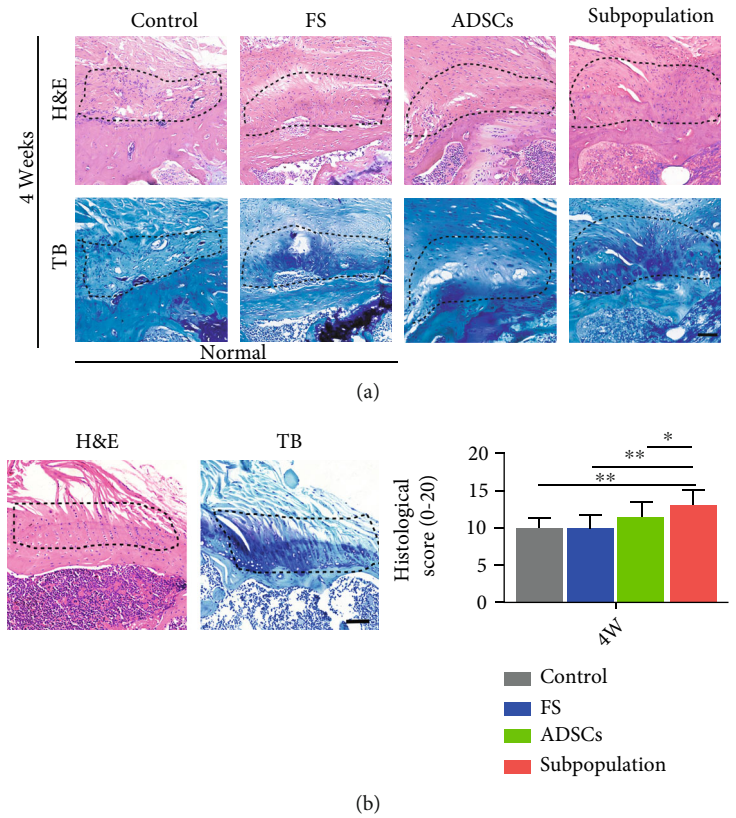

Figure 5: Representative pictures of the supraspinatus tendon humeral head insertion at postoperative four weeks. (a) H&E staining and TB staining images for all groups. (b) Modified tendon maturing score of the repaired enthesis. Area outlined by the dotted line represents the tendon enthesis. Scale bar = 200 μm. $^{*}P < 0.05$.

For trilineage differentiation potential, the osteogenic, chondrogenic, and adipogenic differentiation of subpopulation cells was identified using positive staining for Alizarin Red, Oil Red O, and Alcian Blue. Compared to ADSCs, the subpopulation cells showed lower osteogenic and adipogenic differential potential, while no significant difference was noted in chondrogenic differential potential (Figures 3(b) and 3(c)).

3.3. Tenogenic Differentiation Potential. The isolated subpopulation cells exposed to tenogenic-induced medium for 14 days showed a significant enhancement in tenogenic gene (EGR1, SCX, and TNMD) expression compared to the ADSC group ($P < 0.05$ for all, Figure 4(a)). Specifically, the gene expression of EGR1, SCX, and TNMD increased by factors of 3.13 ± 1.26, 5.15 ± 1.81, and 6.25 ± 1.58, respectively. The immunofluorescence assay revealed that the subpopulation cells had a significantly increased expression of Tnmd, compared to that in the ADSC group (Figure 4(b)). In addition, the subpopulation cells synthesized more collagen than the ADSCs, as shown by picrosirius red staining (Figure 4 (c)). The results revealed that the subpopulation cells have superior tenogenic differentiation.

3.4. Histological Evaluation. The regenerated enthesis in the rotator cuff for all groups was evaluated using H&E and TB staining. At four weeks after the operation, the interface in the control and FS groups with areas of direct tendon-bone contact through a fibrovascular scar was poorly organized and showed a few inflammatory cells, while the repaired insertion site in the ADSCs or subpopulation group contained more newborn collagen organization and became more organized. In the semiquantitative histologic scoring, based on a blinded analysis of the repaired site, no significant differences were observed between the control and FS groups. Meanwhile, the histological score in the ADSC group was slightly higher than that of the FS or control group, without a statistical difference. Unexpectedly, the subpopulation group score was significantly higher than those of the other groups (Figure 5, $P < 0.05$). The results of histological assessments showed that the subpopulation cells may promote tendon enthesis healing, as evidenced by superior bone-tendon insertion maturation in the subpopulation group.

3.5. Tensile Properties. In biomechanical testing (Supplementary Figure S1), all specimens ruptured at the insertion site. At four weeks after the operation, the failure load and ultimate stress in the subpopulation group were significantly higher than those in the other groups ($P < 0.05$). The failure load in the group was significantly greater than that in the control and FS groups ($P < 0.05$), while there was no significant difference in the ultimate stress. No differences in failure load and ultimate stress

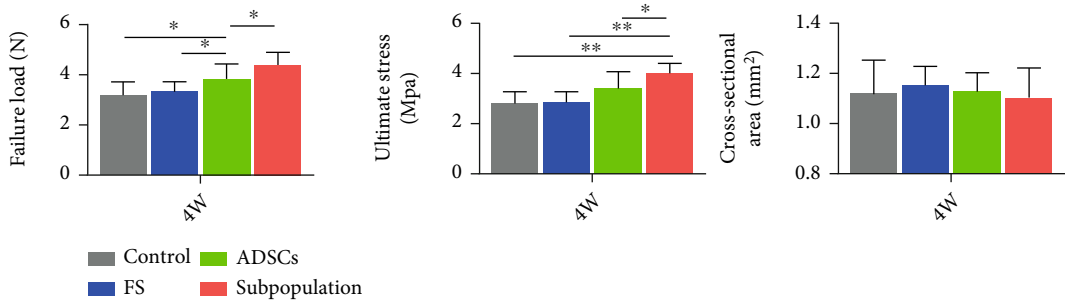

Figure 6: Biomechanical properties of the repaired enthesis in the rotator cuff, including failure load, ultimate stress, and CSA for all groups at postoperative week 4. CSA: cross-sectional area. $^{*}P < 0.05$.

were found between the FS and control groups at four weeks postoperatively. Meanwhile, there was no significant difference in CSA between the groups. These outcomes indicated that the subpopulation cells were able to promote the biomechanical healing quality of tendon enthesis of the rotator cuff.

4. Discussion

RCT is a widespread problem in orthopedics and sports medicine that seriously affects quality of life. Clinically, arthroscopic surgery is usually performed to reconstruct the tendon to the humeral footprint. Due to the high retear rate, mesenchymal stem cells have attracted considerable attention as regenerative medicinal agents for rotator cuff healing [29]. For example, ADSCs are easily obtained from the rich fat tissue of several animals, including humans, mice, rats, canines, and cattle, and have the capacity to differentiate into tendon fibroblasts, bone, and cartilage to augment the healing response [30–33]. However, the high intrinsic heterogeneity of ASCs hinders the translation of MSC-based therapies into the clinic [14]. To date, stem cell therapies for RCT have not yielded satisfactory results, thus necessitating the development of a potential solution to the problem of tendon enthesis healing in the rotator cuff.

It is necessary to select a suitable cell type for transplantation, which should ideally possess high proliferative capacity and tissue specificity. Recently, more attention has been paid to the selection of antigenically defined subpopulations of stem cells sorted based on the expression of specific surface molecules [34, 35]. Previous studies have shown that CD271+ MSCs from the synovial membrane demonstrated excellent cartilage repair, while CD105-depleted ADSCs showed great osteogenic differentiation [16]. In the present study, SSEA-4+CD90+PDGFRA+ subpopulation cells were successfully isolated directly from the adipose tissue fractions, avoiding the processes of early marker changes associated with plate culture. Meanwhile, better characterization and standardization of the subpopulation cells could assure the safety of cell therapies and speed up the progress of the field from bench to bedside. On the other hand, the previous studies have shown that SCX is critically involved in the development of tendon progenitors, and EGR1 is an essential transcription factor for the subsequent tendon collagen fiber differentiation and maturation [36]. The gene expression of TNMD is widely regarded as a late-stage tenogenic marker [37, 38]. The subpopulation cells showed promise for enhancing tenogenic differentiation with respect to the unsorted ADSCs, as evidenced by the significant upregulation of SCX, TNMD, and EGR1 expression. Interestingly, collagen deposition was also elevated in the sorted SSEA-4 +CD90+PDGFRA+ subpopulation cells, as shown by picrosirius red staining. These findings may suggest that the subpopulation cells extracted from adipose tissue can be an ideal cell source for tendon or ligament repair in vivo.

A fibrin sealant, well known as a useful delivery carrier matrix, has been widely applied in various traumas and regenerative medicine fields. Furthermore, previous studies indicated that using a fibrin sealant as a degradable graft scaffold could effectively slow the release of biologically active factors and avoid local explosive release [39, 40]. Gulotta et al. reported the addition of MSCs loaded with a fibrin sealant to the healing rotator cuff insertion site to determine the effect of cell-based strategies. In our study, we used a method to load ADSCs and sorted subpopulation cells via the absorbable fibrin sealant with a custom size and shape, demonstrating their therapeutic efficacy in a murine rotator cuff injury model. In addition, a control group without any treatment and an FS group without any MSCs were designated to eliminate the effect of the fibrin sealant on rotator cuff healing, and no positive or negative effects of the fibrin sealant on the rotator cuff healing process were identified histologically or biomechanically.

Our study had several limitations. First, although rodents are frequently utilized as a model of acute rotator cuff tears, this method does not reflect the clinical processes of chronic degeneration tendon rupture, which can result in muscle atrophy, fibrosis, fatty degeneration, and tendon retraction occurring in human patients. Second, we could not determine the specific growth factors or cytokines secreted from ADSCs or subpopulation cells that promoted rotator cuff healing in vivo, and future studies may be needed to explore the special role of MSC-related growth factors or cytokines in the healing site. Third, we evaluated tendon enthesis regeneration at a single time point. It is possible that implantation of the subpopulation cells could have demonstrated a more profound effect on RC healing over a

longer period. Finally, we investigated only a single dose of ADSCs or subpopulation cells preloaded with the fibrin sealant for implantation; more animals and optimized doses would result in better results and decreased error bars.

5. Conclusion

In conclusion, for the first time, SSEA-4+CD90+PDGFRA+ subpopulation cells were successfully isolated from the adipose tissue fractions directly, showing clonogenicity and high proliferation capacity. In addition, these subpopulation cells express specific markers of MSCs and can differentiate into tenogenic potential. Furthermore, we investigated the effects of subpopulation cells on the healing process of tendon enthesis in a mouse rotator cuff model. The subpopulation of cells could enhance the early stage of repaired tendon enthesis with improved collagen fiber organization and biomechanical strength.

Data Availability

The data used to support the findings of this study are included in the article.

Conflicts of Interest

The authors declare no competing financial interests.

Authors' Contributions

Q.S. and C.D. designed experiments. Y.C. and Y.X. performed experiments, analyzed data, and wrote the manuscript. G.D. assisted in the experiments and preparation of the manuscript. Q.S. and C.D. supervised the study. Yang Chen and Yan Xu contributed equally to this work.

Acknowledgments

This work was supported by the Natural Science Foundation of Hunan Province (No. 2020JJ4874). This investigation was performed at the Xiangya Hospital, Central South University, Changsha, China.

Supplementary Materials

Supplementary Figure S1: biomechanical test of the regenerated rotator cuff in mice. (A) Gross picture of the supraspinatus tendon enthesis for the biomechanical test and (B) an example of the load-displacement curve. *(Supplementary Materials)*

References

[1] P. B. de Witte, A. Kolk, F. Overes, R. G. H. H. Nelissen, and M. Reijnierse, "Rotator cuff calcific tendinitis: ultrasound-guided needling and lavage versus subacromial corticosteroids: five-year outcomes of a randomized controlled trial," *The American Journal of Sports Medicine*, vol. 45, no. 14, pp. 3305–3314, 2017.

[2] R. C. Mather 3rd, L. Koenig, D. Acevedo et al., "The societal and economic value of rotator cuff repair," *The Journal of Bone and Joint Surgery American*, vol. 95, no. 22, pp. 1993–2000, 2013.

[3] R. Kluger, P. Bock, M. Mittlböck, W. Krampla, and A. Engel, "Long-term survivorship of rotator cuff repairs using ultrasound and magnetic resonance imaging analysis," *The American Journal of Sports Medicine*, vol. 39, no. 10, pp. 2071–2081, 2011.

[4] G. Villatte, R. Erivan, G. Nourissat et al., "Allograft and autograft provide similar retear rates for the management of large and massive rotator cuff tears: a review and meta-analysis," *Knee Surgery, Sports Traumatology, Arthroscopy*, 2021.

[5] K. A. Derwin, L. M. Galatz, A. Ratcliffe, and S. Thomopoulos, "Enthesis repair: challenges and opportunities for effective tendon-to-bone healing," *The Journal of Bone and Joint Surgery American*, vol. 100, no. 16, article e109, 2018.

[6] C. Zhu, S. Pongkitwitoon, J. Qiu, S. Thomopoulos, and Y. Xia, "Design and fabrication of a hierarchically structured scaffold for tendon-to-bone repair," *Advanced Materials*, vol. 30, no. 16, article e1707306, 2018.

[7] V. Bunpetch, Z. Y. Zhang, X. Zhang et al., "Strategies for MSC expansion and MSC-based microtissue for bone regeneration," *Biomaterials*, vol. 196, pp. 67–79, 2019.

[8] W. Z. Zhuang, Y. H. Lin, L. J. Su et al., "Mesenchymal stem/stromal cell-based therapy: mechanism, systemic safety and biodistribution for precision clinical applications," *Journal of Biomedical Science*, vol. 28, no. 1, p. 28, 2021.

[9] C. D. Eliasberg, A. Dar, A. R. Jensen et al., "Perivascular stem cells diminish muscle atrophy following massive rotator cuff tears in a small animal model," *The Journal of Bone and Joint Surgery American*, vol. 99, no. 4, pp. 331–341, 2017.

[10] M. N. Pantelic and L. M. Larkin, "Stem cells for skeletal muscle tissue engineering," *Tissue Engineering Part B: Reviews*, vol. 24, no. 5, pp. 373–391, 2018.

[11] Y. S. Kim, H. J. Lee, J. H. Ok, J. S. Park, and D. W. Kim, "Survivorship of implanted bone marrow-derived mesenchymal stem cells in acute rotator cuff tear," *Journal of Shoulder and Elbow Surgery*, vol. 22, no. 8, pp. 1037–1045, 2013.

[12] H. Orbay, A. C. Uysal, H. Hyakusoku, and H. Mizuno, "Differentiated and undifferentiated adipose-derived stem cells improve function in rats with peripheral nerve gaps," *Journal of Plastic, Reconstructive & Aesthetic Surgery*, vol. 65, no. 5, pp. 657–664, 2012.

[13] J. W. Kuhbier, B. Weyand, C. Radtke, P. M. Vogt, C. Kasper, and K. Reimers, "Isolation, characterization, differentiation, and application of adipose-derived stem cells," *Advances in Biochemical Engineering Biotechnology*, vol. 123, pp. 55–105, 2010.

[14] A. I. Gonçalves, D. Berdecka, M. T. Rodrigues et al., "Evaluation of tenogenic differentiation potential of selected subpopulations of human adipose-derived stem cells," *Journal of Tissue Engineering and Regenerative Medicine*, vol. 13, no. 12, pp. 2204–2217, 2019.

[15] L. H. Shevinsky, B. B. Knowles, I. Damjanov, and D. Solter, "Monoclonal antibody to murine embryos defines a stage-specific embryonic antigen expressed on mouse embryos and human teratocarcinoma cells," *Cell*, vol. 30, no. 3, pp. 697–705, 1982.

[16] V. Pérez-Silos, A. Camacho-Morales, and L. Fuentes-Mera, "Mesenchymal stem cells subpopulations: application for orthopedic regenerative medicine," *Stem Cells International*, vol. 2016, Article ID 3187491, 9 pages, 2016.

[17] G. Bartoletti, C. Dong, M. Umar, and F. He, "Pdgfra regulates multipotent cell differentiation towards chondrocytes via inhibiting Wnt 9a/beta-catenin pathway during chondrocranial cartilage development," *Developmental Biology*, vol. 466, no. 1-2, pp. 36–46, 2020.

[18] T. Harvey, S. Flamenco, and C. M. Fan, "A *Tppp3*$^{+}$*Pdgfra*$^{+}$ tendon stem cell population contributes to regeneration and reveals a shared role for PDGF signalling in regeneration and fibrosis," *Nature Cell Biology*, vol. 21, no. 12, pp. 1490–1503, 2019.

[19] S. M. Mihaila, A. M. Frias, R. P. Pirraco et al., "Human adipose tissue-derived SSEA-4 subpopulation multi-differentiation potential towards the endothelial and osteogenic lineages," *Tissue Engineering Part A*, vol. 19, no. 1-2, pp. 235–246, 2013.

[20] T. Rada, T. C. Santos, A. P. Marques et al., "Osteogenic differentiation of two distinct subpopulations of human adipose-derived stem cells: an in vitro and in vivo study," *Journal of Tissue Engineering and Regenerative Medicine*, vol. 6, no. 1, pp. 1–11, 2012.

[21] A. H. Lebaschi, X.-H. Deng, C. L. Camp et al., "Biomechanical, histologic, and molecular evaluation of tendon healing in a new murine model of rotator cuff repair," *Arthroscopy: The Journal of Arthroscopic & Related Surgery*, vol. 34, no. 4, pp. 1173–1183, 2018.

[22] S. Wada, A. H. Lebaschi, Y. Nakagawa et al., "Postoperative tendon loading with treadmill running delays tendon-to-bone healing: immunohistochemical evaluation in a murine rotator cuff repair model," *Journal of Orthopaedic Research*, vol. 37, no. 7, pp. 1628–1637, 2019.

[23] T. Zhang, Y. Chen, C. Chen et al., "Treadmill exercise facilitated rotator cuff healing is coupled with regulating periphery neuropeptides expression in a murine model," *Journal of Orthopaedic Research*, vol. 39, no. 3, pp. 680–692, 2021.

[24] X. Huang, G. Q. Fei, W. J. Liu et al., "Adipose-derived mesenchymal stem cells protect against CMS-induced depression-like behaviors in mice via regulating the Nrf2/HO-1 and TLR4/NF-*κ*B signaling pathways," *Acta Pharmacologica Sinica*, vol. 41, no. 5, pp. 612–619, 2020.

[25] X. Li, S. Pongkitwitoon, H. Lu, C. Lee, R. Gelberman, and S. Thomopoulos, "CTGF induces tenogenic differentiation and proliferation of adipose-derived stromal cells," *Journal of Orthopaedic Research*, vol. 37, no. 3, pp. 574–582, 2019.

[26] D. Wang, H. Tan, A. H. Lebaschi et al., "Kartogenin enhances collagen organization and mechanical strength of the repaired enthesis in a murine model of rotator cuff repair," *Arthroscopy: The Journal of Arthroscopic & Related Surgery*, vol. 34, no. 9, pp. 2579–2587, 2018.

[27] J. Ide, K. Kikukawa, J. Hirose et al., "The effect of a local application of fibroblast growth factor-2 on tendon-to- bone remodeling in rats with acute injury and repair of the supraspinatus tendon," *Journal of Shoulder and Elbow Surgery*, vol. 18, no. 3, pp. 391–398, 2009.

[28] M. Dominici, K. le Blanc, I. Mueller et al., "Minimal criteria for defining multipotent mesenchymal stromal cells. The International Society for Cellular Therapy position statement," *Cytotherapy*, vol. 8, no. 4, pp. 315–317, 2006.

[29] F. Mocini, A. S. Monteleone, P. Piazza et al., "The role of adipose derived stem cells in the treatment of rotator cuff tears: from basic science to clinical application," *Orthopedic Reviews*, vol. 12, article 8682, Supplement 1, 2020.

[30] K. S. Lee, H. W. Kang, H. T. Lee et al., "Sequential sub-passage decreases the differentiation potential of canine adipose-derived mesenchymal stem cells," *Research in Veterinary Science*, vol. 96, no. 2, pp. 267–275, 2014.

[31] T. Lu, H. Xiong, K. Wang, S. Wang, Y. Ma, and W. Guan, "Isolation and characterization of adipose-derived mesenchymal stem cells (ADSCs) from cattle," *Applied Biochemistry and Biotechnology*, vol. 174, no. 2, pp. 719–728, 2014.

[32] P. D. Megaloikonomos, G. N. Panagopoulos, M. Bami et al., "Harvesting, isolation and differentiation of rat adipose-derived stem cells," *Current Pharmaceutical Biotechnology*, vol. 19, no. 1, pp. 19–29, 2018.

[33] M. J. Shin, I. K. Shim, D. M. Kim et al., "Engineered cell sheets for the effective delivery of adipose-derived stem cells for tendon-to-bone healing," *The American Journal of Sports Medicine*, vol. 48, no. 13, pp. 3347–3358, 2020.

[34] K. S. Johal, V. C. Lees, and A. J. Reid, "Adipose-derived stem cells: selecting for translational success," *Regenerative Medicine*, vol. 10, no. 1, pp. 79–96, 2015.

[35] M. Mo, S. Wang, Y. Zhou, H. Li, and Y. Wu, "Mesenchymal stem cell subpopulations: phenotype, property and therapeutic potential," *Cellular and Molecular Life Sciences*, vol. 73, no. 17, pp. 3311–3321, 2016.

[36] H. Liu, S. Zhu, C. Zhang et al., "Crucial transcription factors in tendon development and differentiation: their potential for tendon regeneration," *Cell and Tissue Research*, vol. 356, no. 2, pp. 287–298, 2014.

[37] C. Shukunami, A. Takimoto, M. Oro, and Y. Hiraki, "Scleraxis positively regulates the expression of tenomodulin, a differentiation marker of tenocytes," *Developmental Biology*, vol. 298, no. 1, pp. 234–247, 2006.

[38] Q. Liu, Y. Zhu, J. Qi et al., "Isolation and characterization of turkey bone marrow-derived mesenchymal stem cells," *Journal of Orthopaedic Research*, vol. 37, no. 6, pp. 1419–1428, 2019.

[39] B. S. Kim, F. Shkembi, and J. Lee, "In vitro and in vivo evaluation of commercially available fibrin gel as a carrier of alendronate for bone tissue engineering," *BioMed Research International*, vol. 2017, Article ID 6434169, 10 pages, 2017.

[40] Z. Wang, Y. Chen, H. Xiao et al., "The enhancement effect of acetylcholine and pyridostigmine on bone-tendon interface healing in a murine rotator cuff model," *The American Journal of Sports Medicine*, vol. 49, no. 4, pp. 909–917, 2021.

Hindawi
Stem Cells International
Volume 2022, Article ID 2976185, 15 pages
https://doi.org/10.1155/2022/2976185

Research Article

Constructing Tissue-Engineered Dressing Membranes with Adipose-Derived Stem Cells and Acellular Dermal Matrix for Diabetic Wound Healing: A Comparative Study of Hypoxia- or Normoxia-Culture Modes

Wen Zhou,[1] Xin Zhao,[2] Xin Shi,[3] Can Chen,[4] Yanpeng Cao ,[2] and Jun Liu [2,3]

[1]*Clinical Nursing Teaching and Research Section, The Second Xiangya Hospital, Central South University, Changsha, China*
[2]*Department of Limbs (Foot and Hand) Microsurgery, Affiliated Chenzhou Hospital, Hengyang Medical School, University of South China, Chenzhou, China*
[3]*The First School of Clinical Medicine, Southern Medical University, Guangzhou, China*
[4]*Department of Orthopedics, Xiangya Hospital, Central South University, Changsha, China*

Correspondence should be addressed to Yanpeng Cao; yanpengcao@163.com and Jun Liu; liujunheliyun@163.com

Received 21 December 2021; Revised 22 February 2022; Accepted 16 March 2022; Published 5 May 2022

Academic Editor: Gehua Zhen

Diabetes foot ulcer (DFU) is a serious complication of diabetes, characterized by impaired vascular function, limited angiogenesis, and chronic inflammation. Direct stem cell injection on treating DFU is far from satisfactory in clinical practice, as this therapy neither protects nor localizes the injected cell suspension at the chronic ulcer site. Meanwhile, most of injected cells gradually perished within several days due to senescence or apoptosis. Acellular dermal matrix (ADM) has the potential to act as excellent cell delivery vehicles, considering it is highly biomimetic to native dermal tissue, has low immunogenicity, and suitable for stem cell attachment and proliferation. Hypoxia culture has significantly enhanced effects on the survival ability of in vitro cultured stem cells, indicating this culture mode is a suitable way for inhibiting the senescence or apoptosis of transplanted cells. In the current study, we, respectively, culture adipose-derived stem cells (ADSCs) on an ADM membrane under a hypoxia or normoxia condition to construct two kinds of tissue-engineered dressing membranes (H-ADSCs/ADM and N-ADSCs/ADM) and then comparatively evaluated their efficacy on DFU healing using a diabetic rat model. In vitro results showed that hypoxia precondition could stimulate the ADSCs secreting VEGF-A, and the culture medium from hypoxia-preconditioned ADSCs could enhance the proliferation, migration, and angiogenesis of HUVECs. In vivo results indicated that compared to the N-ADSCs/ADM membrane, the transplanted cells in the H-ADSCs/ADM membrane can survive longer at the chronic ulcer site, consequently improve angiogenesis, inhibit inflammation, and increase extracellular matrix remodeling, eventually accelerating DFU closure. This study provides an innovative covering graft for the treatment of DFU in the clinic.

1. Introduction

Foot ulceration is a serious complication in patient with diabetes, which affects approximately 19-34% of diabetics at least once in their life, thus poses a large burden on the patient and healthcare system [1, 2]. Regrettably, the healing process of diabetes foot ulcer (DFU) is very slow and difficult, which has a profound negative impact on the patient's quality of life [3, 4]. Currently, various therapeutic regimens are being developed, but their efficacy on DFU remains unsatisfactory [5]. Therefore, developing more effective treatment strategies is necessary.

Mesenchymal stem cells (MSCs), which having pluripotent properties and capacity for long-term self-renewal, are known to be effective in enhancing DFU healing [6, 7]. Increasing evidence has demonstrated that the therapeutic benefits of MSCs on DFU healing are mainly contributed to their ability to recruit cells; to release growth factors,

chemokines, cytokines, and proteins; to promote angiogenesis; and reduce apoptosis and oxidative stress [8, 9]. According to literatures, MSCs can be isolated from peripheral blood, bone marrow, placenta, oral mucosa, amniotic fluid, umbilical cord, adipose tissue, and so on [10]. Currently, adipose-derived stem cells (ADSCs) were the most commonly used cell source in the wound healing, due to their easy accessibility, abundant sources, subcutaneous location, and longer incubation time maintaining proliferating ability and differentiation potential [11–13]. Previous studies indicated that ADSCs systemically improve angiogenesis and DFU healing via increasing epithelialization and granulation tissue formation, anti-inflammatory, and antiapoptotic effects and release of angiogenic cytokines [11, 12]. Moreover, few small clinical trials showed that ADSCs treated patients with DFU caused improved ulcer evolution, lower pain scores, and improved claudication walking distances with no reported complications [11, 12]. However, owing to the harsh environment of chronic ulcer sites, the majority of transplanted ADSCs inactivated rapidly and only a few of them are ultimately involved in the wound healing. More seriously, only part of transplanted cells can adhere to chronic ulcer site, which may hinder wound healing homogeneously and rapidly. To address these shortcomings, some researchers transplanted the MSCs into chronic ulcer site by loading them on a scaffold, and in vivo experimental results showed that this transplantation mode was effective for enhancing wound healing [14, 15]. In this transplantation mode, the scaffold acted as a three-dimensional (3D) network for cell attachment, thus ensures the transplanted cells distributed homogeneously. In addition, the scaffold provided some biochemical and mechanical signals to enhance the attached cell proliferation and differentiation, thus beneficial for DFU healing [16]. Among the scaffolds used in loading MSCs, acellular dermal matrix (ADM) has attracted wide attention owing to their low immunogenicity, high biocompatibility, good biodegradability, and high similarity to normal skin dermis in morphology and ingredients [17, 18]. Milan et.al accelerated DFU healing using ADM and human umbilical cord perivascular cells [19]. Meanwhile, Chu et.al constructed a therapeutic graft for DFU healing by seeding BMSCs on ADM [20]. In this study, we are intended to construct a tissue-engineered graft as dressing membrane for DFU healing with the mode of loading ADSCs on an ADM membrane. Regrettably, most of the transplanted BMSCs can only function about 7 days under the injured microenvironment of DFU due to cell inactivation [20]. Thus, extending the time of transplanted MSC survival in vivo may be a promising and possible solution to improve its therapeutic efficiency on DFU healing.

Oxygen concentration has been considered as a vital factor in regulating the survival, proliferation, and differentiation of MSCs [21–23]. A prior study has demonstrated that hypoxia pretreatment increases MSC survival in vivo, which would extend the function duration of transplanted cells at the wound site [22]. In addition, the conditioned media from hypoxia cultured MSCs is more effective for enhancing wound healing in comparison with normoxia-cultured MSCs because it contains more bioactive substance beneficial for cell survival and tube formation [24]. These studies imply that the hypoxia pretreatment may be an effective approach for extending the survival time of transplanted MSCs at the chronic ulcer site, thus enhancing its therapeutic efficiency on DFU healing.

In this study, two kinds of tissue-engineered dressing membranes were prepared by, respectively, culturing ADSCs on an ADM membrane under a hypoxia or normoxia condition. Additionally, a streptozotocin-induced diabetic rat model was used to comparatively evaluate the two dressing membranes on DFU healing.

2. Materials and Methods

2.1. Ethics Statement. The experimental protocol for using of Sprague-Dawley (SD) rats in our study was authorized by the Animal Ethics Committee of Chenzhou No. 1 People's Hospital (approval No. 2019045). At the end of final experiments and observations, all the rats were humanely euthanized. Fresh skin tissue used in this study was obtained free of charge with the informed consent of the donor who had been amputated in a car accident, and all procedures were approved by the Ethics Committee of Chenzhou No. 1 People's Hospital (approval No. 2022019).

2.2. ADSC Isolation and Identification. Inguinal subcutaneous adipose tissue was acquired from 3-week-old SD rats and washed with PBS for 3 times. After that, the adipose tissues (about 0.8 cm^3) were minced with sterile surgical scissors and digested with 0.1% type I collagenase (Gibco, USA) for 1.5 hours at 37°C with gentle shake followed by complete medium containing 10% fetal bovine serum (FBS) to neutralize the collagenase. After the suspension was centrifuged at 1000 rpm for 5 min, the cell pellet was resuspended in complete medium (DMEM/F12, 10% FBS, 1% antibiotics, Gibco, USA) and incubated at 37°C in 5% CO_2. Cells were passaged when reaching 80-90% confluence. The cells in passage 3 were used for further experiments.

These isolated cells were identified by flow cytometry analysis using monoclonal antibodies for CD11b, CD29, CD34, CD44, CD45, and CD73 (RAXMX-09011 Kit, Cyagen, United States). Meanwhile, these isolated cells were also identified by evaluating their potential of osteogenic, chondrogenic, and adipogenic differentiation.

2.3. Preparation of ADM Membrane. Fresh skin tissues were harvested from the donors at Chenzhou No. 1 People's Hospital, who were undergoing traumatic amputation owing to car accident. Additionally, we excluded in the donors with transmittable diseases, such as human immunodeficiency virus (HIV), hepatitis, syphilis, and human T-cell lymphotropic virus (HTLV).

The acquired skin tissues were incised into square shapes with 2 cm in diameter followed by PBS washing for 15 min and then decellularized within 10 mM Tris buffer containing 5 mM ethylenediaminetetraacetic acid for 12 hours. After mechanically detaching the epidermal layer from the dermis, the tissues were decellularized within 1% Triton X-100 containing 1.5 M potassium chloride and 50 mM Tris buffer for

12 hours. In order to clear the nuclear substance of the dermis, 100 μg/mL RNase together with 150 IU/mL DNase was used to digest the dermis, and then, the processed dermis was rinsed in PBS for 12 hours. After the acquired ADM was sectioned into a shape of thin slice (100 μm), they were lyophilized by a vacuum freeze-drier (FD8-5T, SIM, USA) and then trimmed into a circle shape with 2 cm in diameter. Finally, ADM membrane was acquired.

During decellularization, the abovementioned solutions were added with 1% penicillin-streptomycin-amphotericin B (03-033-1B, BioInd, Israel) and protease inhibitor (1 tablet/300 mL, S8820-20TAB, Sigma). Specially, protease inhibitor (1 tablet/300 mL, S8820-20TAB, Sigma) was not added into nuclease solution.

2.4. Evaluation of ADM Membrane. After fixed in 4% neutral paraformaldehyde for 1 day, the ADM membrane or natural dermis tissue (NDT) was embedded within paraffin and sectioned with 5 μm thickness for hematoxylin & eosin (H&E), 4′,6-diamidino-2-phenylindole (DAPI), and Masson's trichrome (MT) staining. H&E staining combined with DAPI was used for observing the elimination of cellular components in the ADM membrane, while MT staining was used for observing the preservation of collagen in the ADM. In order to comparatively characterize the ultrastructural difference between ADM membrane and NDT, they were, respectively, fixed with 0.25% glutaraldehyde solution and sputter-coated with gold for scanning electron microscope (SEM) (S-3400 N; Hitachi, Japan).

2.5. Fabrication and Evaluation of H-ADSCs/ADM and N-ADSCs/ADM. After washing the ADM membrane (100 μm thick, 2 cm diameter) within PBS for 5 min, the ADM membrane was placed on 6-well plates and a concentrated ADSC solution (1.0×10^6 cells/800 μL, passage 3) was seeded on the top of the ADM membrane. The plates were cultured under normoxic (21% O_2) condition for 2 days and then refresh the culture medium. Part of plates was randomly selected and cultured under normoxic (21% O_2) condition for 48 hours, while the other part of plates was cultured under hypoxic (1% O_2) conditions for 48 hours. Thus, the H-ADSCs/ADM or the N-ADSCs/ADM was acquired.

After fixed in 4% neutral paraformaldehyde for 1 day, the H-ADSCs/ADM or the N-ADSCs/ADM was embedded within paraffin and sectioned with 5 μm thickness for H&E and DAPI staining.

2.6. Collection of the Culture Medium from H-ADSCs/ADM or N-ADSCs/ADM. After harvesting the H-ADSCs/ADM or the N-ADSCs/ADM, the two kinds of culture medium were, respectively, added to a centrifugal filter unit with a 3 kDa cutoff (Millipore, USA) and centrifuged at 3000 rpm to concentrate the medium by 50-fold. After that, the concentrated hypoxia- or normoxia-culture medium was mixed with FBS-free endothelial cell medium at a ratio of 1 : 3 and marked as H medium and N medium.

2.7. Cytocompatibility of ADM. After 48 hours incubation under a normoxic or hypoxic condition, the live cells or the dead cells in the H-ADSCs/ADM or the N-ADSCs/ADM ($n = 4$, per group) were, respectively, stained with Calcein-AM (green) or EthD-1 (red) according to the instrument of Live/Dead Assay kit (40747ES76, Yeasen, Shanghai, China). Cell viability was calculated as follows: (live cells/total cells) × 100%. Additionally, the H-ADSCs/ADM or the N-ADSCs/ADM was washed by PBS to remove the unattached cells and then observed with SEM for the adhered cells.

2.8. Enzyme-Linked Immunosorbent Assay (ELISA) for Angiogenic-Related Growth Factors. The levels of vascular endothelial growth factor-A (VEGF-A), hepatocyte growth factor (HGF), and fibroblast growth factor (FGF) that were secreted by ADSCs on the ADM under normoxic or hypoxic condition were tested by ELISA. In brief, the supernatant was concentrated and measured by ELISA kits (VEGF: ab100786, Abcam, USA; HGF, ER0027, Fine Biotech; FGF, KA4283, Abnova) according to the manufacturer's instructions ($n = 3$).

2.9. Culture Medium from Hypoxia-Preconditioned ADSCs on HUVEC Bioactivities. The effects of culture medium from hypoxia- or normoxia-preconditioned ADSCs on the proliferation of HUVECs were tested by a CCK8 kit (70-CCK8100, MultiSciences, China) ($n = 4$). HUVECs were obtained commercially (CP-H082, Procell Life Science, China). In brief, HUVECs (1000/well) were seeded in a 96-well plate and cultured by H medium or N medium. At 0, 1, 2, and 3 days of culture, CCK8 reagent was added into the culture medium of each well and then incubated at 37°C for 2 hours. The cell proliferation was measured by absorbance at 450 nm using a microplate reader (BioTek, USA).

The effects of culture medium from hypoxia- or normoxia-preconditioned ADSCs on the migration of the HUVECs were tested using wound healing assays ($n = 3$). Briefly, HUVECs were seeded in the 24-well culture plates at 4×10^4 cells per well and cultured for 48 hours in the incubator until reaching about 90% confluence. A sterile 100 μL pipette tip was used to scratch a straight line. Then, H medium or N medium was added into the 24-well plate. Images were obtained at 48 hours and analyzed.

The angiogenic activity of hypoxia- or normoxia-preconditioned ADSCs was evaluated by tube formation assay ($n = 3$). HUVECs (1.5×10^5/well) were seeded on a Matrigel (E1270, Sigma-Aldrich) substrate and incubated with H medium or N medium at 37°C in 5% CO_2. After 12 hours of incubation, the cord-like structures were captured and counted by phase-contrast microscopy. HUVECs cultured without H medium or N medium were used as the control group.

2.10. Streptozotocin-Induced Diabetic Rat Model. Adult male SD rats (10-week-old, weighing 200-250 g) were raised in a 12-hour light/dark cycle and temperature-controlled (25°C) and humidity cage, with free access to food and water. Streptozotocin (1% STZ, 75 mg/kg, S0130, Sigma, USA) was intraperitoneally injected into the abdominal cavity of all rats and fasted for solids 18 hours, and blood glucose levels were

Table 1: Primer sequences used for qRT-PCR analysis.

Gene	Primer sequence	Species
IL-1β	Forward: 5′-ATAGCAGCTTTCGACAGTGAG-3′ Reverse: 5′-GTCAACTATGTCCCGACCATT-3′	Rat
IL-6	Forward: 5′-GACTGATGTTGTTGACAGCCACTGC-3′ Reverse: 5′-TAGCCACTCCTTCTGTGACTCTAACT-3′	Rat
NF-κB	Forward: 5′-CGATCTGTTTCCCCTCATCT-3′ Reverse: 5′-TGCTTCTCTCCCCAGGAATA-3′	Rat
β-Actin	Forward: 5′-ATCTGGCACCACACCTTC-3′ Reverse: 5′-AGCCAGGTCCAGACGCA-3′	Rat

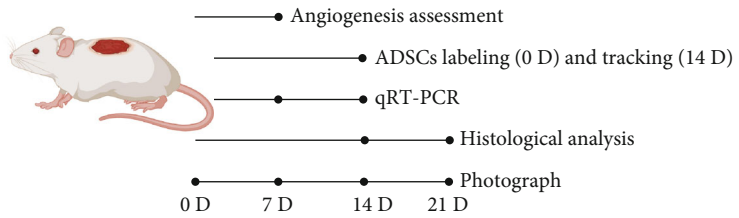

Figure 1: Flowchart depicting the experimental design for in vivo evaluation of ADM, N-ADSCs/ADM, and H-ADSCs/ADM in a diabetic wound rat model.

monitored by an electronic glucometer on days 0, 3, and 7. The animals with blood glucose level higher than 15 mM, weight loss, polyuria, and polydipsia were diagnosed as diabetic and used for the creation of skin wounds. After 2-week observation, the diabetic SD rats were anesthetized with 50 mg/kg pentobarbital sodium (Sigma). After shaving the rats with an electric clipper, dorsal skin was sanitized with 5% povidone-iodine solution; then, an excisional skin wound with 2 cm in diameter was created on the dorsal by a scalpel; thus, a diabetic wound model was acquired. The diabetic wounds were covered with three dressing membranes: commercial ADM (ADM group), N-ADSCs/ADM (N-ADSCs/ADM group), and H-ADSCs/ADM (H-ADSCs/ADM group). Commercial ADM membrane was bought in Beijing Jayyalife Biological Technology Co., Ltd. (J-1, Jayyalife, Beijing, China). All operations were performed by two independent investigators (Xin Shi and Yanpeng Cao) ($n = 8$).

2.11. ADSC Labeling and Tracking. In order to track the implanted cells at the DFU healing site, the ADSCs in the H-ADSCs/ADM or the N-ADSCs/ADM were prestained with fluorescent solution (Vybrant™ DiO, ThermoFisher, Ireland) for 20 min at 37°C prior to implantation, respectively. At 14 days after transplantation, the rats were sacrificed to harvest the circular full-thickness skin tissue at the center of the wound, frozen sections were prepared, and the cell nucleus was stained using DAPI. A fluorescence microscope (ApoTome; Zeiss) with an excitation wavelength of 594 nm was used to detect DiO-labeled cells at the DFU healing site.

2.12. Diabetic Wound Closure. At days 0, 7, 14, and 21 after surgery, the wounds of each diabetic rat were photographed, and wound-size reduction was calculated by two independent investigators (Yanpeng Cao and Xin Shi) using Image-Pro Plus (version 6.0.0; Media Cybernetics Inc.). The percentage of diabetic wound closure was calculated using the equation: the percentage of diabetic wound closure = $(W0 - Wt)/A0 \times 100\%$, where "W0" indicates the initial diabetic wound area and "Wt" is the diabetic wound area at the measured timepoint ($n = 8$).

2.13. Histological Analysis. The diabetic rats were anesthetized 14 and 21 days after operation. The circular full-thickness skin tissue (about 2.5 cm in diameter) was incised at the center of the wound and then fixed within 4% paraformaldehyde for 24 hours. The fixed skin specimens were dehydrated in graded ethanol, cleared by xylene, infiltrated by paraffin wax and embedded within paraffin blocks. After cross-sections of 5 μm in thickness were prepared from paraffin blocks, slides were stained using standard protocols for H&E and MT staining for histological analysis. H&E images were captured for wound epithelization, and MT images were used for collagen contents. For H&E images, the level of reepithelialization was calculated according to following: reepithelialization (%) = (the length of the neo − epithelium across the surface of the wound/the length of wound between wound edges) × 100%. For MT images, the level of collagen deposition in the diabetic wound was measured by calculating the mean staining intensity for collagen of wound beds by the image analysis software Image-Pro Plus 6.0 software ($n = 8$).

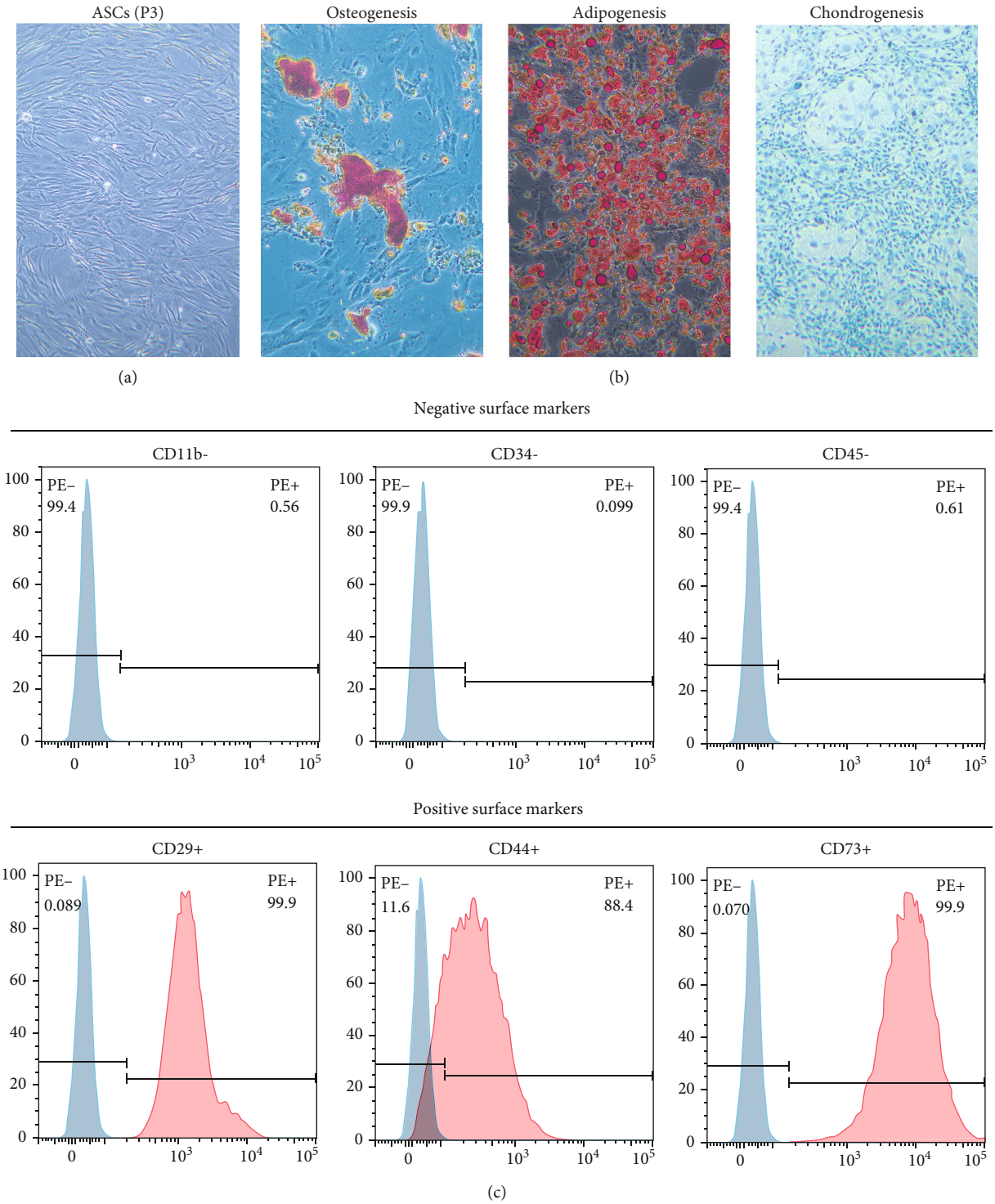

Figure 2: Isolation and identification of ADSCs. (a) The morphology of the isolated ADSCs from rat at passage 2. Bar = 100 μm. (b) Osteogenic differentiation, chondrogenic differentiation, and adipogenic differentiation of ADSCs revealed by Alizarin Red, Alcian blue, and Oil red O staining. Bar = 100 μm. (c) The expression of cell surface markers related to stem cell phenotype in ADSCs using flow cytometry analysis, which were positive for CD29, CD44, and CD73 and negative for CD11b, CD34, and CD45.

2.14. Angiogenesis Assessment. At day 7 postoperation, the diabetic rats were euthanized and skin specimens on dorsal were harvested, respectively, and the undersurface of the skin was photographed to observe the newly formed blood vessels. After that, skin specimens were fixed in 4% paraformaldehyde, immersed at 4°C in 30% sucrose overnight, and then sectioned at 20 μm on a freezing microtome. The sections were blocked with PBS containing 5% of normal

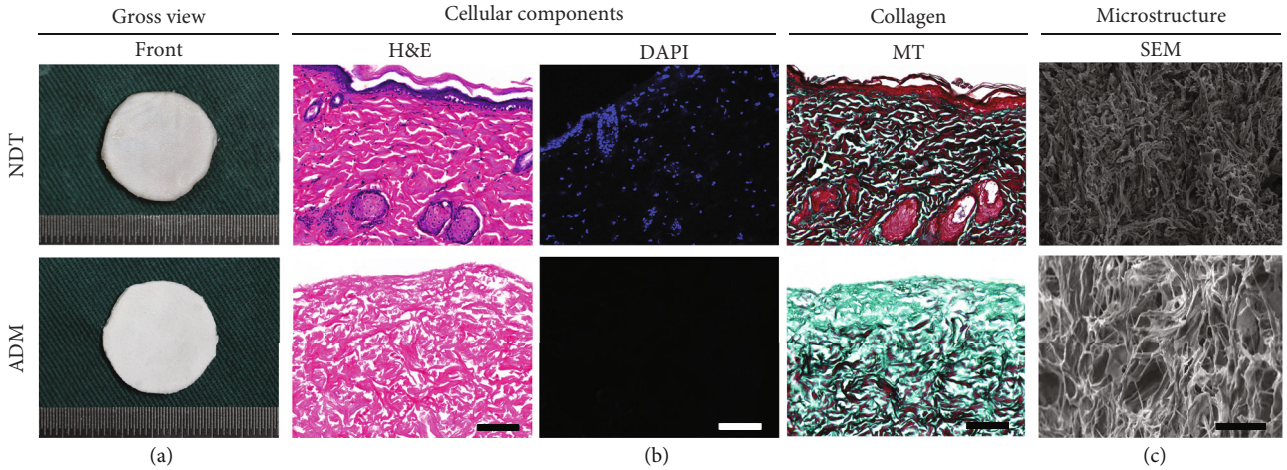

Figure 3: Appearance and morphology of ADM. (a) Gross appearance of acellular dermal matrix (ADM) membrane and natural dermis tissue (NDT). (b) Histological analysis of the ADM membrane and NDT. Sections were stained with H&E, DAPI, and MT. Bar = 100 μm. (c) Scanning electron micrographs of the ADM membrane and NDT. Bar = 100 μm.

goat serum and 0.01% of Triton X-100 for 1 hour at room temperature. After 3 washes in PBS, samples were incubated with mouse anti-CD31 antibody (ab24590, Abcam, USA) at 4°C overnight. After that, the sections were incubated with goat anti-mouse IgG H&L secondary antibody (ab150113, Abcam, USA) at room temperature for 90 min. After staining the nuclei with DAPI, these sections were captured with a fluorescence microscope (ApoTome 2, Carl Zeiss, Germany), and vessel density was quantified from at least three random visual fields per section between the wound edges using the Image-Pro Plus 6.0 software ($n = 8$).

2.15. Quantitative Real-Time Polymerase Chain Reaction (qRT-PCR). At days 7 and 14 postoperation, the diabetic rats were euthanized and skin specimens on dorsal were harvested, respectively. The total RNA of skin wound tissue was extracted using Trizol (Invitrogen, Waltham, MA, USA) according to the manufacturer's protocols. And then, cDNA was synthesized from total RNA (1 μg) using Prime ScriptTM RT Master Mix (Takara Bio Inc., Shiga, Japan) at 37°C for 30 min and 85°C for 10 s. In this study, the primer sequences used for all PCR reactions are shown in Table 1, and β-actin was used as the housekeeping gene. The expression of the genes was normalized against the housekeeping gene β-actin, and the results were quantified relative to the corresponding gene expression of ADM group, which was standardized to 1 ($n = 4$).The groups, interventions, and timepoints for evaluations are listed in Figure 1.

2.16. Statistical Analysis. All values are represented as mean ± standard deviation. The Student t-test was used for the comparison between two groups, and the one-way analysis of variance with a post hoc test was used for the comparison above two groups. A value of "$P < 0.05$" was considered statistically significant. All the statistical analyses were performed using the Statistical Package for the Social Sciences 25.0 software (SPSS, United States).

3. Results

3.1. Isolation and Identification of ADSCs. Under phase-contrast microscope, these isolated cells in the culture plate presented a spindle shape in morphology (Figure 2(a)). In addition, after osteogenic, chondrogenic, or adipogenic induction, Alizarin Red, Alcian blue, or Oil Red O images determined that the isolated cells were capable of differentiating into osteocytes, chondrocytes, or adipocytes (Figure 2(b)). Using flow cytometry analysis, we found that these isolated cells are positive for CD29, CD44, and CD73, while negative for CD11b, CD34, and CD45 (Figure 2(c)).

3.2. Appearance and Morphology of ADM. The ADM membrane was white in color with a thickness about 100 μm (Figure 3(a)). Histologically, the ADM membrane showed no cellular content in the H&E- and DAPI-stained images (Figure 3(b)). MT staining determined that the collagen content in the ADM membrane presented a similar pattern with normal dermis (Figure 3(b)). SEM images determined that the ADM well preserved the microstructure of normal dermis (Figure 3(c)).

3.3. Viability of ADSCs on the ADM under Normoxic or Hypoxic Condition. Using Live/Dead assay, most of the ADSCs on the ADM under normoxic or hypoxic condition were positive for green fluorescence (live cells), while a few of ADSCs were positive for red fluorescence (dead cells). Statistically, the viability of ADSCs on the ADM membrane cultured under normoxic or hypoxic condition was lower than that on the TCPS without significant difference (Figure 4(a)). In addition, SEM images showed that a dense layer of viable ADSCs was well attached on the outer surface of ADM membrane after normoxic culture or hypoxic culture (Figure 4(b)). These results indicated that 48 hours of hypoxia culture was harmless for ADSCs on an ADM membrane.

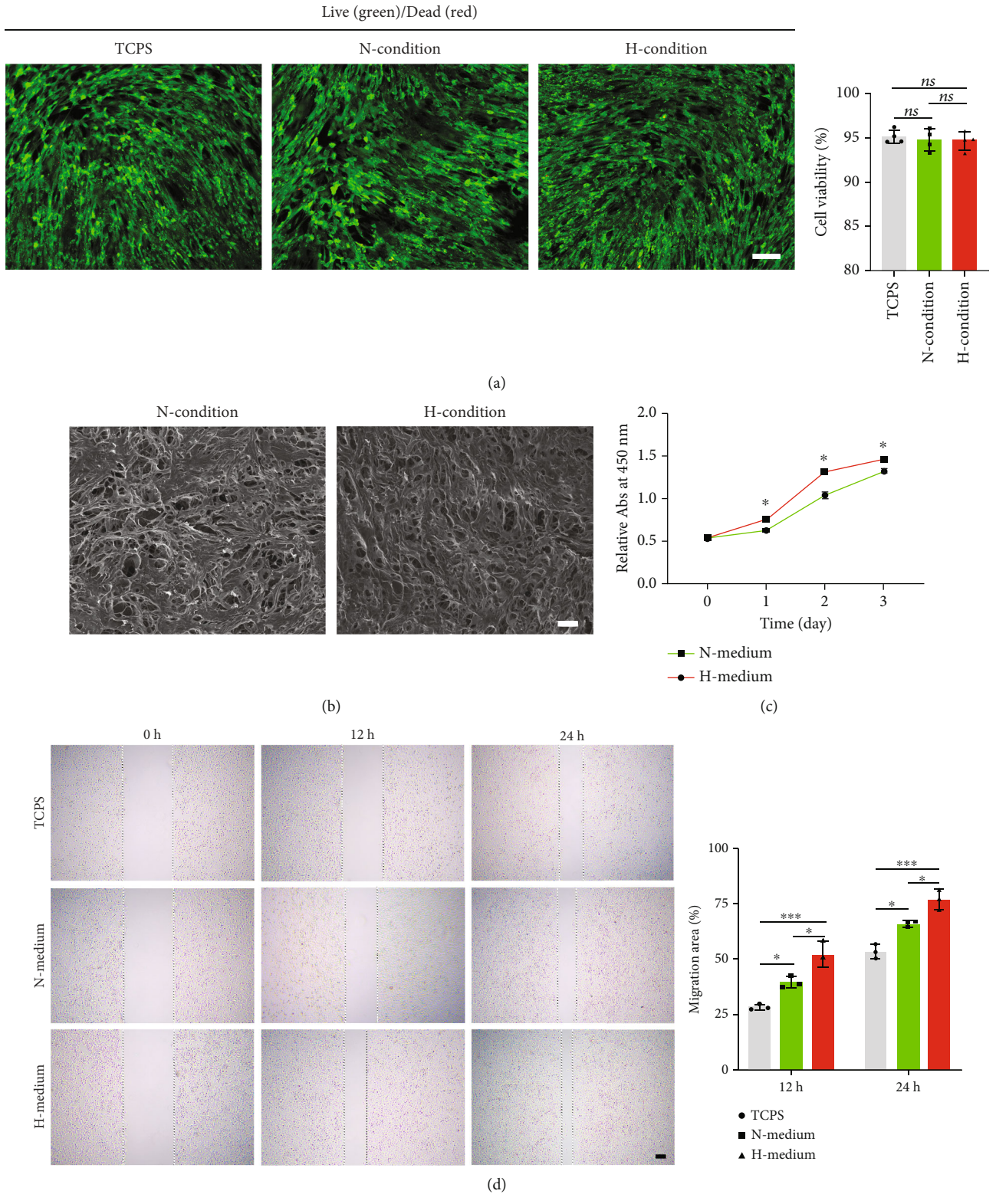

Figure 4: Continued.

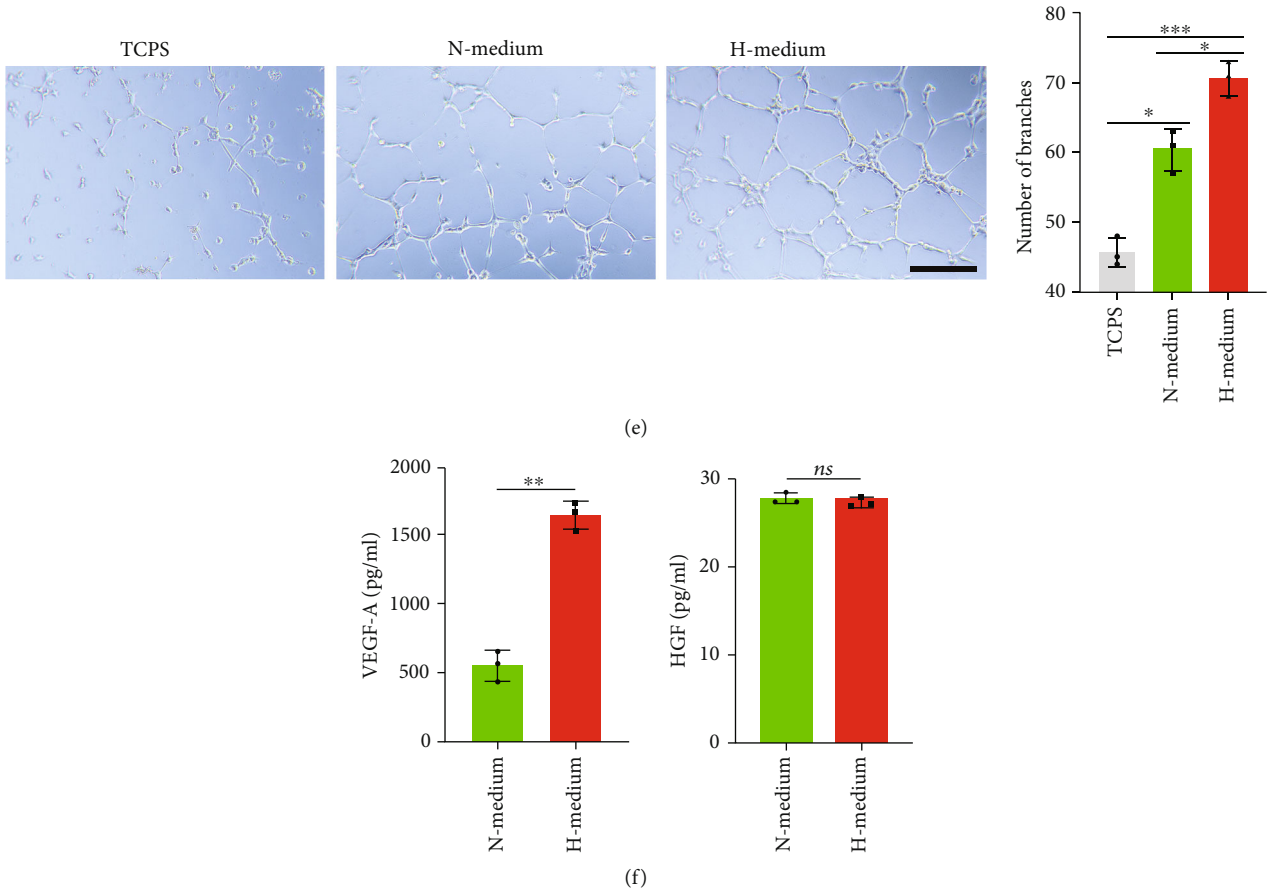

Figure 4: (a) Live/dead cell analysis for the ADM membrane on which ADSCs had been seeded and cultured under normoxic or hypoxic condition. Representative images show the live (green) and dead (red) ADSCs in the TCPS and the ADM membrane cultured under normoxic or hypoxic condition and the viability analysis for the cells on the TCPS and ADM membrane, $n = 4$ per group. (b) Scanning electron micrographs of the ADM membrane on which ADSCs had been cocultured under normoxic or hypoxic condition for 48 hours. (c) Proliferation of HUVECs influenced by H medium and N medium was evaluated with Cell Counting Kit-8 (CCK8) assay at 0,1, 2, and 3 days after cell seeding, $n = 4$ per group. (d) Representative images of scratch on HUVECs at 0, 12, and 24 hours after treated by H medium and N medium. The migration of HUVECs was significantly increased by H medium, $n = 3$ per group. (e) In vitro tube formation of HUVECs at 12 hours under the stimulation of C medium and H medium. Bar = 100 μm, $n = 3$ per group. (f) The content of angiogenic-related growth factors (VEGF-A, HGF, and FGF) in culture medium from hypoxia- or normoxia-preconditioned ADSCs determined by ELISA, the FGF content was too low to be measured. $n = 3$ per group. All data are shown as means ± standard deviation ($^*P < 0.05$, $^{**}P < 0.01$, and $^{***}P < 0.001$).

3.4. Culture Medium from Hypoxia-Preconditioned ADSCs Improves the Proliferation and Migration of HUVECs. In order to evaluate the possible effect of culture medium from hypoxia-preconditioned ADSCs, CCK8 assays were performed. As showed in Figure 4(c), CCK8 assay showed that the HUVECs cultured within the H medium showed significantly higher absorption than the HUVECs cultured within the N medium at 1, 2, and 3 days ($P < 0.05$ for all). This result indicates that culture medium from hypoxia-preconditioned ADSCs could significantly stimulate the proliferation of HUVECs.

The migration-promoting effect of culture medium from hypoxia-preconditioned ADSCs was confirmed by wound healing assays. As showed in Figure 4(d), H medium and N medium both facilitated wound closure at 12 hours or 24 hours. The percentage of the migration area at 12 hours or 24 hours was significantly larger after treatment with H medium ($P < 0.05$ for all). This result implied that culture medium from hypoxia-preconditioned ADSCs could dramatically induce the migration of HUVECs.

3.5. Culture Medium from Hypoxia-Preconditioned ADSCs Stimulates Angiogenesis In Vitro. In order to evaluate the effect of culture medium from hypoxia-preconditioned ADSCs on angiogenic capacity, tube formation assays were performed to analyze the number of branches formed by HUVECs. As showed in Figure 4(e), the number of branches in the H medium group was significantly higher than that of N medium group ($P < 0.05$). This outcome indicates that culture medium from hypoxia-preconditioned ADSCs could facilitate angiogenesis in vitro.

3.6. Culture Medium from Hypoxia-Preconditioned ADSCs Contains More VEGF-A. To comparatively evaluate the

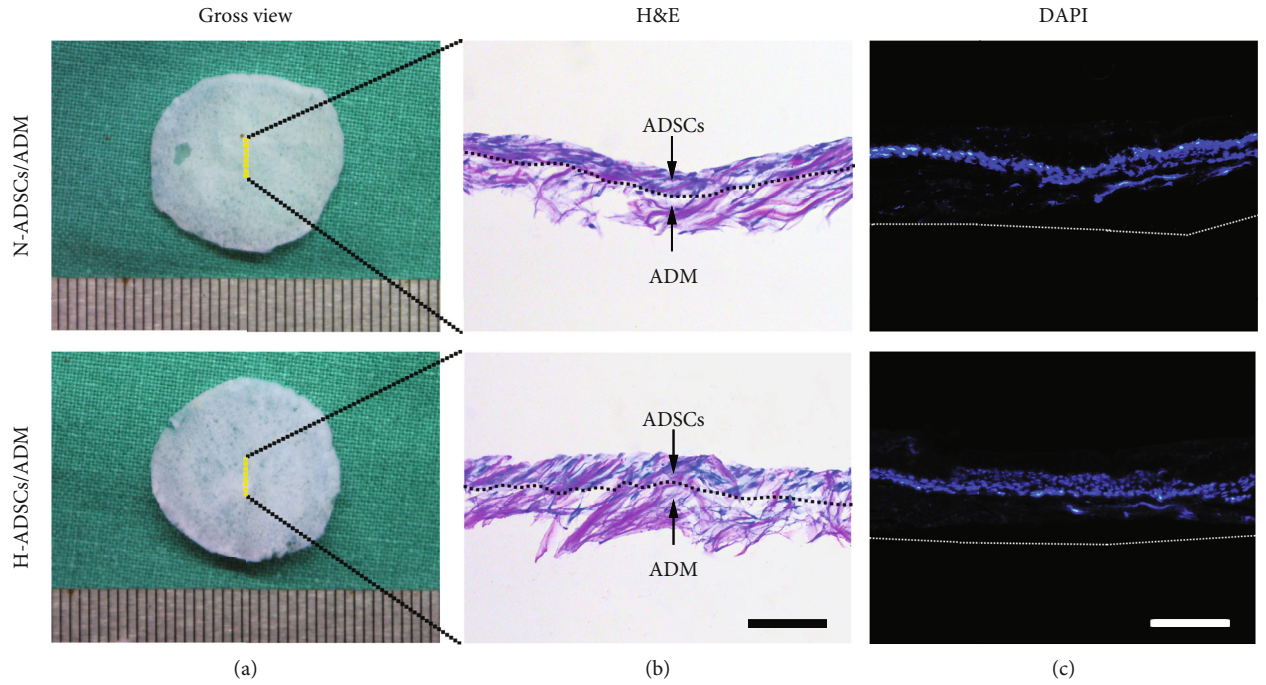

Figure 5: Morphological appearance of H-ADSCs/ADM. (a) Gross appearance, (b) histological morphology, and (c) DAPI images of the N-ADSCs/ADM membrane and the H-ADSCs/ADM membrane. The dotted line in (b) represents the boundary between the ADSCs and the ADM membrane. The dotted line represents the bottom of the ADM membrane. Bar = 100 mm.

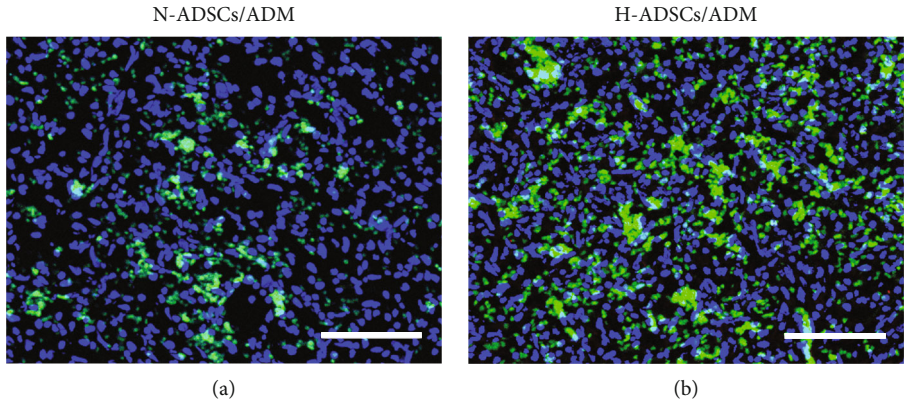

Figure 6: Hypoxia-precondition enhances the survival ability of ADSCs at DFU healing site. ADSC tracing in vivo at postoperative day 14. (a) Skin wound treated with N-ADSCs/ADM membrane with DiO labeling. (b) Skin wound treated with H-ADSCs/ADM membrane with DiO labeling. Bar = 100 mm.

content of angiogenic-related growth factors in culture medium from hypoxia- or normoxia-preconditioned ADSCs, ELISA assay was performed. As depicted in Figure 4(f), culture medium from hypoxia-preconditioned ADSCs contains more VEGF-A than culture medium from normoxia-preconditioned ADSCs ($P < 0.05$). As for HGF, no significant differences were found between the culture medium from hypoxia-preconditioned ADSCs and the culture medium from normoxia-preconditioned ADSCs. Regrettably, the FGF content was too low to be measured.

3.7. Morphological Appearance of H-ADSCs/ADM. Both the H-ADSCs/ADM and the N-ADSCs/ADM showed a white membranous membrane in gross appearance (Figure 5(a)). Histologically, a dense layer of ADSCs was attached on the surface of the ADM membrane with a few cells entering the deeper interstices of the ADM (Figure 5(b)). In addition, as showed in DAPI images of H-ADSCs/ADM or N-ADSCs/ADM, a dense layer of viable ADSCs was well attached on the outer surface of ADM (Figure 5(c)).

3.8. In Vivo Cell Tracking Analysis. There are more DiO-labeled ADSCs at the H-ADSCs/ADM-treated DFU healing site compared to the N-ADSCs/ADM-treated DFU healing site at postoperative day 14 (Figure 6), which implied that the hypoxia-precondition could enhance the survival ability of ADSCs at DFU healing site.

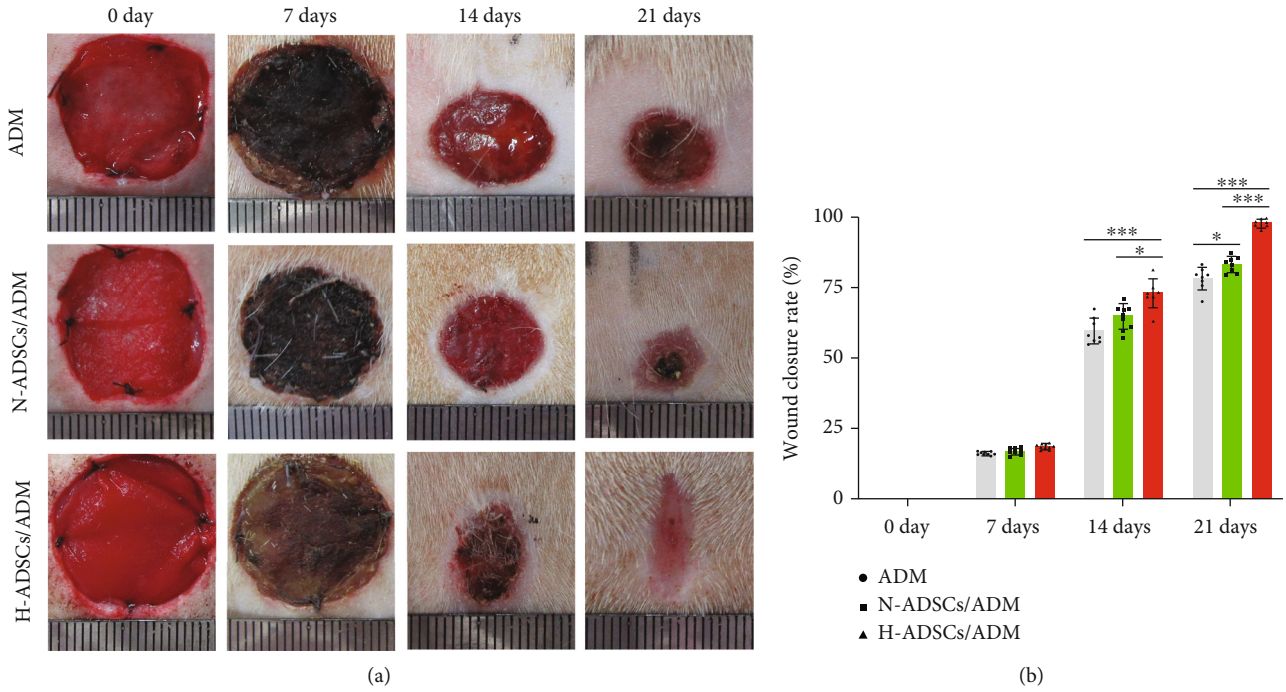

Figure 7: H-ADSCs/ADM facilitating diabetic wound healing. (a) Photos of the skin wound healing in diabetic rat among the ADM, N-ADSCs/ADM, and H-ADSCs/ADM groups at postoperative 0, 7, 14, and 21 days. (b) Statistical analysis of wound area among the three groups at postoperative 0, 7, 14, and 21 days, $n = 8$ per group. All data are shown as means ± standard deviation ($^{*}P < 0.05$, $^{**}P < 0.01$, and $^{***}P < 0.001$).

3.9. Wound Closure Analysis. As showed in gross images of the wounds (Figure 7(a)), there are no apparent complications or excessive scarring in any of the conditions at any timepoint. New epidermis grew from the edge of skin wound and gradually extended to the center of skin wound, resulting in the reduction of wound area. The rats in the H-ADSCs/ADM group showed an almost complete wound closure after 21 days. The result of wound closure quantification (Figure 7(b)) showed that there are no differences among groups at days 7, while some differences were observed at day 14. Specifically, at day 21, the H-ADSCs/ADM group showed a significantly ($P < 0.05$) higher wound closure than the other groups ($P < 0.05$ for all).

3.10. Histological Analysis. The extent of reepithelialization of skin wounds was evaluated on the images of H&E-stained sections (Figure 8(a)). The rats in the H-ADSCs/ADM group or N-ADSCs/ADM group showed significantly higher value in the reepithelialization rate than that of the ADM group at postoperative day 14 or 21. In addition, the reepithelialization rate of the H-ADSCs/ADM group was significantly higher than the N-ADSCs/ADM group at postoperative day 21 (Figure 8(b)).

The collagen deposition and maturation of healed skin wounds were evaluated according to the images of MT-stained sections. As shown in Figure 8(a), on postoperative day 14, extensive deposition of collagen fibers could be seen in the wound bed of the H-ADSCs/ADM group or N-ADSCs/ADM group, while in the ADM group, lots of immature collagen was formed surrounding the skin fibroblasts in the ADM group. On postoperative day 21, more collagen fibers in the H-ADSCs/ADM group were deposited at the wound healing site with a pattern of thick and wavy appearance compared to the N-ADSCs/ADM and ADM groups. More importantly, the hair follicles were regenerated at the wounds of the H-ADSCs/ADM group, when compared with the N-ADSCs/ADM and ADM groups. Quantitatively, the collagen content in the H-ADSCs/ADM group was significantly higher than that of N-ADSCs/ADM and ADM groups at postoperative day 14 or 21 (Figure 8(b)). These results implied that H-ADSCs/ADM was capable of enhancing the repair of diabetic wounds.

3.11. H-ADSCs/ADM Membrane Stimulating Angiogenesis in Diabetic Wounds. Angiogenesis in the DFUs was characterized by the immunofluorescence staining of CD31, a transmembrane protein expressed at the early stage of vascular development. As showed in Figure 9(a), the quantity of CD31 significantly increased in the wounds treated with the H-ADSCs/ADM membrane when compared to that of the N-ADSCs/ADM and ADM groups. The quantification analysis of CD31 showed that significantly more blood vessels were formed in wound bed of the H-ADSCs/ADM group compared to the N-ADSCs/ADM and ADM groups, and significantly more vessels were detected in the wounds of the N-ADSCs/ADM group when compared with the wounds in the ADM group (Figure 9(b)).

3.12. H-ADSCs/ADM Membrane Inhibiting the Gene Expression of Proinflammatory Cytokine in Diabetic Wounds. The expression of proinflammatory cytokines (IL-1β, IL-6, and NF-κB) in the wound tissues of the ADM, N-

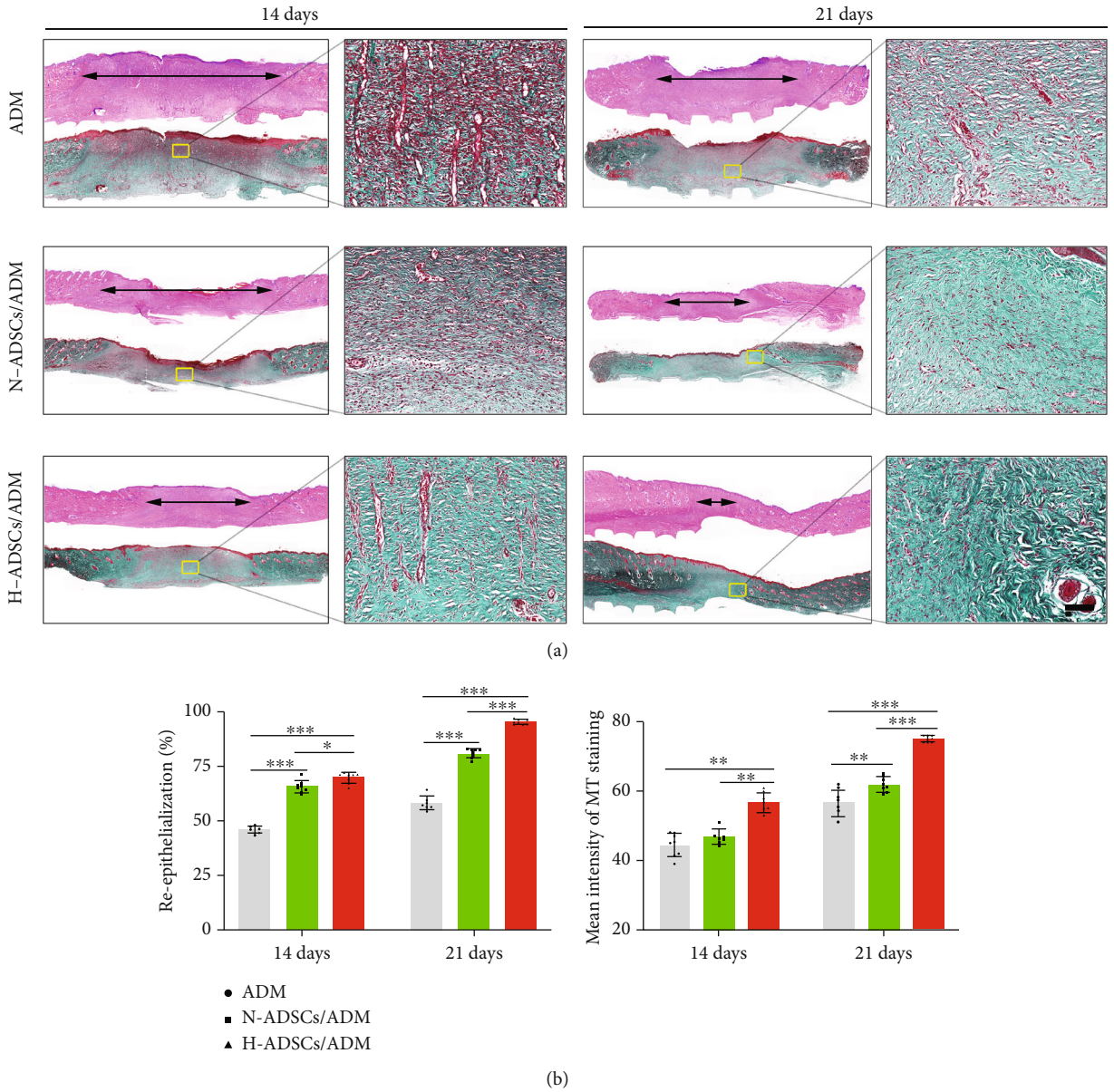

Figure 8: H-ADSCs/ADM facilitating reepithelialization and collagen deposition in diabetic wounds. (a) The images of H&E- and MT-stained sections in the ADM, N-ADSCs/ADM, and H-ADSCs/ADM groups at 14 or 21 days after the operation. "Double-headed black arrows" mean the edges of the scars. Bar = 100 μm. (b) Quantitative analysis of the reepithelialization extent and the mean intensity of MT staining in the histological sections of the ADM, N-ADSCs/ADM, and H-ADSCs/ADM groups, $n = 8$ per group. All data are shown as means ± standard deviation ($^{*}P < 0.05$, $^{**}P < 0.01$, and $^{***}P < 0.001$).

ADSCs/ADM, and H-ADSCs/ADM groups was evaluated by qRT-PCR. Our results showed that H-ADSCs/ADM membrane significantly downregulated the expression of IL-1β, IL-6, and NF-κB compared with the ADM and N-ADSCs/ADM groups at 7 days postwounding. Additionally, at 14 days postwounding, the expression of IL-1β, IL-6, and NF-κB in H-ADSCs/ADM groups was obviously lower than the other two groups (Figure 10).

4. Discussion

DFUs are a serious complication of diabetes, which is characterized by impaired vascular function, limited angiogenesis, and chronic inflammation [25, 26]. Direct MSC injections on treating DFUs are far from satisfactory in clinical practice, as this therapy neither protects nor localizes the injected cell suspension at the chronic ulcer site [27]. Meanwhile, most of injected MSCs gradually perished within several days due to senescence or apoptosis [28]. ADM has the potential to act as excellent cell delivery vehicles, considering it is highly biomimetic to native dermal tissue, has low immunogenicity, and suitable for stem cell attachment and proliferation [29, 30]. Hypoxia culture has significantly enhanced effects on the survival ability of in vitro cultured MSCs [28], indicating this culture mode is a suitable way for inhibiting the senescence

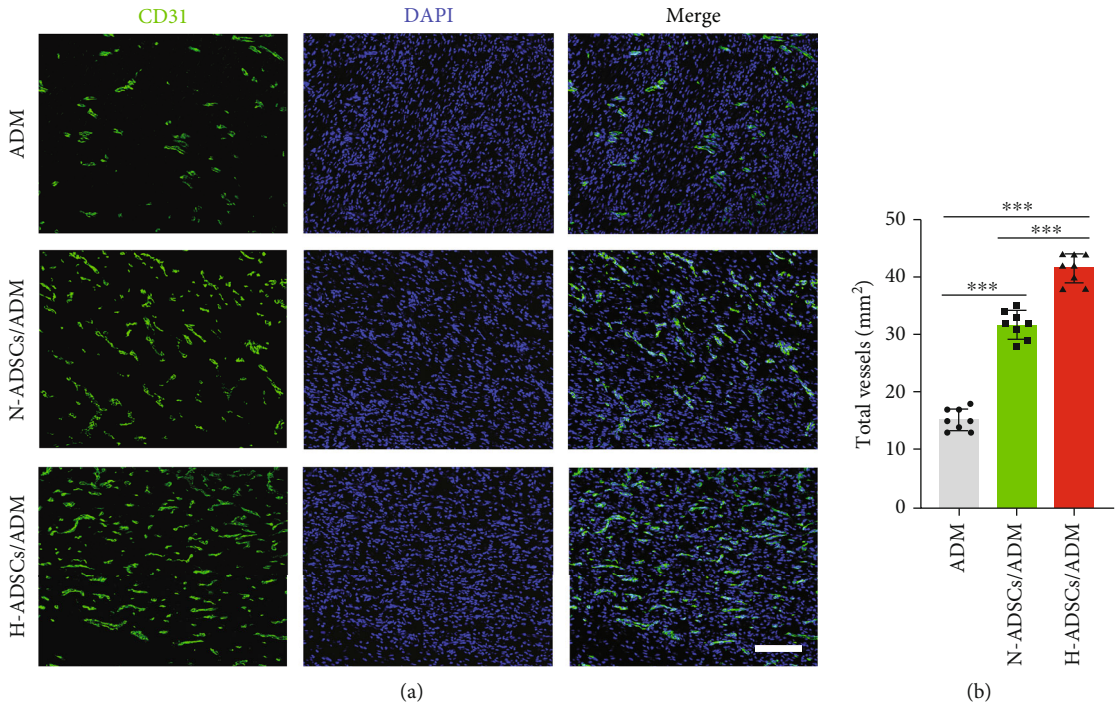

Figure 9: H-ADSCs/ADM membrane stimulating angiogenesis in diabetic wounds. (a) Immunofluorescence analysis of sections for CD31 showed the formation of microvessels in the ADM, N-ADSCs/ADM, and H-ADSCs/ADM groups. Bar = 100 μm. (b) CD31 area quantification showed the quantitative analysis of the number of total blood vessels in wounds at day 7 postoperation, $n = 8$ per group. All data are shown as means ± standard deviation ($^{*}P < 0.05$, $^{**}P < 0.01$, and $^{***}P < 0.001$).

or apoptosis of transplanted cells. Therefore, in the current study, we, respectively, culture ADSCs on an ADM membrane under a hypoxia or normoxia condition to construct two kinds of tissue-engineered dressing membranes (H-ADSCs/ADM and N-ADSCs/ADM) and then comparatively evaluated their efficacy on DFU healing using a diabetic rat model. The in vivo results indicated that the transplanted cells in the H-ADSCs/ADM can survive longer at the chronic ulcer site, consequently improve angiogenesis, inhibit inflammation, and increase extracellular matrix remodeling, eventually accelerating DFU closure. This study provides a new covering graft for the treatment of DFU.

Currently, the stem cells isolated from adipose (ADSCs), bone marrow (BMSCs), or umbilical cord blood (UCB-MSCs) have seen success in accelerating diabetic wound healing. Among them, ADSCs are the most commonly used cell source, owing to its advantages of relative abundance and easy accessibility [16, 31]. As for ADSC-based strategies for wound healing, extending the survival time of transplanted cells and improving its function in stimulating angiogenesis at the chronic ulcer site are the most significant challenges. Prior studies have shown that hypoxia pretreatment can increase MSC survival and improve its function in stimulating angiogenesis [22, 28, 32]. Therefore, in the presented study, we engineered a dressing membrane by culturing ADSCs on an ADM under a hypoxia condition. In consideration that appropriate hypoxic culture conditions are of great significance for promoting MSC survival and stimulating the paracrine activities of MSCs, we firstly explored the optimal culture conditions by selecting a suitable oxygen tension. ADSCs have been shown to reside in a lower (1-5%) oxygen tension than that normally used in ambient cell culture (20-21%) [33]. Due to the lack of vascularization, in the early period of DFU healing, the oxygen tension may be lower than 4% [34]. Thus, we selected 1% O_2 oxygen tension as hypoxia culture parameter for constructing the required dressing membrane. Stubbs et al. found that compared to normoxic culture condition, hypoxic culture condition could improve the survival of ADSCs [35]. In addition, Zhang et al. revealed that hypoxia-cultured ADSCs secreted more angiogenic factors than the normoxic cultured ADSCs [36]. Another study showed that the supernatant from hypoxia-preconditioned ADSCs was capable of improving endothelial cell survival and angiogenesis capacity [35]. Our in vitro study also showed that the supernatant from hypoxia-preconditioned ADSCs contains more VEGF-A and exhibited better function in promoting the proliferation, migration, and tube formation of HUVECs than that from ADSCs under normoxia.

Despite the difference in preparing covering grafts for the treatment of DFU, the results of the in vitro study showed that both methods had similar cell loading efficiency and viability. After cell incubation, both hypoxia culture and normoxia culture resulted in a dense layer of viable cells on the outer surface of ADM. This result indicates that both culture methods can be a harmless approach for culturing ADSCs on an ADM membrane. More importantly, the supernatant from hypoxia culture showed significantly higher bioactive molecules associated with angiogenesis compared with the supernatant from normoxia culture, indicating that hypoxia

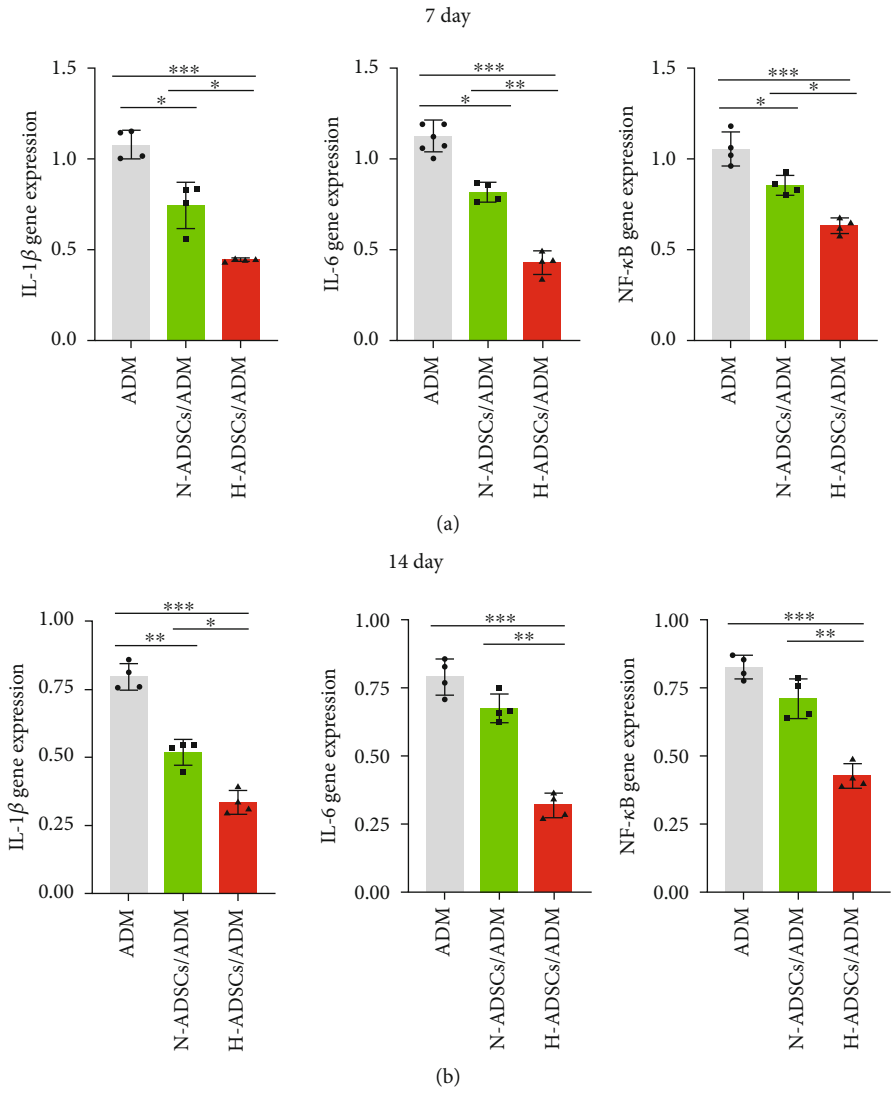

Figure 10: H-ADSCs/ADM membrane inhibiting the gene expression of proinflammatory cytokine in diabetic wounds. The expression of proinflammatory cytokines (IL-1β, IL-6, and NF-κB) in the wound tissues of the ADM, N-ADSCs/ADM, and H-ADSCs/ADM groups was evaluated by qRT-PCR. The gene expression levels of IL-1β, IL-6, and NF-κB at (a) 7 days and (b) 14 days, $n = 4$ per group. All data are shown as means ± standard deviation ($^*P < 0.05$, $^{**}P < 0.01$, and $^{***}P < 0.001$).

culture was an effective means for stimulating ADSCs secreting angiogenesis-related molecules.

In this study, we determined that the streptozotocin-induced diabetic rats treated with the H-ADSCs/ADM showed a significantly better healing speed in skin wound closure than the rats treated with N-ADSCs/ADM, as characterized by the improved angiogenesis, optimized local inflammation, and increased extracellular matrix remodeling. The reasons for this healing difference in skin wound may be that (1) skin wound closure is proceeded by the initial inflammatory phase, middle proliferative phase, and last remodeling phase, which involves multiple cells, growth factors, and extracellular signals [37]. In the case of diabetes, the skin wounds are usually characterized by continuous inflammation, cell dysfunction, and limited angiogenesis, resulting in delayed wound healing [16]. Owing to the ability of ADSCs differentiating into different lineages and secreting angiogenic or anti-inflammatory molecules, the potential of ADSCs for wound healing has been shown in several studies [11, 12]. This may be the important reason why the skin wound in the N-ADSCs/ADM and H-ADSCs/ADM groups closed significantly quicker than the ADM group. (2) The implanted ADSCs in the H-ADSCs/ADM could tolerate local hypoxia better than the ADSCs in the N-ADSCs/ADM and survived better at the chronic ulcer site. These survived ADSCs at the wound site could release more and longer biomolecules to optimize local immune environment [38, 39], as well as stimulating angiogenesis, thus resulting in an improvement of wound healing. In addition, the more survived ADSCs at the wound lesion may serve as a cell source that can directly differentiate into endothelial cells or fibrocytes, thus enhancing the formation of granulation tissues at the skin wound. Regrettably, we still need more in-depth studies to prove our explanations.

This study has confirmed that H-ADSCs/ADM is a novel covering graft for treating diabetic wounds. However, there remain several limitations. Firstly, owing to the lack of the technology, it is hard to measure the exact oxygen concentration at the H-ADSCs/ADM-mediated DFU healing site. In this study, we selected 1% O_2 oxygen tension as hypoxia culture parameter for constructing the H-ADSCs/ADM membrane. Logically speaking, this culture parameter may be inaccurate. Next step, we should seek a suitable technology to accurately measure the exact oxygen concentration at H-ADSCs/ADM-mediated DFU healing site and then used this oxygen concentration as a reference to optimize the hypoxia culture parameters. Secondly, our animal experiments were conducted in streptozotocin-induced diabetic rats, which cannot completely imitate the type 2 diabetes observed in the clinic. Thus, the H-ADSCs/ADM membrane of this study may not be simply translated to treat DFU of humans. In the next step, diabetic rats with type 2 diabetes should be used to test the function of our graft again. Thirdly, given the secretion of angiogenic and anti-inflammatory molecules, the implanted ADSCs with the potential of stimulating tumor growth cannot be ignored in clinical setting. Despite these limitations, this study provides a basis for the clinical application of the H-ADSCs/ADM membrane in the treatment of diabetic wound.

5. Conclusion

In summary, a novel tissue-engineered dressing membrane (H-ADSCs/ADM) was constructed by culturing ADSCs on an ADM membrane under a hypoxia condition. This study indicated that ADM is an ideal biomaterial for ADSC delivery in a wound healing scenario. Additionally, in vitro results showed that the ADSCs in the ADM cultured under a hypoxia condition secreted more VEGF-A, and their culture medium presented better properties in promoting the proliferation, migration, and tube formation of HUVECs. In vivo results showed hypoxia-culture mode could prolong the cell survival time of H-ADSCs/ADM membrane at the chronic ulcer site, consequently improve angiogenesis, inhibit inflammation, and increase extracellular matrix remodeling, eventually accelerating DFU closure. This study showed that H-ADSCs/ADM membrane may offer innovative strategies for DFU treatment in the clinic.

Data Availability

The raw data supporting the conclusions of this article will be made available by the authors, without under reservation.

Conflicts of Interest

The authors declare that the research was conducted in the absence of any commercial or financial relationships that could be construed as a potential conflict of interest.

Authors' Contributions

J L contributed to conceptualization and supervision. W Z, Y-P C, X S, and X Z performed methodology and validation. X S, W Z, X Z, and Y-P C completed data curation and analysis. X S and C C contributed to writing—original draft preparation. Y-P C, W Z, and C C contributed to writing—review and editing. J L did funding acquisition. All authors have read and agreed to the published version of the manuscript.

Acknowledgments

This work was supported by the Natural Science Foundation of Hunan Province, China (2017JJ2006), Foundation of Bureau of Science and Technology of Chenzhou, China (ZDYF2020023), Innovative Project of Chenzhou No. 1 People's Hospital, China (XZ201735), and Foundation of Bureau of Science and Technology of Chenzhou, China (lcy12021009).

References

[1] D. G. Armstrong, A. J. M. Boulton, and S. A. Bus, "Diabetic foot ulcers and their recurrence," *The New England Journal of Medicine*, vol. 376, no. 24, pp. 2367–2375, 2017.

[2] M. Kerr, E. Barron, P. Chadwick et al., "The cost of diabetic foot ulcers and amputations to the National Health Service in England," *Diabetic Medicine*, vol. 36, no. 8, pp. 995–1002, 2019.

[3] J. Z. Lim, N. S. Ng, and C. Thomas, "Prevention and treatment of diabetic foot ulcers," *Journal of the Royal Society of Medicine*, vol. 110, no. 3, pp. 104–109, 2017.

[4] N. Singh, D. G. Armstrong, and B. A. Lipsky, "Preventing foot ulcers in patients with diabetes," *Journal of the American Medical Association*, vol. 293, no. 2, pp. 217–228, 2005.

[5] E. Everett and N. Mathioudakis, "Update on management of diabetic foot ulcers," *Annals of the New York Academy of Sciences*, vol. 1411, no. 1, pp. 153–165, 2018.

[6] Y. Cao, X. Gang, C. Sun, and G. Wang, "Mesenchymal stem cells improve healing of diabetic foot ulcer," *Journal Diabetes Research*, vol. 2017, p. 9328347, 2017.

[7] S. N. Dash, N. R. Dash, B. Guru, and P. C. Mohapatra, "Towards reaching the target: clinical application of mesenchymal stem cells for diabetic foot ulcers," *Rejuvenation Research*, vol. 17, no. 1, pp. 40–53, 2014.

[8] Q. Wu, B. Chen, and Z. Liang, "Mesenchymal stem cells as a prospective therapy for the diabetic foot," *Stem Cells International*, vol. 2016, Article ID 4612167, 18 pages, 2016.

[9] S. M. Becerra-Bayona, V. A. Solarte-David, C. L. Sossa et al., "Mesenchymal stem cells derivatives as a novel and potential therapeutic approach to treat diabetic foot ulcers," *Endocrinology, Diabetes & Metabolism Case Reports*, vol. 2020, 2020.

[10] A. Uccelli, L. Moretta, and V. Pistoia, "Mesenchymal stem cells in health and disease," *Nature Reviews. Immunology*, vol. 8, no. 9, pp. 726–736, 2008.

[11] M. Gadelkarim, A. I. Abushouk, E. Ghanem, A. M. Hamaad, A. M. Saad, and M. M. Abdel-Daim, "Adipose-derived stem cells: effectiveness and advances in delivery in diabetic wound healing," *Biomedicine & Pharmacotherapy*, vol. 107, pp. 625–633, 2018.

[12] W. U. Hassan, U. Greiser, and W. Wang, "Role of adipose-derived stem cells in wound healing," *Wound Repair and Regeneration*, vol. 22, no. 3, pp. 313–325, 2014.

[13] Y. Qi, J. Ma, S. Li, and W. Liu, "Applicability of adipose-derived mesenchymal stem cells in treatment of patients with type 2 diabetes," *Stem Cell Research & Therapy*, vol. 10, no. 1, p. 274, 2019.

[14] T. Weng, W. Zhang, Y. Xia et al., "3D bioprinting for skin tissue engineering: current status and perspectives," *Journal of Tissue Engineering*, vol. 12, 2021.

[15] Á. Sierra-Sánchez, K. H. Kim, G. Blasco-Morente, and S. Arias-Santiago, "Cellular human tissue-engineered skin substitutes investigated for deep and difficult to heal injuries," *NPJ Regenerative Medicine*, vol. 6, no. 1, p. 35, 2021.

[16] H. Cho, M. R. Blatchley, E. J. Duh, and S. Gerecht, "Acellular and cellular approaches to improve diabetic wound healing," *Advanced Drug Delivery Reviews*, vol. 146, pp. 267–288, 2019.

[17] L. Tognetti, E. Pianigiani, F. Ierardi et al., "The use of human acellular dermal matrices in advanced wound healing and surgical procedures: state of the art," *Dermatologic Therapy*, vol. 34, no. 4, article e14987, 2021.

[18] C. Dai, S. Shih, and A. Khachemoune, "Skin substitutes for acute and chronic wound healing: an updated review," *The Journal of Dermatological Treatment*, vol. 31, no. 6, pp. 639–648, 2020.

[19] P. B. Milan, N. Lotfibakhshaiesh, M. T. Joghataie et al., "Accelerated wound healing in a diabetic rat model using decellularized dermal matrix and human umbilical cord perivascular cells," *Acta Biomaterialia*, vol. 45, pp. 234–246, 2016.

[20] J. Chu, P. Shi, X. Deng et al., "Dynamic multiphoton imaging of acellular dermal matrix scaffolds seeded with mesenchymal stem cells in diabetic wound healing," *Journal of Biophotonics*, vol. 11, no. 7, article e201700336, 2018.

[21] X. Hu, R. Wu, L. A. Shehadeh et al., "Severe hypoxia exerts parallel and cell-specific regulation of gene expression and alternative splicing in human mesenchymal stem cells," *BMC Genomics*, vol. 15, no. 1, p. 303, 2014.

[22] J. Beegle, K. Lakatos, S. Kalomoiris et al., "Hypoxic preconditioning of mesenchymal stromal cells induces metabolic changes, enhances survival, and promotes cell retention in vivo," *Stem Cells*, vol. 33, no. 6, pp. 1818–1828, 2015.

[23] M. Zayed, K. Iohara, H. Watanabe, M. Ishikawa, M. Tominaga, and M. Nakashima, "Characterization of stable hypoxia-preconditioned dental pulp stem cells compared with mobilized dental pulp stem cells for application for pulp regenerative therapy," *Stem Cell Research & Therapy*, vol. 12, no. 1, p. 302, 2021.

[24] L. Chen, Y. Xu, J. Zhao et al., "Conditioned medium from hypoxic bone marrow-derived mesenchymal stem cells enhances wound healing in mice," *PLoS One*, vol. 9, no. 4, article e96161, 2014.

[25] V. Falanga, "Wound healing and its impairment in the diabetic foot," *Lancet*, vol. 366, no. 9498, pp. 1736–1743, 2005.

[26] O. Ochoa, F. M. Torres, and P. K. Shireman, "Chemokines and diabetic wound healing," *Vascular*, vol. 15, no. 6, pp. 350–355, 2007.

[27] S. Baldari, G. Di Rocco, M. Piccoli, M. Pozzobon, M. Muraca, and G. Toietta, "Challenges and strategies for improving the regenerative effects of mesenchymal stromal cell-based therapies," *International Journal of Molecular Sciences*, vol. 18, no. 10, p. 2087, 2017.

[28] Y. Yang, E. H. Lee, and Z. Yang, "Hypoxia conditioned mesenchymal stem cells in tissue regeneration application," *Tissue Engineering. Part B, Reviews*, 2022.

[29] H. Xing, H. Lee, L. Luo, and T. R. Kyriakides, "Extracellular matrix-derived biomaterials in engineering cell function," *Biotechnology Advances*, vol. 42, p. 107421, 2020.

[30] X. Guo, D. Mu, and F. Gao, "Efficacy and safety of acellular dermal matrix in diabetic foot ulcer treatment: a systematic review and meta-analysis," *International Journal of Surgery*, vol. 40, pp. 1–7, 2017.

[31] G. T. Kirby, S. J. Mills, A. J. Cowin, and L. E. Smith, "Stem cells for cutaneous wound healing," *BioMed Research International*, vol. 2015, Article ID 285869, 2015.

[32] X. Wan, M. K. Xie, H. Xu et al., "Hypoxia-preconditioned adipose-derived stem cells combined with scaffold promote urethral reconstruction by upregulation of angiogenesis and glycolysis," *Stem Cell Research & Therapy*, vol. 11, no. 1, 2020.

[33] J. R. Choi, K. W. Yong, and W. K. Z. Wan Safwani, "Effect of hypoxia on human adipose-derived mesenchymal stem cells and its potential clinical applications," *Cellular and Molecular Life Sciences*, vol. 74, no. 14, pp. 2587–2600, 2017.

[34] K. Kang, J. B. Chuai, B. D. Xie et al., "Mesenchymal stromal cells from patients with cyanotic congenital heart disease are optimal candidate for cardiac tissue engineering," *Biomaterials*, vol. 230, p. 119574, 2020.

[35] S. L. Stubbs, S. T. Hsiao, H. M. Peshavariya, S. Y. Lim, G. J. Dusting, and R. J. Dilley, "Hypoxic preconditioning enhances survival of human adipose-derived stem cells and conditions endothelial cells in vitro," *Stem Cells and Development*, vol. 21, no. 11, pp. 1887–1896, 2012.

[36] W. Zhang, L. Liu, Y. Huo, Y. Yang, and Y. Wang, "Hypoxia-pretreated human MSCs attenuate acute kidney injury through enhanced angiogenic and antioxidative capacities," *BioMed Research International*, vol. 2014, Article ID 462472, 10 pages, 2014.

[37] P. Martin, "Wound healing–aiming for perfect skin regeneration," *Science*, vol. 276, no. 5309, pp. 75–81, 1997.

[38] H. Shen, I. Kormpakis, N. Havlioglu et al., "The effect of mesenchymal stromal cell sheets on the inflammatory stage of flexor tendon healing," *Stem Cell Research & Therapy*, vol. 7, no. 1, p. 144, 2016.

[39] P. Sukho, J. W. Hesselink, N. Kops, J. Kirpensteijn, F. Verseijden, and Y. M. Bastiaansen-Jenniskens, "Human mesenchymal stromal cell sheets induce macrophages predominantly to an anti-inflammatory phenotype," *Stem Cells and Development*, vol. 27, no. 13, pp. 922–934, 2018.

Hindawi
Stem Cells International
Volume 2022, Article ID 6342594, 17 pages
https://doi.org/10.1155/2022/6342594

Research Article

Administration of Melatonin in Diabetic Retinopathy Is Effective and Improves the Efficacy of Mesenchymal Stem Cell Treatment

Samraa H. Abdel-Kawi[1] **and Khalid S. Hashem**[2]

[1]*Department of Medical Histology and Cell Biology, Faculty of Medicine, Beni-Suef University, Beni-Suef, Egypt 62511*
[2]*Department of Biochemistry and Chemistry of Nutrition, Faculty of Veterinary Medicine, Beni-Suef University, Beni-Suef, Egypt 62511*

Correspondence should be addressed to Khalid S. Hashem; khaled.mohamed2@vet.bsu.edu.eg

Received 23 October 2021; Accepted 26 March 2022; Published 11 April 2022

Academic Editor: Yi Zhang

Stem cell transplantation is a promising therapeutic technique for the treatment of a variety of diseases; nevertheless, stem cell therapy may not always work as well as it could. The goal of this study was to test the hypothesis that employing a powerful antioxidant like melatonin improves stem cell transplantation success and potentiates stem cell function in the therapy of diabetic retinopathy. For this purpose, 50 adult male rats were divided into the following: control group: this group received 0.5 ml of 0.1 M of sodium citrate buffer (pH = 4.5) (intraperitoneal (I.P.)). The confirmed diabetic rats were divided into 4 groups: diabetic group: confirmed diabetic rats received no treatments with a regular follow of the blood glucose profile for 8 weeks; melatonin group: confirmed diabetic rats received melatonin (5 mg/kg/day); stem cell group: the confirmed diabetic rats were given intravitreal injection of stem cells (2 μl cell suspension of stem cells (3×10^4 cells/μl)); and melatonin+stem cell group: confirmed diabetic rats received melatonin (5 mg/kg/day), orally once daily for 8 weeks, and 2 μl cell suspension of stem cells (3×10^4 cells/μl) was carefully injected into the vitreous cavity. Our results showed that administration of melatonin and/or stem cell restored the retinal oxidative/antioxidant redox and reduced retinal inflammatory mediators. Coadministration of melatonin and stem cells enhanced the number of transplanted stem cells in the retinal tissue and significantly reduced retinal BDEF, VEGF, APOA1, and RBP4 levels as compared to melatonin and/or stem alone. We may conclude that rats treated with melatonin and stem cells had their retinal oxidative/antioxidant redox values restored to normal and their histological abnormalities reduced. These findings support the hypothesis that interactions with the BDEF, VEGF, APOA1, and RBP4 signaling pathways are responsible for these effects.

1. Introduction

Diabetes mellitus (DM) affects the body's metabolism. Diabetes complications have recently become a prominent issue [1]. These complications include many disorders such as retinal, renal, neuronal, and cardiovascular disruption [2].

Diabetic retinopathy (DR) is defined as a vascular alteration in the retinal cells. This change has the potential to cause blindness and vision loss. The pathophysiological mechanisms of DR are not fully understood [3]. Long-term hyperglycemia increases the production of reactive oxygen species (ROS) in the retina, which is the most well-established mechanism that could explain DR. [4] Furthermore, inflammatory mediators such as TNF, interleukins (ILs), and cyclooxygenase-II (COX-II) play a crucial role in the etiology of DR. [5]

In response to diabetic-induced tissue injury, pigment epithelium-derived factor (PEDF) and vascular endothelial growth factor (VEGF) are formed [6] and it is thought that VEGF is the primary cause in the vascular alterations and abnormities in DR. [7] A prior study discovered a link between excessive VEGF production and lipid peroxidation in DR. [8] Apolipoprotein A1 (APOA1) and retinol-binding protein (RBP4) have recently been discovered to be more significantly expressed in retinal degenerative diseases and retinal detachment [9]; such overexpression

indicates the massive damage of the barriers of the retina and so a dysfunction and damage of retina is developed. APOA1 is one of the most important components of high-density lipoprotein (HDL). Although, RBP4 is a hepatic adipocyte that acts as a transporter protein, many previous studies reported that RBP4 is incorporated in retinal dysfunction and degeneration [10, 11].

Many limitations and restrictions have been reported to the current therapies of DR, and most of these traditional therapies are not effective. So, it becomes a provoked need to find an effective approach for managing DR. [12] Moreover, controlling blood glucose and blood pressure is considered a potent protocol to control the massive progression of retinal damage in DR. [13] In the therapy of progressed damage retina in DR, photocoagulation by laser, intraocular injection of anti-VEGF, and steroid injection are all viable treatments, although they all have possible side effects [14]. As mentioned previously, many researchers seek alternative effective therapies for DR.

The transplantation of stem cell is considered a modern effective promising interference which can restore the damaged tissues and cells. This effect could be attributed to stem cells' ability to proliferate and differentiate [15].

Stem cell transplantation in the retinal tissue is an effective and appealing technique for replacing or repairing damaged retinal pigment epithelium and photoreceptors [16]. Retinal stem cell transplantation is a viable alternative therapy for patients with DR who want to regain their vision [17, 18].

Transplantation of stem cells in the retina has many advantages, but there are many limitation and disadvantages of using stem cells such as low survival rate. This is considered one of the key reasons which restricts the efficiency of stem cell treatment [19, 20]. Inflammation and oxidative damage are considered the primary bulwark against the proper survival and implantation of stem cells. Many earlier studies suggested that the antioxidant content of the stem cells has the ability to inhibit the ROS and inflammatory response at the injured tissue. As a result, stem cell transplantation could protect against ROS-induced apoptosis [21]. As information regarding the effect of using an exogenous antioxidant on the antistress ability of stem cells against exogenous stresses, particularly on DR, is lacking, our aim was to investigate the effect of using a well-established antioxidant on the efficacy of stem cell transplantation in DR.

Melatonin's unique molecular structure confers a powerful antioxidant action since it is both lipophilic and hydrophilic. The unique characteristics of melatonin enable it to easily traverse all body barriers and enter in numerous organelles, including mitochondria, where ROS are formed [22]. It also possesses direct free radical scavenging characteristics due to its ability to create a variety of antioxidant enzymes which regulate the oxidative/antioxidant redox such as glutathione peroxidase (GPx) and glutathione reductase (GR) which have an important role in regulating GSH metabolism, catalase (CAT), and superoxide dismutase (SOD) which have free radical scavenging activity [23].

Melatonin has the ability to reduce the inflammatory reaction via inhibiting many inflammatory mediators [24]. This anti-inflammatory action could be linked to its capacity to suppress NF-B activation, which expresses various inflammatory genes like IL-6, TNF, and IL-1 [8]. Furthermore, melatonin has an anti-inflammatory impact through inhibiting COX-II [25]. In light of this, our target is to evaluate the role of melatonin in increasing stem cell anti-ROS capability and therapeutic efficiency in DR, as well as the relationship between ROS, inflammatory, and vasculogenic mediators.

2. Materials and Methods

2.1. Chemicals: Streptozotocin (STZ). The streptozotocin vial (1 g) was provided by Sigma Company (Sigma-Aldrich, Egypt) in the form of powder.

2.2. Isolated and Cultivation of Bone Marrow-Derived Mesenchymal Stem Cells (BM-Derived MSCs). MSCs were isolated for a period of four weeks. Rats were sacrificed; then, the bilateral femora and tibias were extracted and put in Dulbecco's modified Eagle medium (DMEM; Gibco/BRL) under sterile circumstances. MSCs were isolated and cultivated according to Jiang et al. [26].

2.3. Animals. The experiment involved 50 mature male albino rats weighing 200-250 g on average. Before the experiments, the rats were given a two-week acclimatization period in the laboratory. They were housed in metal cages (3 rats in each cage) and kept in conventional laboratory conditions, including $(25 \pm 2^{\circ}C)$ room temperature, 70 percent relative humidity, and a 12-hour dark-light cycle with free access to food and water. The National Institutes of Health (NIH) standard for the laboratory animal use was followed for all procedures involving drug administration and tissue and blood collection (NIH Publications No. 8023, revised 1978).

2.4. Induction of Diabetes. STZ (60 mg/kg BW, I.P.) was injected to create diabetes [7, 27, 28]. All animals were starved for twenty-four hours before induction of diabetes. Diabetic rats were defined as those that had blood glucose level of 200 mg/dl or higher after 48 hours of the injection and were monitored for 8 weeks [29].

2.5. Experimental Animals. After the end of the acclimation period, these rats were divided into five equal groups ($n = 10$): control group: animals were I.P. injected with 0.5 ml of 0.1 M sodium citrate buffer (pH = 4.5) (intraperitoneal (I.P.)). The confirmed diabetic rats were divided into 4 groups: diabetic group: confirmed diabetic rats received no treatments with a regular follow of the blood glucose profile for 8 weeks; melatonin group: confirmed diabetic rats were orally administered melatonin (5 mg/kg/day) [30], as a suspension in 1 mL of 0.1 M sodium citrate buffer (pH = 4.5) once daily till the end of the 8^{th} week; stem cell group: 4 weeks later to the confirmation of diabetes [31], the confirmed diabetic rats were given intravitreal injection of stem cells. To begin, diabetic rats were sedated with 2 percent pentobarbital sodium intraperitoneally, and the limbs and head were well secured to allow access to the eyes. From the corneoscleral limbus of the eye, a 10 l microsyringe

linked to a 30 G needle was inserted into the vitreous cavity, and 2 l stem cell suspension (3104 cells/l) was gently injected into the vitreous cavity. All injections were effective, as evidenced by no bleeding after 30 seconds of observation [32], and rats were kept under careful observation for about 4 weeks later [33]. Melatonin+stem cell group: confirmed diabetic rats were given melatonin (5 mg/kg body weight once daily for 8 weeks) [30], as an oral suspension. For preparing the suspension, 1 mL of 0.1 M sodium citrate buffer (pH = 4.5) was used. Then, 2 μl cell suspension of stem cells (3×10^4 cells/μl) was carefully injected into the vitreous cavity [32] and still under observation 28 days later. At the end of the experiment, blood samples were collected from the medial canthus of the eye, and then, rats were sacrificed by decapitation [33] (Figure 1).

2.6. Vitreous Sample Collection. Vitreous samples were suctioned directly into a 5 ml syringe using a three-port 25-gauge transconjunctival suture-less vitrectomy device (TSV25G; Alcon Constellation; Alcon Laboratories, Fort Worth, TX) according to Ding et al. [34].

2.7. Retina Collection for Biochemical Investigations. The retinas of the left eyes were dissected as soon as rats were killed and kept refrigerated at -70°C until biochemical studies could be performed. For the biochemical experiments, retina samples were homogenized using a tissue homogenizer in a cold phosphate-buffered saline (diluted as 1 : 5; pH 7.2) (Ortoalresa, Spain). After centrifuging homogenates at 10,000 g for 30 minutes, the supernatants were stored at -80°C for biochemical tests.

2.8. Fluorescent Microscopic Examination. To elucidate fluorescent-labeled mesenchymal stem cells, sections of stem cells and melatonin+stem cells were examined under fluorescent microscopy (Figure 2). The bromodeoxyuridine-(BrdU-) positive cells in the sections were identified by staining the section with rat anti-BrdU (1 : 100, Neomarkers) and goat anti-rat Ig GFITC (1 : 100, Kpl) [35] (Figure 2).

2.9. Measurement of Blood Glucose, Glycated Hemoglobin A1C (HbA1C), and C-Peptide Linkage. A glucose assay kit (Sigma-Aldrich, Egypt, Cat. No. GAGO20) was used to determine the blood glucose level. For detecting HbA1C, glycohemoglobin absorbance and total hemoglobin fraction were measured at 415 nm compared to the prepared standard hemoglobin [36]. A C-peptide ELISA assay kit (Sigma-Aldrich, Egypt, Product no. EZRMCP2) was used for detecting C-peptide linkage.

2.10. Measurement of Retinal Oxidant/Antioxidant Redox. All the used kits for measuring the retinal oxidant/antioxidant status were purchased from Sigma-Aldrich, Egypt. A GSH (reduced glutathione) test kit (Cat. no. 099M4064V) [37], glutathione reductase (GR) test kit (Cat no. GRSA) [38], catalase (CAT) assay kit (Cat. no. CAT 100) [39], superoxide dismutase activity (SOD) assay kit (Cat. no. BCCC1068) [40], total antioxidant capacity (TAC) (Cat. no. 059M4154V) [41], and malondialdehyde (MDA) assay kit (Cat. no. 6A20K07390) [42] were used to evaluate the retinal oxidant/antioxidant redox.

2.11. Measurement of Retinal Inflammatory Markers. All the used kits for measuring the retinal inflammatory markers were purchased from Sigma-Aldrich, Egypt. A tumor necrosis factor-α (TNF-α) ELISA kit (Cat. no. RAB0479), interleukin 1-β (IL-1β) ELISA kit (Cat. no. RAB0278), interleukin 6 (IL-6) ELISA kit (Cat. no RAB0311), and cyclooxygenase II (COX-II) ELISA kits (Cat. no. RAB1034) were used.

2.12. Measurement of BEDF, VEGF, APOA1, and RBP4 by Using the Western Blot Technique. The concentrations of cerebral BEDF, VEGF, APOA1, and RBP4 were determined by immunoblotting with the appropriate antibody, and the proteins were subsequently separated by gel electrophoresis according to their molecular weight and the intensity of the bands was compared to that of β-actin using the image analysis programme ChemiDoc MP imager (Markham Ontario L3R 8T4, Canada) [43, 44].

2.13. Retina Preparation for Histological Study. Each rat's tissue (retina) was evaluated graphically after the eye was removed. The tissue was taken for histological examination, washed in normal saline, and immediately immersed in 10% buffered formalin. According to conventional methods, they were gradually dehydrated, paraffin embedded, sectioned into 5 μm slices, and stained with hematoxylin and eosin for histologic evaluation [45].

2.14. .Immunohistochemical Study for Detection of COX-II and VEGF. To remove paraffin, the sections were submerged in dimethyl benzene for 30 minutes and then rinsed in aqueous ethanol for 5 minutes each time. Endogenous peroxidases were then blocked for 15 minutes with 0.3 percent hydrogen peroxidase before being rinsed with ultrapure water. After that, the sections were treated by microwaving them for 10 minutes at 700 W in 0.01 M citric acid buffer (pH 6.0). An anti-VEGF polyclonal antibody (RB-222-R7; Lab Vision Corporation Laboratories, Fremont, California, USA) and anti-COX-II polyclonal antibody (Cat. No. 06-735; Sigma-Aldrich, Egypt) were incubated overnight at 4°C on the sections after thorough washing. After that, the pieces were immersed in DAB and multispectral image analysis was used to quantify them [46].

2.15. Morphometric Study. The morphometric measurements were done by using a Leica Qwin 500 LTD image analyzer (Leica, Cambridge, UK). All measurements were taken in five sections from VEGF and anti-cox-2 immunostained sections from each animal. The mean area percentage of COX-II and VEGF immunoreactivity was measured in 10 random nonoverlapping fields per section using a binary mode with ×40 objective lens.

2.16. Statistical Analysis. SPSS software, version 16, was used for statistical analysis. All data were expressed as mean value ± standard error (SE). For comparison of rat groups, a one-way analysis of variance (ANOVA) test will be utilized, followed by the Tukey–Kramer post-ANOVA test.

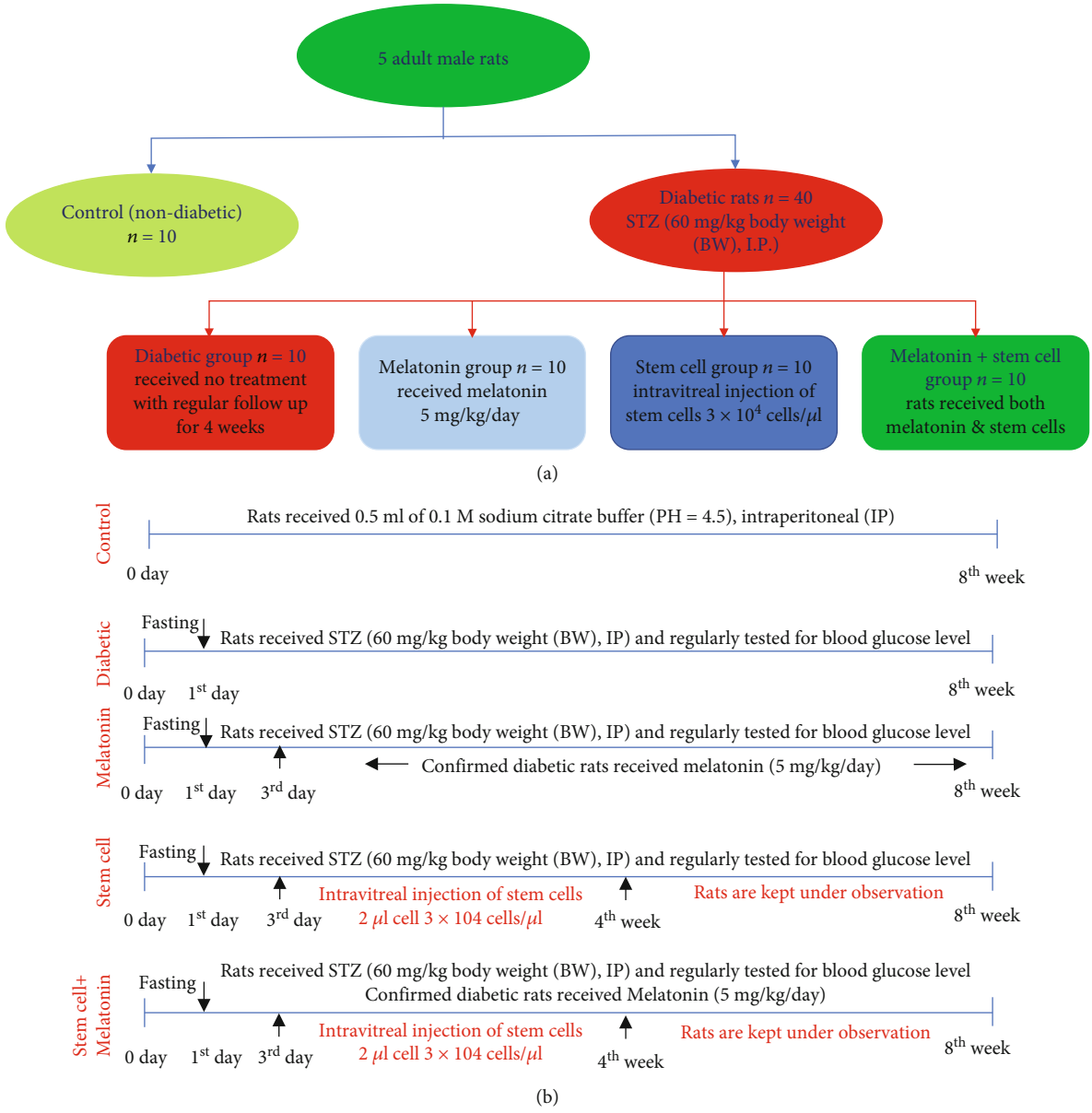

Figure 1: (a) Rat grouping. (b) Experimental design shows the protocol of treatment of each group.

P value less than 0.05 ($P < 0.05$) was considered to indicate a significant difference.

3. Results

3.1. Changes in the Glucose Profile of Different Treated Groups. Our results in Table 1 showed a significant increase in blood glucose level and HbA1C (74.4%, 271.6%), respectively, as compared to the control group. Melatonin administration significantly reduced blood glucose level and HbA1C (29.6%, 37.1%), respectively, in comparison to the diabetic group. Stem cell administration showed a nonsignificant decrease in blood glucose level and HbA1C as compared to the diabetic group. Coadministration of melatonin and stem cells in the melatonin+stem cell group significantly decreased the blood glucose level and HbA1C (30.7%, 42.3%) as compared to the diabetic group. Moreover, C-peptide linkage showed a significant reduction in the diabetic group (92.7%) as compared to the control group. Melatonin administration significantly increased C-peptide linkage (600%) as compared to the diabetic group. Stem cell administration showed a nonsignificant difference in C-peptide linkage as compared to the diabetic group. Coadministration of melatonin and stem cells in the melatonin+stem cell group showed a significant increase in C-peptide linkage (733%) as compared to the diabetic group.

3.2. Changes in Retinal Oxidative/Antioxidant Status. Our results in Table 2 showed a significant decrease in GSH concentration, GR, CAT, and SOD activities, and TAC content

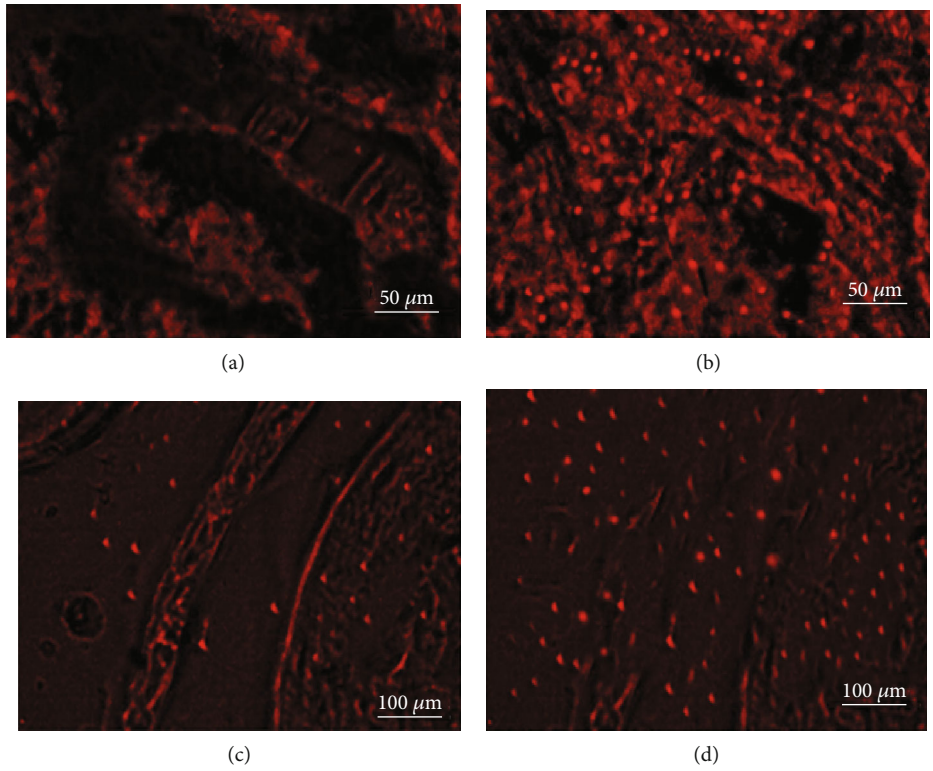

(a) (b) (c) (d)

Figure 2: Photomicrograph of sections of retinas shows a positive immunofluorescent: (a, c) stem cell group (50 μm and 100 μm, respectively) and (b, d) melatonin+stem cell group (50 μm and 100 μm, respectively).

Table 1: Changes in the blood glucose profile in different treated groups.

	Blood sugar	HbA1C	C-peptide linkage
Control	69 ± 1.2	4.31 ± 0.56	4.16 ± 0.02
Diabetic	270 ± 2.1^{a}	15.98 ± 0.93^{a}	0.3 ± 0.001^{a}
Melatonin	$190 \pm 1.1^{a,b}$	$10 \pm 0.86^{a,b}$	$2.1 \pm 0.01^{a,b}$
Stem cells	268 ± 2.3^{a}	14.2 ± 1.05^{a}	0.45 ± 0.001^{a}
Melatonin + stem cells	$187 \pm 1.2^{a,b}$	$9.04 \pm 0.23^{a,b}$	$2.5 \pm 0.01^{a,b}$

Values were expressed as means ± SE. a indicates a significant difference as compared to the control group at P value < 0.05, and b indicates a significant difference as compared to the diabetic group at P value < 0.05.

with a significant increase in MDA level as compared to the control group ($P < 0.05$). Melatonin administration significantly increased GSH concentration, GR, CAT, and SOD activities, and TAC content and significantly reduced MDA level as compared to the diabetic group at $P < 0.05$. Also, stem cell administration significantly increased GSH concentration, GR, CAT, and SOD activities, and TAC content and significantly reduced MDA level as compared to the diabetic group at $P < 0.05$. Coadministration of melatonin and stem cells in the melatonin+stem cell group significantly increased GSH concentration, GR, CAT, and SOD activities, and TAC content and significantly reduced MDA level as compared to the diabetic group at $P < 0.05$. Moreover, there were no significant differences of oxidant/antioxidant status between melatonin, stem cell, and melatonin+stem cell, and control groups at $P < 0.05$.

3.3. Changes of Retinal Inflammatory Markers in Different Treated Groups. Our results in Table 3 showed a significant increase in TNF-α, IL-1β, IL-10, and COX-II levels as compared to the control group at $P < 0.05$. Melatonin administration significantly reduced TNF-α, IL-1β, IL-10, and COX-II levels as compared to the diabetic group at $P < 0.05$. Also, stem cell administration significantly decreased TNF-α, IL-1β, IL-10, and COX-II levels as compared to the diabetic group at $P < 0.05$. Coadministration of melatonin and stem cells in the melatonin+stem cell group significantly decreased TNF-α, IL-1β, IL-10, and COX-II levels as

Table 2: Changes in retinal oxidative/antioxidant status.

	GSH	GR	CAT	SOD	TAC	MDA
Control	50 ± 1.09	70 ± 0.76	90 ± 0.43	66 ± 0.76	210 ± 1.87	27.54 ± 1.09
Diabetic	10.12 ± 0.98[a]	20 ± 0.23[a]	8.43 ± 0.06[a]	15 ± 0.73[a]	51.32 ± 1.33[a]	85 ± 2.09[a]
Melatonin	45 ± 1.11[b]	66.2 ± 2.01[b]	87.22 ± 2[b]	63.12 ± 1.3[b]	200 ± 1.02[b]	26.32 ± 1.08[b]
Stem cells	44.22 ± 1.11[b]	63 ± 1.71[b]	84 ± 1.04[b]	61.2 ± 2.09[b]	197 ± 2.09[b]	30.12 ± 1.03
Melatonin+stem cells	48.2 ± 0.76[b]	67.32 ± 1.09[b]	88.43 ± 1.06[b]	64.41 ± 0.72[b]	208 ± 1.54[b]	25.1 ± 1.6[b]

Values were expressed as means ± SE. a indicates a significant difference as compared to the control group at P value < 0.05, and b indicates a significant difference as compared to the diabetic group at P value < 0.05.

Table 3: Changes of retinal inflammatory markers in different treated groups.

	TNF-α	IL-1β	IL-6	COX-11
Control	25 ± 0.19	20 ± 0.76	32 ± 0.13	30 ± 0.96
Diabetic	90.13 ± 0.98[a]	110 ± 0.53[a]	160.8 ± 0.96[a]	200 ± 0.49[a]
Melatonin	45 ± 0.12[a,b]	66.2 ± 2.01[a,b]	89 ± 1.1[a,b]	51.14 ± 0.53[a,b]
Stem cells	46.24 ± 1.1[a,b]	85 ± 1.71[a,b]	90 ± 1.4[a,b]	67.2 ± 0.99[a,b]
Melatonin+stem cells	27.02 ± 0.6[b]	24.36 ± 0.12[b]	35.44 ± 0.16[b]	32.11 ± 0.12[b]

Values were expressed as means ± SE. a indicates a significant difference as compared to the control group at P value < 0.05, and b indicates a significant difference as compared to the diabetic group at P value < 0.05.

compared to the diabetic group at $P < 0.05$. Moreover, there were no significant differences in TNF-α, IL-1β, IL-10, and COX-II levels in the stem+melatonin group and control group at $P < 0.05$.

3.4. Changes of BEDF, VEGF, APOA1, and PRP4 of Different Treated Groups. Our results in Figure 3 showed a significant increase in BEDF, VEGF, APOA1, and PRP4 protein concentrations as compared to the control group at $P < 0.05$. Melatonin administration significantly reduced BEDF, VEGF, APOA1, and PRP4 protein concentrations as compared to the diabetic group at $P < 0.05$. Also, stem cell administration significantly decreased BEDF, VEGF, APOA1, and PRP4 protein concentrations as compared to the diabetic group at $P < 0.05$. Coadministration of melatonin and stem cells in the melatonin+stem cell group significantly decreased BEDF, VEGF, APOA1, and PRP4 protein concentrations as compared to the diabetic group at $P < 0.05$. Moreover, there were no significant differences in BEDF, VEGF, APOA1, and PRP4 protein concentrations in the stem+melatonin group and control group at $P < 0.05$.

3.5. Histopathological Study of Retinal Tissues. As shown in Figure 4(a), the control group shows the normal architecture of well-organized layers of the retina consisting of the photoreceptor layer, outer nuclear layer, outer plexiform layer, inner nuclear layer, inner plexiform layer, and ganglion cell layer. The diabetic group shows disorganization of retinal layers with near-total disappearance of nuclei of the outer nuclear layer, disruption of the outer plexiform layer, and appearance of empty spaces within the inner nuclear layer. Neovascularization in the ganglion cell layer with dilated congested blood capillaries is also noticed (Figure 4(b)). It shows apparent marked reduction of retinal thickness in comparison with the control group and marked disorganization of retinal layers with the appearance of spaces within the outer nuclear layer and many spaces in the inner nuclear layer. Multiple cavities within the photoreceptor layer are also detected. Retinal folding with disruption of the outer plexiform layer is seen, and dilated congested blood vessels and a reduction in the counts of ganglion cells in the ganglion cell layer can be detected (Figure 4(c)). It shows neovascularization in the ganglion cell layer (Figure 4(d)). It shows an increased number of supporting cells with dark nuclei within the ganglion cell layer (Figure 4(e)). Melatonin and stem cells groups, respectively, show well-organized retinal layers but with the appearance of many small empty spaces in the photoreceptor layer, outer nuclear layer, and inner nuclear layer. Neovascularization is still found in the ganglion cell layer (Figures 4(f) and 4(g)). In the melatonin+stem cell group, the total retinal thickness is preserved, the inner nuclear layer appears with higher cell density, the inner plexiform layer preserves its reticular appearance with no widening of the spaces between its fibers, and the ganglion cell layer consisted of one row of ganglion cells (Figure 4(h)).

3.6. Changes of COX-II Immunohistochemical Reaction in Retinal Tissues in Different Groups. As shown in Figure 5(a), the control group showed no immunoreactivity. In Figure 5(b), the diabetic group showed a strong positive COX-II immunoreactivity (brown color). In Figures 5(c) and 5(d)), melatonin and stem cell groups, respectively, displayed a positive immunoreactivity (brown color). In

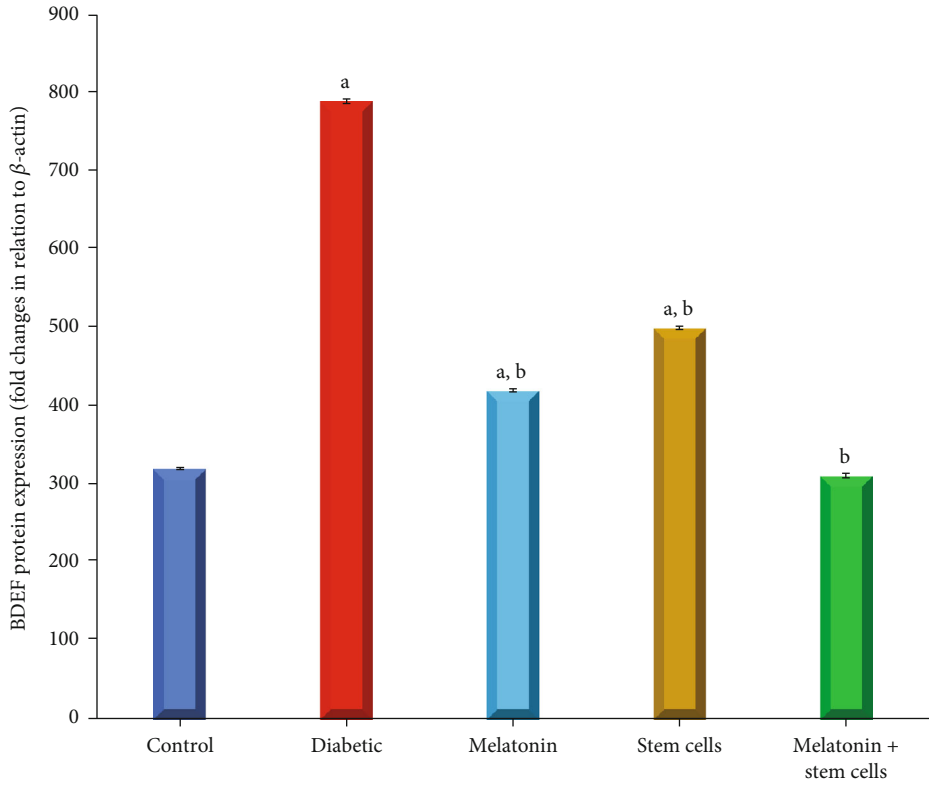

(a)

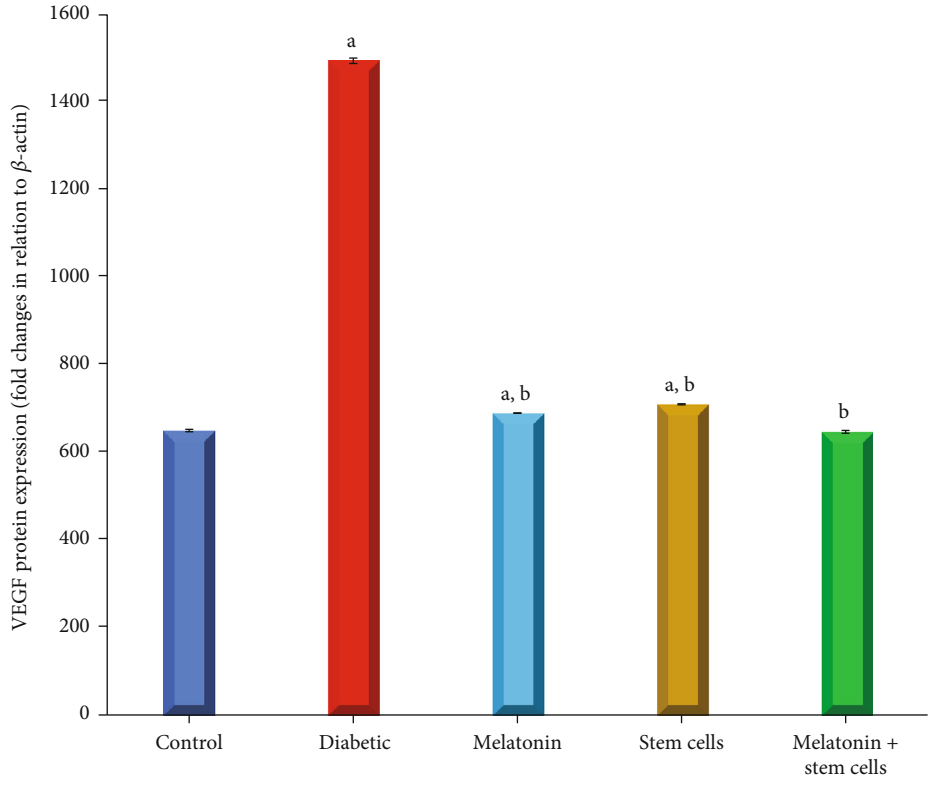

(b)

Figure 3: Continued.

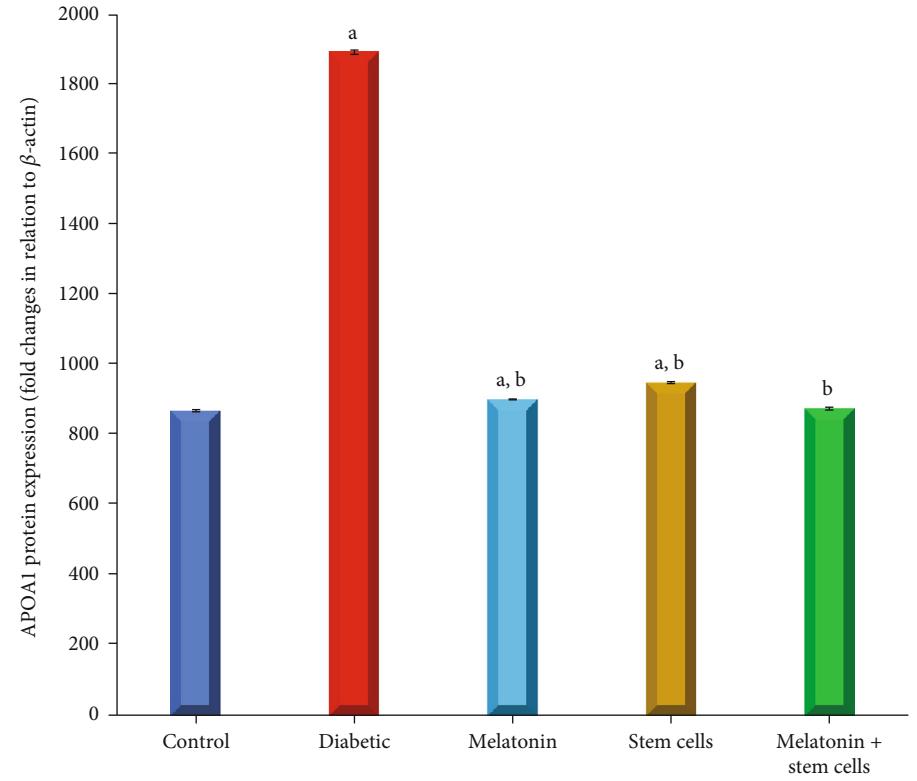

(c)

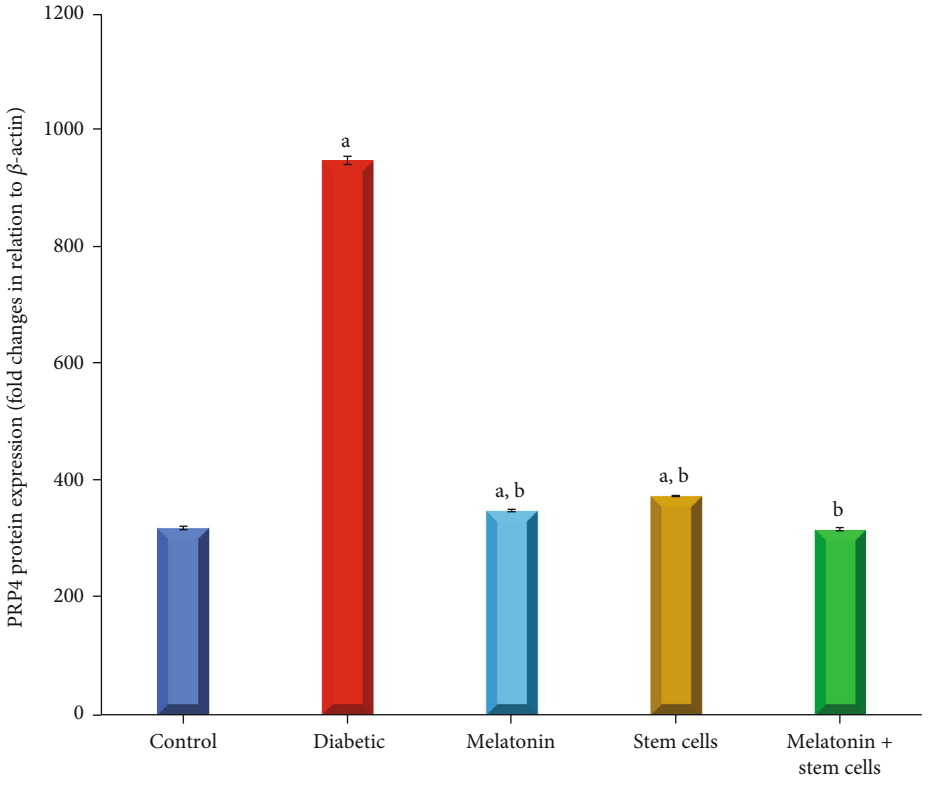

(d)

Figure 3: Continued.

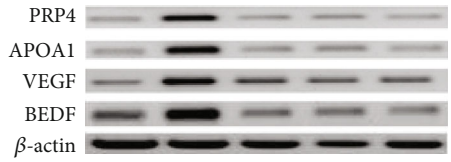

(e)

Figure 3: The changes of BDEF, VEGF, ABOA1, and PRP4 protein expression in different groups. The effect of melatonin and/or stem cell on diabetic rats on the expression levels of BDEF (a), VEGF (b), ABOA1 (c), and PRP4 (d) and (e) images of western blotting bands of the measured protein expression in different groups. Data are presented as mean ± SE ($n = 10$). a indicates a significant difference compared to the control group, and b indicates a significant change compared to the diabetic group at $P < 0.05$ using ANOVA followed by Tukey–Kramer as the post-ANOVA test.

Figure 5(e), the melatonin+stem cell group showed a negative immunoreactivity. In Figure 5(f), the optical density of COX-II was represented as means ± SE ($n = 10$). a indicates a significant difference as compared to the control group at $P < 0.05$. b indicates a significant difference as compared to the diabetic group at $P < 0.05$. The magnification is ×200.

3.7. Changes of VEGF Immunohistochemical Reactions in Retinal Tissues of Different Groups. As shown in Figure 6(a)), the control group showed no immunoreactivity. In Figure 6(b), the diabetic group showed a strong positive VEGF immunoreactivity (brown color) in the ganglion cell layer (GCL). In Figures 6(c) and 6(d)), the melatonin and stem cell groups, respectively, displayed a positive immunoreactivity (brown color) in GCL. In Figure 6(e), the melatonin+stem cell group showed a negative immunoreactivity. In Figure 6(d)), the optical density of VEGF was represented as means ± SE ($n = 10$). a indicates a significant difference as compared to the control group at $P < 0.05$. b indicates a significant difference as compared to the diabetic group at $P < 0.05$. The magnification is ×200.

4. Discussion

Diabetic retinopathy (DR) is provoked microvascular sequelae of diabetes mellitus (DM) which may cause a vision loss [47]. The rapid progression of DM and its complication worldwide give DR great importance [48, 49]. Oxidative and inflammatory stressors are considered crucial limiting factors in the formation of DR. [50]

The overproduction of ROS impairs the retinal vessels, which leads to the development of DR. Diabetes-induced oxidative damage in the retina could be attributed to the activation of nuclear factor-κB (NF-κB) [51] and reduction nuclear factor erythroid 2-related factor 2 (Nrf2) expression [52]. Based on our obtained results, the disturbance of retinal oxidative/antioxidant redox is manifested by reduction of retinal GSH concentration, GR, CAT, and SOD activities, and TAC with a concurrent increase in MDA concentration. Even if blood glucose levels return to normal, oxidative damage produced by diabetes might linger for a long time [53]. Additionally, hyperglycemia triggers many inflammatory mediators in the retinal vasculature such as IL-1β, TNF-α, IL-6, and COX-II [54]. Moreover, inflammation, oxidative stress, and autophagy all play a role in the etiology of diabetic retinopathy [23].

PEDF is a glycoprotein that was discovered in foetal human retinal pigment epithelial cell culture for the first time [55]. It has strong antioxidant properties and is abundantly expressed in the retina. PEDF expression was shown to be higher in the diabetic group compared to the control group, which is consistent with previous findings [56]. Other researchers, on the other hand, found that hyperglycemia caused a considerable drop in PEDF expression [57]. The overexpression of PEDF expression could be a protective response of the retina to the diabetic effect [58, 59].

VEGF overexpression has been observed in the retinas and vitreous humors of diabetic animals and people in a number of earlier studies [60]. VEGF is produced in retinal tissue in response to a variety of stimuli [61]. In early DR, VEGF increases the retinal vascular permeability [62]. The fundamental cause of mediating VEGF and the development of DR is thought to be oxidative stress [63].

Lipids have an important role in the onset of DR. APOA1 is one of the fundamental proteins which enters in the formation of HDL. It removes deleterious oxidized lipids from the retinal tissue [64].

In agreement with our findings, Simó et al. recorded that vitreous humor content of APO1 significantly increased in DR. [65] The overexpression of APOA1 could be attributed to its potent scavenging power for oxidative reactants [66] and anti-inflammatory effect [67].

RBP4 is considered one of the most important cardiovascular protective agents, and it is closely related to insulin resistance [68]. Previous studies documented the role of RBP4 in early vascular dysfunction [69, 70].

Many proinflammatory mediators such as TNF-α, IL-1β, IL-6, and COX-II were stimulated by RBP4 [71]. The overexpression of RBP4 in the diabetic group induces endothelial cell inflammation, which, followed by an impairment of retinal vascularity, leads to too much increase in the retinal vascular permeability [34] and progressive retinal degeneration [72].

The results of our histology analysis showed empty spaces between the outer and inner nuclear layers. An apparent loss in retinal thickness and disorganized retinal layers are detected in DR. It was also shown that the outer and

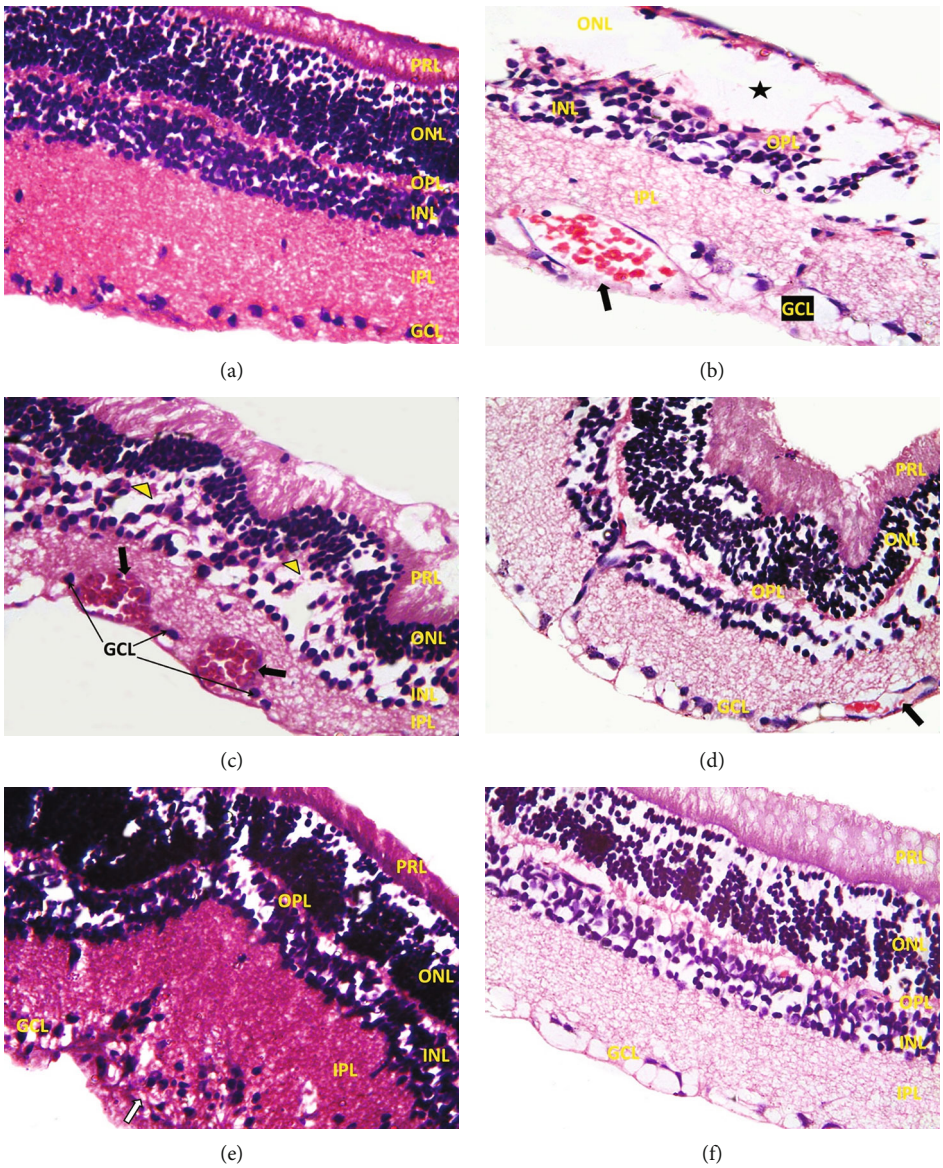

Figure 4: Continued.

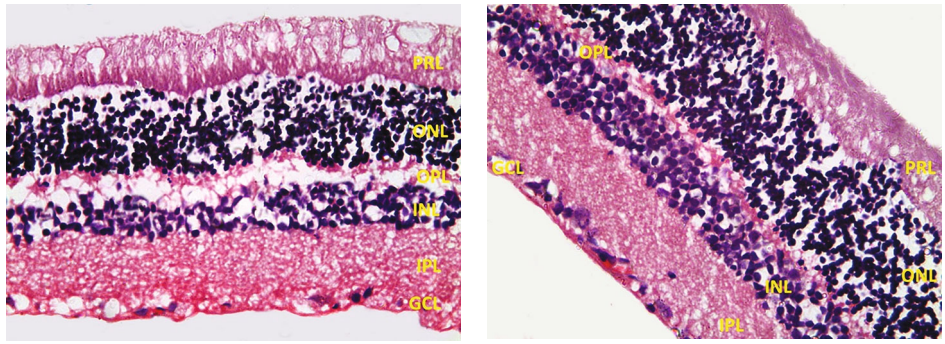

(g) (h)

Figure 4: Photograph of the retinas' sections stained with H&E. (a) Control group shows normal histological structure of well-organized retinal layers formed by the photoreceptor layer (PRL), outer nuclear layer (ONL), outer plexiform layer (OPL), inner nuclear layer (INL), inner plexiform layer (IPL), and ganglion cell layer (GCL). (b) Diabetic group shows disorganization of retinal layers with near-total disappearance of nuclei of the outer nuclear layer (ONL) (Astrix), disruption of the outer plexiform layer (OPL), and appearance of empty spaces within the inner nuclear layer (INL). Neovascularization in the ganglion cell layer (GCL) with dilated congested blood capillaries (arrow) is also noticed. (c) Diabetic group shows apparent marked reduction of retinal thickness in comparison to the control group and marked disorganization of retinal layers with the appearance of spaces between the nuclei of the outer nuclear layer (ONL) and many spaces in the inner nuclear layer (INL). Multiple cavities within the photoreceptor layer (PRL) are also detected. Retinal folding with disruption of the outer plexiform layer is seen (arrowheads). Dilated congested blood vessels (arrows) and a reduction in the counts of ganglion cells within the ganglion cell layer (GCL) can be detected (retina). (d) Diabetic group shows neovascularization within the ganglion cell layer (GCL). (e) Diabetic group shows an increased number of supporting cells with dark nuclei within the ganglion cell layer. (f, g) Melatonin and stem cell groups, respectively, show well-organized retinal layers but with appearance of many small empty spaces in PRL, ONL, and INL. Neovascularization is still found in GCL. (h) Melatonin+stem cell group: the total retinal thickness is apparently preserved, the inner nuclear layer (INL) appears with higher cell density, the inner plexiform layer (IPL) preserves its reticular appearance with no widening of the spaces between its fibers, and (d) the ganglion cell layer (GCL) is formed by one row of ganglion cells (GC). H&E, ×400.

inner plexiform layers were disrupted. This was in line with the findings of prior research [73].

These findings could be contributed to the progressive loss of retinal nerve cells leading to a reduction in retinal thickness. Apoptosis of neurons in the retinal tissue, which are further phagocytized by glial cells, may also contribute to the appearance of empty spaces [74]. The dysfunction of blood-retinal barriers leads to accumulation of fluids in the inner and outer retinal plexiform layer, and so separation between retinal cells occurs and retinal edema takes place [75].

As mentioned previously, treatment with a well-known potent anti-inflammatory and an antioxidant agent such as melatonin has a great effect on DR. In diabetic rats, a significant reduction of melatonin formation has been recorded. This reduction could be attributed to the low expression of melatonin production-regulating enzymes such as aryl alkyl amine N-acetyl transferase (AANAT) [76]. Consistent with our results, the concentration of melatonin was lower in patients with DR than non-DR individuals [77]. Melatonin has also been shown to reduce oxidative stress, which helps to alleviate histopathological changes in the retina [78].

Melatonin activates the PI3K/Akt-Nrf2 signaling pathway, which boosts cellular antioxidant defences and lowers VEGF production [8]. Melatonin's capacity to reduce ROS and malondialdehyde (MDA) as well as control apoptosis and inflammation in diabetic retinopathy rats by regulating the MAPK pathway could explain the lower BEDF in the melatonin group compared to the diabetic group [79]. The protective effect of melatonin on the retinal tissue was previously studied by Djordjevic et al. [80]. The significant reduction of APOA1 in the melatonin group might be due to the consumption of APOA1 in HDL synthesis [81]. RBP4 expression was reduced in the melatonin group compared to the diabetic group. As previously discussed, RBP4 is released in response to retinal vascular degeneration. In accordance with our results, a significant reduction of retinal vascular damage, cytokines, and other inflammatory mediators was recorded with melatonin administration [7].

The use of stem cells to heal injured neural tissues becomes a viable option. Following the transplantation, there was a gradual integration of the transplanted stem cells into the retinal milieu, as well as proliferation and differentiation of the transplanted stem cells into target cells [82]. However, these therapies' efficacy falls short of expectations [83]. There are many challenges and limitation of the use of stem cell transplantation in retinal degeneration and DR. Following stem cell transplantations, many previous studies have reported retinal detachment, visual loss [84], and inflammation [85]. Moreover, the low survival rate of transplanted stem cells represents one of the main obstacles in stem cell therapy. The low survival rate could be attributed to the oxidative stress and inflammatory environment at the injured site [86]. So it is a logical approach to counter these effects by using a potent antioxidant and anti-inflammatory substance. Many previous

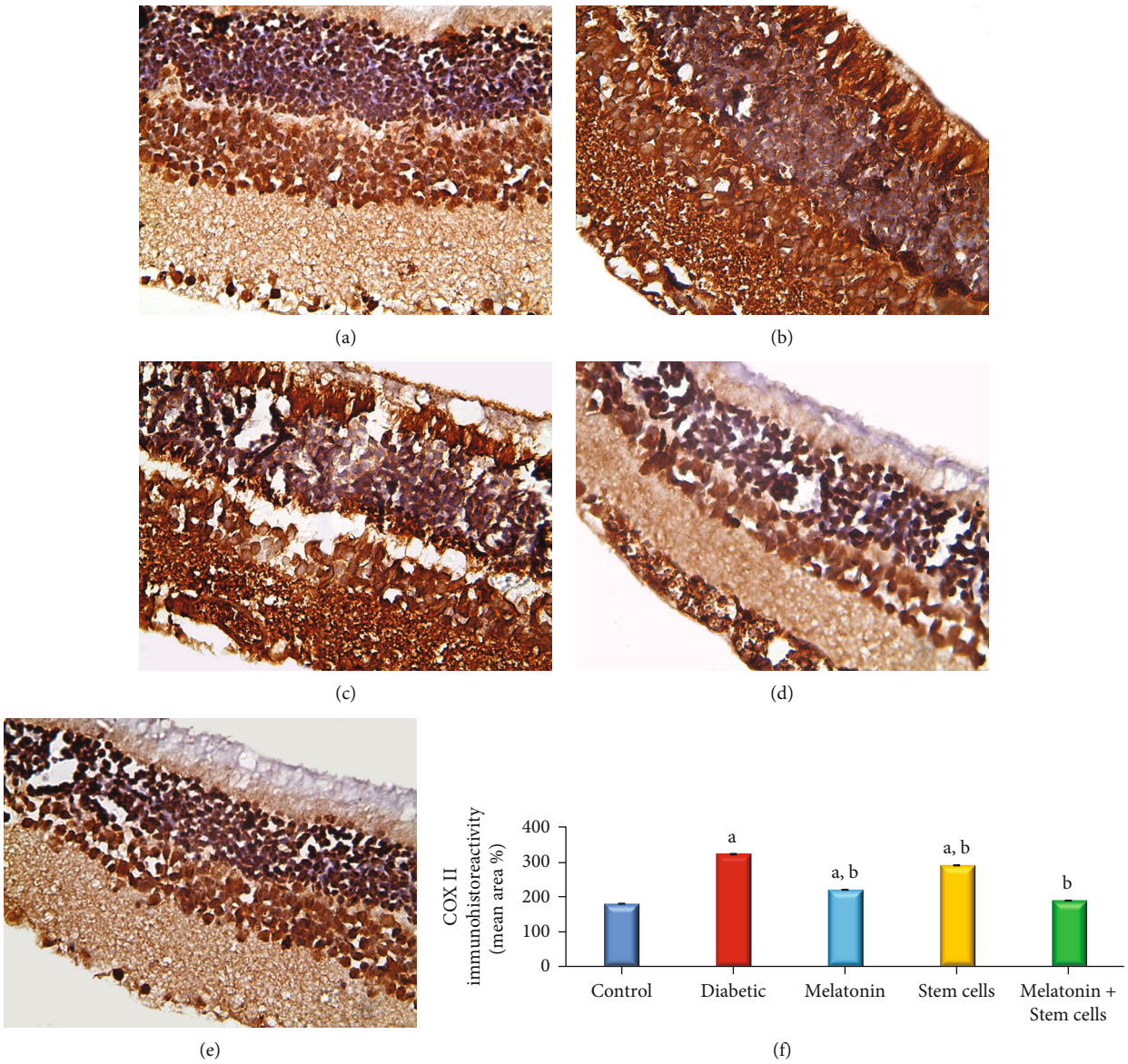

Figure 5: Photomicrograph of COX-II immunohistochemically stained retinal sections (magnification, ×200). (a) Control group showed no immunoreactivity. (b) Diabetic group showed a strong positive COX-II immunoreactivity (brown color). (c, d) Melatonin and stem cell groups, respectively, displayed a positive immunoreactivity (brown color). (e) The melatonin+stem cell group showed a negative immunoreactivity. (f) The optical density of COX-II was represented as means ± SE ($n = 10$). a indicates a significant difference as compared to the control group at $P < 0.05$. b indicates a significant difference as compared to the diabetic group at $P < 0.05$.

cotreatments in stem cell therapy have been studied, such as N-acetylcysteine (NAC), which dramatically enhanced the survival of muscle-derived stem cells (MDSCs) and cardiac function in an acute myocardial infarction model [87].

In diabetic retinopathies, there are not enough data on antioxidant cotreatment with stem cells. So, in this work, we looked into the therapeutic effects of melatonin in combination with MSCs on DR.

MSCs reduced hyperglycemia-induced histological alterations in the retinas of STZ-induced diabetic rats, according to our findings. Furthermore, we noticed that MSCs' therapeutic activity is due to their ability to decrease oxidative stress and suppress VEGF release. Because of their anti-inflammatory and antiangiogenic properties, MSCs have therapeutic potential in DR.

In the present study, histopathological examination and morphometric analysis revealed that MSCs were able to improve histopathological alterations of DR by preserving retinal thickness and organization of its different layers. The protection of the retina against oxidative stress and downregulation of VEGF expression may be responsible for the improvement shown with MSCs.

Figure 2 shows the capacity of melatonin to improve stem cell survival and implantation in retinal tissue. This

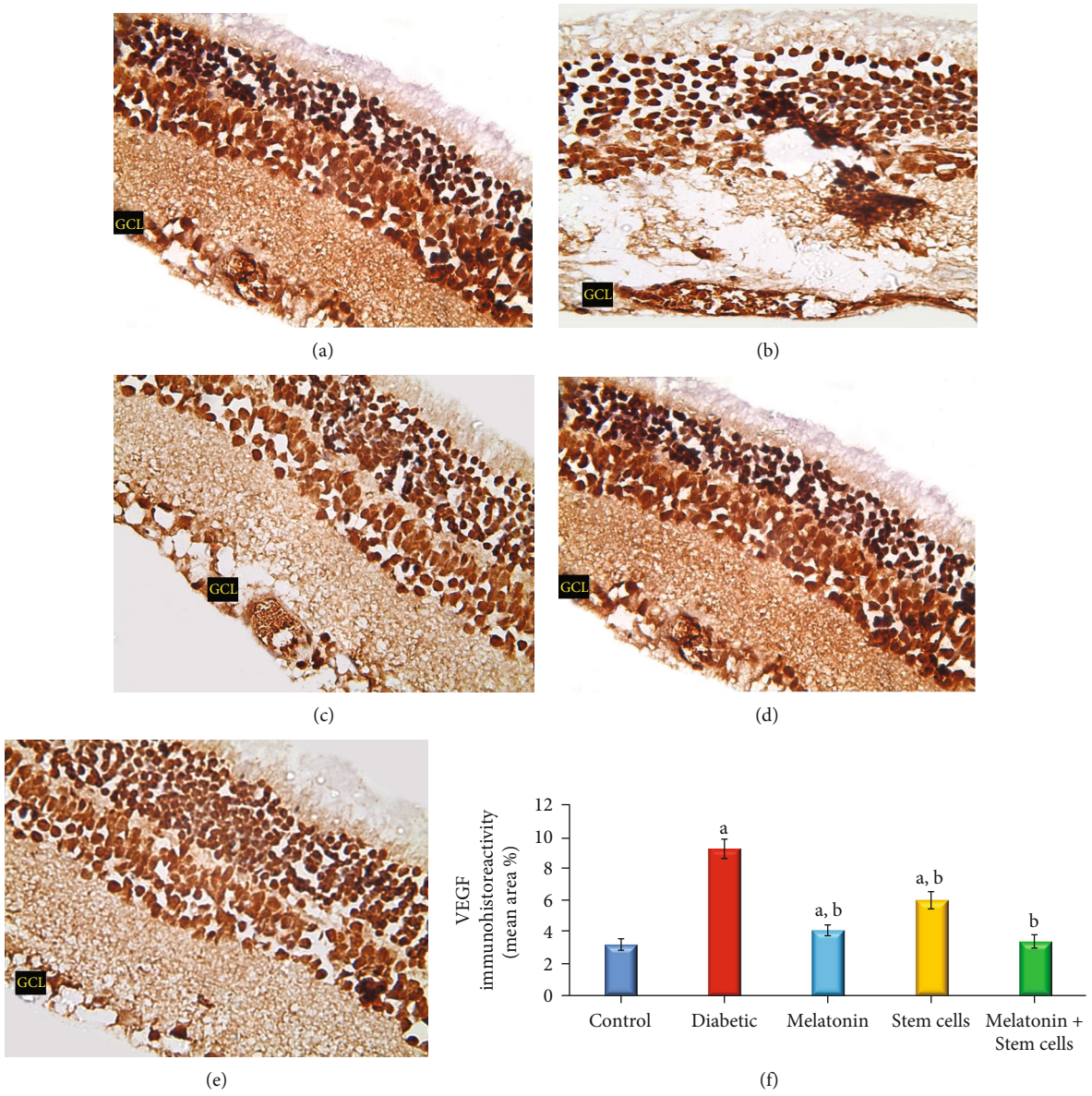

Figure 6: Photomicrograph of VEGF immunohistochemically stained retinal sections (magnification, ×200). (a) The control group showed no immunoreactivity. (b) The diabetic group showed a strong positive VEGF immunoreactivity (brown color) in the ganglion cell layer (GCL). (c, d) Melatonin and stem cell groups, respectively, displayed a positive immunoreactivity (brown color) in GCL. (e) The melatonin+stem cell group showed a negative immunoreactivity. (f) The optical density of VEGF was represented as means ± SE ($n = 10$). a indicates a significant difference as compared to the control group at $P < 0.05$. b indicates a significant difference as compared to the diabetic group at $P < 0.05$.

finding is supported by a previous study which indicated that melatonin medication improved the efficacy of adipose-derived mesenchymal stem cell (ADSC) therapy in rats with acute interstitial cystitis [88].

5. Conclusion

In conclusion, the present study demonstrates that administration of melatonin alleviates oxidative and inflammatory changes in DR. Administration of melatonin and stem cell in DR restores retinal oxidative/antioxidant redox and reduces retinal inflammatory mediators. Melatonin is a promising supportive therapy with stem cell transplantation as it has the capability to regulate retinal BEDF, VEGF, APOA1, and RBP4 gene expression.

Data Availability

Data are available when requested.

Ethical Approval

The Experimental Animal Ethics Committee of Beni-Suef University's Faculty of Veterinary Medicine was the guide

of this study, and all experimental procedures followed the National Institutes of Health's (NIH) standard for the care and use of laboratory animals (NIH Publications No. 8023, revised 1978).

Conflicts of Interest

The authors declare no conflict of interest.

Authors' Contributions

K.H. and S.A. were responsible for the conceptualization, methodology, software, and investigation and wrote the original draft. K.H. was responsible for the formal analysis and reviewed and edited the paper. All authors have read and agreed to the published version of the manuscript.

Acknowledgments

The authors acknowledge the staff members of histological and biochemical laboratories, Beni-Suef University, for their kind support and help during all the steps of this work.

References

[1] B.-Y. Peng, N. K. Dubey, V. K. Mishra et al., "Addressing stem cell therapeutic approaches in pathobiology of diabetes and its complications," *Journal of Diabetes Research*, vol. 2018, 16 pages, 2018.

[2] N. E. Babiker, A. Gassoum, N. E. Abdelraheem et al., "The progress of stem cells in the treatment of diabetes mellitus type 1," *Progress in Stem Cell*, vol. 4, no. 1, pp. 175–188, 2017.

[3] A. K. W. Lai and A. C. Lo, "Animal models of diabetic retinopathy: summary and comparison," *Journal of Diabetes Research*, vol. 2013, 29 pages, 2013.

[4] A. M. A. El-Asrar, "Role of inflammation in the pathogenesis of diabetic retinopathy," *Middle East African Journal of Ophthalmology*, vol. 19, no. 1, pp. 70–74, 2012.

[5] Y. Wooff, S. M. Man, R. Aggio-Bruce, R. Natoli, and N. Fernando, "IL-1 family members mediate cell death, inflammation and angiogenesis in retinal degenerative diseases," *Frontiers in Immunology*, vol. 10, p. 1618, 2019.

[6] T. Curtis, T. Gardiner, and A. Stitt, "Microvascular lesions of diabetic retinopathy: clues towards understanding pathogenesis," *Eye*, vol. 23, no. 7, pp. 1496–1508, 2009.

[7] G. Özdemir, Y. Ergün, S. Bakariş, M. Kılınç, H. Durdu, and E. Ganiyusufoğlu, "Melatonin prevents retinal oxidative stress and vascular changes in diabetic rats," *Eye*, vol. 28, no. 8, pp. 1020–1027, 2014.

[8] T. Jiang, Q. Chang, J. Cai, J. Fan, X. Zhang, and G. Xu, "Protective effects of melatonin on retinal inflammation and oxidative stress in experimental diabetic retinopathy," *Biochemistry Research International*, vol. 2016, 13 pages, 2016.

[9] Z. Wu, N. Ding, M. Yu et al., "Identification of potential biomarkers for rhegmatogenous retinal detachment associated with choroidal detachment by vitreous iTRAQ-based proteomic profiling," *International Journal of Molecular Sciences*, vol. 17, no. 12, p. 2052, 2016.

[10] C. L. Cioffi, N. Dobri, E. E. Freeman et al., "Design, synthesis, and evaluation of nonretinoid retinol binding protein 4 antagonists for the potential treatment of atrophic age-related macular degeneration and Stargardt disease," *Journal of Medicinal Chemistry*, vol. 57, no. 18, pp. 7731–7757, 2014.

[11] C. L. Cioffi, B. Racz, E. E. Freeman et al., "Bicyclic octahydrocyclopenta pyrrolo antagonists of retinol binding protein 4: potential treatment of atrophic age-related macular degeneration and Stargardt disease," *Journal of Medicinal Chemistry*, vol. 58, no. 15, pp. 5863–5888, 2015.

[12] Y. Wang, X. Meng, and H. Yan, "Niaspan inhibits diabetic retinopathy-induced vascular inflammation by downregulating the tumor necrosis factor-α pathway," *Molecular Medicine Reports*, vol. 15, no. 3, pp. 1263–1271, 2017.

[13] C. Hernández, A. Simó-Servat, P. Bogdanov, and R. Simó, "Diabetic retinopathy: new therapeutic perspectives based on pathogenic mechanisms," *Journal of Endocrinological Investigation*, vol. 40, no. 9, pp. 925–935, 2017.

[14] A. Fiori, V. Terlizzi, H. Kremer et al., "Mesenchymal stromal/stem cells as potential therapy in diabetic retinopathy," *Immunobiology*, vol. 223, no. 12, pp. 729–743, 2018.

[15] M. L. Graham, J. L. Janecek, J. A. Kittredge, B. J. Hering, and H. J. Schuurman, "The streptozotocin-induced diabetic nude mouse model: differences between animals from different sources," *Comparative Medicine*, vol. 61, no. 4, pp. 356–360, 2011.

[16] W. Zakrzewski, M. Dobrzyński, M. Szymonowicz, and Z. Rybak, "Stem cells: past, present, and future," *Stem Cell Research & Therapy*, vol. 10, no. 1, pp. 1–22, 2019.

[17] K. Ben M'Barek and C. Monville, "Cell therapy for retinal dystrophies: from cell suspension formulation to complex retinal tissue bioengineering," *Stem Cells International*, vol. 2019, Article ID 4568979, 14 pages, 2019.

[18] K. B. M'Barek, W. Habeler, and C. Monville, "Stem cell-based RPE therapy for retinal diseases: engineering 3D tissues amenable for regenerative medicine," *Retinal Degenerative Diseases*, vol. 1074, pp. 625–632, 2018.

[19] K.-H. Ryu, S. Y. Kim, Y. R. Kim et al., "Tonsil-derived mesenchymal stem cells alleviate concanavalin A-induced acute liver injury," *Experimental Cell Research*, vol. 326, no. 1, pp. 143–154, 2014.

[20] M. Yuasa, K. Ishiwata, T. Sugio et al., "Herpes simplex virus type 2 fulminant hepatitis after umbilical cord blood transplantation for acute myeloid leukemia," *[Rinsho ketsueki] The Japanese journal of clinical hematology*, vol. 55, no. 6, pp. 682–686, 2014.

[21] T. He, T. E. Peterson, E. L. Holmuhamedov et al., "Human endothelial progenitor cells tolerate oxidative stress due to intrinsically high expression of manganese superoxide dismutase," *Arteriosclerosis, Thrombosis, and Vascular Biology*, vol. 24, no. 11, pp. 2021–2027, 2004.

[22] C. Venegas, J. A. García, G. Escames et al., "Extrapineal melatonin: analysis of its subcellular distribution and daily fluctuations," *Journal of Pineal Research*, vol. 52, no. 2, pp. 217–227, 2012.

[23] E. Dehdashtian, S. Mehrzadi, B. Yousefi et al., "Diabetic retinopathy pathogenesis and the ameliorating effects of melatonin; involvement of autophagy, inflammation and oxidative stress," *Life Sciences*, vol. 193, pp. 20–33, 2018.

[24] R. Jahanban-Esfahlan, S. Mehrzadi, R. J. Reiter et al., "Melatonin in regulation of inflammatory pathways in rheumatoid arthritis and osteoarthritis: involvement of circadian clock genes," *British Journal of Pharmacology*, vol. 175, no. 16, pp. 3230–3238, 2018.

[25] P. Trivedi, G. B. Jena, K. B. Tikoo, and V. Kumar, "Melatonin modulated autophagy and Nrf2 signaling pathways in mice with colitis-associated colon carcinogenesis," *Molecular Carcinogenesis*, vol. 55, no. 3, pp. 255–267, 2016.

[26] T.-S. Jiang, L. Cai, W. Y. Ji et al., "Reconstruction of the corneal epithelium with induced marrow mesenchymal stem cells in rats," *Molecular Vision*, vol. 16, pp. 1304–1316, 2010.

[27] A. Gajdosik, A. Gajdosikova, M. Stefek, J. Navarova, and R. Hozova, "Streptozotocin-induced experimental diabetes in male Wistar rats," *General Physiology and Biophysics*, vol. 18, pp. 54–62, 1999.

[28] A. Akbarzadeh, D. Norouzian, M. R. Mehrabi et al., "Induction of diabetes by streptozotocin in rats," *Indian Journal of Clinical Biochemistry*, vol. 22, no. 2, pp. 60–64, 2007.

[29] M. Cesaretti, M. Ginoza, A. B. Ribeiro, and O. Kohlmann Jr, "Systemic hemodynamic and left ventricular function of diabetic-induced hypertensive rats," *Arquivos Brasileiros de Endocrinologia e Metabologia*, vol. 54, no. 9, pp. 842–851, 2010.

[30] V. Brazão, F. H. Santello, R. P. Colato et al., "Melatonin downregulates steroidal hormones, thymocyte apoptosis and inflammatory cytokines in middle-aged T. cruzi infected rats," *Biochimica et Biophysica Acta (BBA)-Molecular Basis of Disease*, vol. 1866, no. 11, article 165914, 2020.

[31] H. Kajiyama, T. S. Hamazaki, M. Tokuhara et al., "Pdx1-transfected adipose tissue-derived stem cells differentiate into insulin-producing cells in vivo and reduce hyperglycemia in diabetic mice," *International Journal of Developmental Biology*, vol. 54, no. 4, pp. 699–705, 2010.

[32] X. Feng, P. Chen, X. Zhao, J. Wang, and H. Wang, "Transplanted embryonic retinal stem cells have the potential to repair the injured retina in mice," *BMC Ophthalmology*, vol. 21, no. 1, pp. 1–11, 2021.

[33] P. K. Ngoc, P. V. Phuc, T. H. Nhung, D. T. Thuy, and N. T. M. Nguyet, "Improving the efficacy of type 1 diabetes therapy by transplantation of immunoisolated insulin-producing cells," *Human Cell*, vol. 24, no. 2, pp. 86–95, 2011.

[34] N. Ding, S. Luo, J. Yu, Y. Zhou, and Z. Wu, "Vitreous levels of apolipoprotein A1 and retinol binding protein 4 in human rhegmatogenous retinal detachment associated with choroidal detachment," *Molecular Vision*, vol. 24, pp. 252–260, 2018.

[35] M. T. Abdel Aziz, M. A. Wassef, L. A. Rashed, S. Mhfouz, and N. Omar, "Mesenchymal Stem Cells Therapy in Acute Renal Failure: Possible Role of Hepatocyte Growth Factor," *Journal of Stem Cell Research & Therapy*, vol. 1, no. 3, pp. 2–7, 2011.

[36] W. Cheneke, S. Suleman, T. Yemane, and G. Abebe, "Assessment of glycemic control using glycated hemoglobin among diabetic patients in Jimma University specialized hospital, Ethiopia," *BMC Research Notes*, vol. 9, no. 1, pp. 1–10, 2016.

[37] E. Beutler, "Improved method for the determination of blood glutathione," *The Journal of Laboratory and Clinical Medicine*, vol. 61, pp. 882–888, 1963.

[38] J. C. Han and G. Y. Han, "A procedure for quantitative determination of Tris(2-carboxyethyl)phosphine, an odorless reducing agent more stable and effective than dithiothreitol," *Analytical Biochemistry*, vol. 220, no. 1, pp. 5–10, 1994.

[39] S. P. Sichak and A. L. Dounce, "Analysis of the peroxidatic mode of action of catalase," *Archives of Biochemistry and Biophysics*, vol. 249, no. 2, pp. 286–295, 1986.

[40] M. Nishikimi, N. A. Rao, and K. Yagi, "The occurrence of superoxide anion in the reaction of reduced phenazine methosulfate and molecular oxygen," *Biochemical and Biophysical Research Communications*, vol. 46, no. 2, pp. 849–854, 1972.

[41] D. Koracevic, G. Koracevic, V. Djordjevic, S. Andrejevic, and V. Cosic, "Method for the measurement of antioxidant activity in human fluids," *Journal of Clinical Pathology*, vol. 54, no. 5, pp. 356–361, 2001.

[42] J. A. Buege and S. D. Aust, "Microsomal lipid peroxidation," *Methods in Enzymology*, vol. 52, pp. 302–310, 1978.

[43] H. M. Marks, *The Progress of Experiment: Science and Therapeutic Reform in the United States 1900-1990*, Cambridge University Press, 2000.

[44] J. Wang, K. Edeen, R. Manzer et al., "Differentiated human alveolar epithelial cells and reversibility of their phenotype in vitro," *American Journal of Respiratory Cell and Molecular Biology*, vol. 36, no. 6, pp. 661–668, 2007.

[45] H. Dawood Yassa, A. Alsayed Mohammed, A. Saleh Moawad, A. Yahia Sedeak, and G. Hassan Abdelfatah, "Role of stem cell therapy in diabetic cardiomyopathy in rats: histological and immunohistochemical study," *Egyptian Journal of Medical Research*, vol. 2, no. 1, pp. 36–55, 2021.

[46] J. D. Bancroft and M. Gamble, *Theory and practice of histological techniques*, Elsevier health sciences, 2008.

[47] R. Williams, M. Airey, H. Baxter, J. Forrester, T. Kennedy-Martin, and A. Girach, "Epidemiology of diabetic retinopathy and macular oedema: a systematic review," *Eye*, vol. 18, no. 10, pp. 963–983, 2004.

[48] N. Maniadakis and E. Konstantakopoulou, "Cost effectiveness of treatments for diabetic retinopathy: a systematic literature review," *PharmacoEconomics*, vol. 37, no. 8, pp. 995–1010, 2019.

[49] K. W. Lee, S. M. Ching, V. Ramachandran et al., "Prevalence and risk factors of gestational diabetes mellitus in Asia: a systematic review and meta-analysis," *BMC Pregnancy and Childbirth*, vol. 18, no. 1, pp. 1–20, 2018.

[50] J. Tang and T. S. Kern, "Inflammation in diabetic retinopathy," *Progress in Retinal and Eye Research*, vol. 30, no. 5, pp. 343–358, 2011.

[51] A. Sui, X. Chen, A. M. Demetriades et al., "Inhibiting NF-κB signaling activation reduces retinal neovascularization by promoting a polarization shift in macrophages," *Investigative Ophthalmology & Visual Science*, vol. 61, no. 6, pp. 4–4, 2020.

[52] W. P. Miller, S. Sunilkumar, J. F. Giordano, A. L. Toro, A. J. Barber, and M. D. Dennis, "The stress response protein REDD1 promotes diabetes-induced oxidative stress in the retina by Keap1-independent Nrf2 degradation," *Journal of Biological Chemistry*, vol. 295, no. 21, pp. 7350–7361, 2020.

[53] R. G. Miller and T. J. Orchard, "Understanding metabolic memory: a tale of two studies," *Diabetes*, vol. 69, no. 3, pp. 291–299, 2020.

[54] A. R. Santiago, R. Boia, I. D. Aires, A. F. Ambrósio, and R. Fernandes, "Sweet stress: coping with vascular dysfunction in diabetic retinopathy," *Frontiers in Physiology*, vol. 9, p. 820, 2018.

[55] B. Boehm, G. Lang, O. Volpert et al., "Low content of the natural ocular anti-angiogenic agent pigment epithelium-derived factor (PEDF) in aqueous humor predicts progression of diabetic retinopathy," *Diabetologia*, vol. 46, no. 3, pp. 394–400, 2003.

[56] M. Matsuoka, N. Ogata, K. Minamino, A. Higuchi, and M. Matsumura, "High levels of pigment epithelium-derived

factor in the retina of a rat model of type 2 diabetes," *Experimental Eye Research*, vol. 82, no. 1, pp. 172–178, 2006.

[57] B. Wang, P. Atherton, R. Patel, G. Manning, and R. Donnelly, "Antiangiogenic effects and transcriptional regulation of pigment epithelium-derived factor in diabetic retinopathy," *Microvascular Research*, vol. 80, no. 1, pp. 31–36, 2010.

[58] A. N. Witmer, "Vascular endothelial growth factors and angiogenesis in eye disease," *Progress in Retinal and Eye Research*, vol. 22, no. 1, pp. 1–29, 2003.

[59] J. Penn, A. Madan, R. B. Caldwell, M. Bartoli, R. W. Caldwell, and M. E. Hartnett, "Vascular endothelial growth factor in eye disease," *Progress in Retinal and Eye Research*, vol. 27, no. 4, pp. 331–371, 2008.

[60] J. M. Sundstrom, C. Hernández, S. R. Weber et al., "Proteomic analysis of early diabetic retinopathy reveals mediators of neurodegenerative brain diseases," *Investigative Ophthalmology & Visual Science*, vol. 59, no. 6, pp. 2264–2274, 2018.

[61] J. Patel, G. M. Saleh, P. G. Hykin, Z. J. Gregor, and I. A. Cree, "Concentration of haemodynamic and inflammatory related cytokines in diabetic retinopathy," *Eye*, vol. 22, no. 2, pp. 223–228, 2008.

[62] Y. Wu, Y. Zuo, R. Chakrabarti, B. Feng, S. Chen, and S. Chakrabarti, "ERK5 contributes to VEGF alteration in diabetic retinopathy," *Journal of Ophthalmology*, vol. 2010, 11 pages, 2010.

[63] S. Simão, D. B Bitoque, S. M Calado, and G. A Silva, "Oxidative stress modulates the expression of VEGF isoforms in the diabetic retina," *New Frontiers in Ophthalmology*, vol. 2, no. 2, pp. 77–83, 2016.

[64] M. H. Davidson, "Apolipoprotein measurements: is more widespread use clinically indicated," *Clinical Cardiology: An International Indexed and Peer-Reviewed Journal for Advances in the Treatment of Cardiovascular Disease*, vol. 32, no. 9, pp. 482–486, 2009.

[65] R. Simó, M. Higuera, M. García-Ramírez, F. Canals, J. García-Arumí, and C. Hernández, "Elevation of apolipoprotein A-I and apolipoprotein H levels in the vitreous fluid and overexpression in the retina of diabetic patients," *Archives of Ophthalmology*, vol. 126, no. 8, pp. 1076–1081, 2008.

[66] F. Robbesyn, N. Augé, C. Vindis et al., "High-density lipoproteins prevent the oxidized low-density lipoprotein–induced endothelial growth factor receptor activation and subsequent matrix metalloproteinase-2 upregulation," *Arteriosclerosis, Thrombosis, and Vascular Biology*, vol. 25, no. 6, pp. 1206–1212, 2005.

[67] R. Simó, M. García-Ramírez, M. Higuera, and C. Hernández, "Apolipoprotein A1 is overexpressed in the retina of diabetic patients," *American Journal of Ophthalmology*, vol. 147, no. 2, pp. 319–325, 2009.

[68] V. Lambadiari, N. P. E. Kadoglou, V. Stasinos et al., "Serum levels of retinol-binding protein-4 are associated with the presence and severity of coronary artery disease," *Cardiovascular Diabetology*, vol. 13, no. 1, pp. 1–8, 2014.

[69] S. E. Park, D. H. Kim, J. H. Lee et al., "Retinol-binding protein-4 is associated with endothelial dysfunction in adults with newly diagnosed type 2 diabetes mellitus," *Atherosclerosis*, vol. 204, no. 1, pp. 23–25, 2009.

[70] A. Solini, F. Stea, E. Santini et al., "Adipocytokine levels mark endothelial function in normotensive individuals," *Cardiovascular Diabetology*, vol. 11, no. 1, pp. 103–107, 2012.

[71] K. M. Farjo, R. A. Farjo, S. Halsey, G. Moiseyev, and J. X. Ma, "Retinol-binding protein 4 induces inflammation in human endothelial cells by an NADPH oxidase-and nuclear factor kappa B-dependent and retinol-independent mechanism," *Molecular and Cellular Biology*, vol. 32, no. 24, pp. 5103–5115, 2012.

[72] M. Du, L. Otalora, A. A. Martin et al., "Transgenic mice overexpressing serum retinol-binding protein develop progressive retinal degeneration through a retinoid-independent mechanism," *Molecular and Cellular Biology*, vol. 35, no. 16, pp. 2771–2789, 2015.

[73] M. Saberi and S. Gholami, "An investigation on the effects of the Aloe Vera extract on the thickness of the retina in male diabetic rats," *Iranian Journal of Veterinary Research*, vol. 13, no. 41, pp. 296–302, 2012.

[74] R. E. Marc, B. W. Jones, C. B. Watt, F. Vazquez-Chona, D. K. Vaughan, and D. T. Organisciak, "Extreme retinal remodeling triggered by light damage: implications for age related macular degeneration," *Molecular Vision*, vol. 14, pp. 782–806, 2008.

[75] X. Zhang, H. Zeng, S. Bao, N. Wang, and M. C. Gillies, "Diabetic macular edema: new concepts in patho-physiology and treatment," *Cell & Bioscience*, vol. 4, no. 1, pp. 1–14, 2014.

[76] D. do Carmo Buonfiglio, R. A. Peliciari-Garcia, F. G. do Amaral et al., "Early-stage retinal melatonin synthesis impairment in streptozotocin-induced diabetic Wistar rats," *Investigative Ophthalmology & Visual Science*, vol. 52, no. 10, pp. 7416–7422, 2011.

[77] T. Hikichi, N. Tateda, and T. Miura, "Alteration of melatonin secretion in patients with type 2 diabetes and proliferative diabetic retinopathy," *Clinical Ophthalmology (Auckland, NZ)*, vol. 5, p. 655, 2011.

[78] T. Gürpınar, N. Ekerbiçer, N. Uysal, T. Barut, F. Tarakçı, and M. I. Tuglu, "The effects of the melatonin treatment on the oxidative stress and apoptosis in diabetic eye and brain," *The Scientific World Journal*, vol. 2012, 5 pages, 2012.

[79] Y. Ma, Q. Zhao, Y. Shao, M. Z. Cao, M. Zhao, and D. Wang, "Melatonin inhibits the inflammation and apoptosis in rats with diabetic retinopathy via MAPK pathway," *European Review for Medical and Pharmacological Sciences*, vol. 23, 3 Suppl, pp. 1–8, 2019.

[80] B. Djordjevic, T. Cvetkovic, T. J. Stoimenov et al., "Oral supplementation with melatonin reduces oxidative damage and concentrations of inducible nitric oxide synthase, VEGF and matrix metalloproteinase 9 in the retina of rats with streptozotocin/nicotinamide induced pre-diabetes," *European Journal of Pharmacology*, vol. 833, pp. 290–297, 2018.

[81] L. Ba, S. Cao, N. Ji, C. Ma, R. Wang, and D. Luo, "Exogenous melatonin treatment in the postharvest storage of pitaya fruits delays senescence and regulates reactive oxygen species metabolism," *Food Science and Technology*, vol. 42, 2021.

[82] M. S. Singh, S. S. Park, T. A. Albini et al., "Retinal stem cell transplantation: balancing safety and potential," *Progress in Retinal and Eye Research*, vol. 75, article 100779, 2020.

[83] S. N. Bhatia, G. H. Underhill, K. S. Zaret, and I. J. Fox, "Cell and tissue engineering for liver disease," *Science Translational Medicine*, vol. 6, no. 245, p. 245sr2, 2014.

[84] A. J. Rong, B. L. Lam, Z. A. Ansari, and T. A. Albini, "Vision loss secondary to autologous adipose stem cell injections: a rising problem," *JAMA Ophthalmology*, vol. 136, no. 1, pp. 97–99, 2018.

[85] H. Surendran, S. Nandakumar, V. B. Reddy K et al., "Transplantation of retinal pigment epithelium and photoreceptors generated concomitantly via small molecule-mediated differentiation rescues visual function in rodent models of retinal degeneration," *Stem Cell Research & Therapy*, vol. 12, no. 1, pp. 1–17, 2021.

[86] W. Chang, B. W. Song, J. Y. Moon et al., "Anti-death strategies against oxidative stress in grafted mesenchymal stem cells," *Histology and Histopathology*, vol. 28, no. 12, pp. 1529–1536, 2013.

[87] L. Drowley, M. Okada, S. Beckman et al., "Cellular antioxidant levels influence muscle stem cell therapy," *Molecular Therapy*, vol. 18, no. 10, pp. 1865–1873, 2010.

[88] Y. T. Chen, H. J. Chiang, C. H. Chen et al., "Melatonin treatment further improves adipose-derived mesenchymal stem cell therapy for acute interstitial cystitis in rat," *Journal of Pineal Research*, vol. 57, no. 3, pp. 248–261, 2014.

Hindawi
Stem Cells International
Volume 2022, Article ID 7538025, 13 pages
https://doi.org/10.1155/2022/7538025

Review Article

Mesenchymal Stem Cell-Derived Extracellular Vesicles: Immunomodulatory Effects and Potential Applications in Intervertebral Disc Degeneration

Shaojun Hu,[1] Hongyuan Xing,[1] Jiangnan Zhang,[2] Zemin Zhu,[3] Ying Yin,[4] Ning Zhang,[1] and Yiying Qi[1]

[1]*Department of Orthopedics, 2nd Affiliated Hospital, School of Medicine, Zhejiang University, 88 Jiefang Road, Zhejiang, 310009 Hangzhou, China*
[2]*Department of Orthopedics Surgery, Wenling 1st People's Hospital, 190 Taiping South Road, Wenling, 317500 Zhejiang, China*
[3]*People's Hospital of Changxing County, Changxing, 313100 Zhejiang Province, China*
[4]*Department of Gastroenterology, Affiliated Zhongda Hospital of Southeast University, Nanjing, 210000 Jiangsu, China*

Correspondence should be addressed to Ning Zhang; zhangning@zju.edu.cn and Yiying Qi; qiyiying@zju.edu.cn

Received 30 May 2021; Revised 25 November 2021; Accepted 5 January 2022; Published 18 February 2022

Academic Editor: Yu Sheng Li

Intervertebral disc (IVD) degenerative disease is a common health problem worldwide. Administration of mesenchymal stem cells (MSCs) in intervertebral disc degeneration (IVDD) has been widely explored in recent years. However, transplantation of MSCs is restricted by several factors. Currently, paracrine signaling is one of the main mechanisms by which MSCs play a therapeutic role in disc regeneration. Extracellular vehicles (EVs) are the main paracrine products of MSCs. They show great potential as an effective alternative to MSCs and play immunomodulation roles such as anti-inflammatory effects, antioxidative stress, antiapoptosis, and antiextracellular matrix (ECM) degradation during treatment of IVDD. This review focuses on the immunomodulatory effect of MSC EVs and their potential applications.

1. Introduction

Low back pain is a disease that causes high rates if disabilities globally [1]. Intervertebral disc degeneration (IVDD) is a major cause of low back pain. However, the cause of IVDD has not been fully elucidated. Mechanical overloading [2], defective nutrient supply, cell death [3], and progressive fibrosis [4] are associated with progression of IVDD. Studies report that degradation of extracellular matrix is the main factor that causes IVDD and is characterized by increased inflammatory mediators expression [5, 6]. Therefore, several therapeutic approaches for treatment of IVDD are based on reducing matrix degradation and downregulating expression of inflammatory factors within the IVD. Cell therapy has widely been explored as an alternative for treatment of IVDD [7–10]. Therefore, several novel therapies including mesenchymal stem cell (MSC) transplantation have been developed [11]. MSCs are a group of cells with multidirectional differentiation and self-expansion abilities. Studies report that MSCs can differentiate into NP-like cells [12–14]. Therefore, the role of MSCs in disc tissue engineering has been widely explored. A major limitation in IVDD treatment is that its inherently avascular and high osmotic pressure harsh environment limits efficacy of therapeutic agents. Moreover, the dense fibrous ring envelope makes limits entry of cells in large quantities [2, 15]. Notably, only a small percentage of MSCs is eventually integrated into the damaged area during the repair process thus promoting tissue regeneration. Therefore, high efficacy of the treatment is not achieved. Recent studies report that paracrine secretion of mesenchymal stem cells is an important mode of tissue repair [16–18]. Extracellular vehicles (EVs) are the main components of paracrine secretion. They can tolerate harsh environment and play an important role in treatment

of intervertebral disc (IVD) [19]. Therefore, MSC EVs have a higher potential for treatment of IVDD compared with MSCs. Immunomodulatory effects and potential applications of MSC EVs and its advantages over MSC transplants in IVDD are presented in the current review.

2. EVs

EVs are structures released by eukaryotic cells and prokaryotic cells. EVs are vesicles enclosed by a lipid bilayer that cannot replicate and do not contain a functional nucleus.

Studies have characterized three main types of extracellular vesicles including: exosomes, microvesicles and apoptotic bodies (Figure 1). Exosomes are small vesicles with a diameter of 50-200 nm, containing biomolecules such as microRNA (miRNA), which are most widely used and have significant medical application. Secretion of exosome is implicated in endocytosis and exocytosis. Early endosomes are formed by plasma membrane invagination, and then late endosomes are formed by vector selection. At last, multivesicular bodies (MVB) formed and fused with plasma membrane to release the substances contained in it referred as exosomes to the extracellular space [20–22]. Microvesicles are derived from plasma membrane and outward budding and a diameter ranging from 200 to 2000 nm, and they express integrins and CD40 [23, 24] and can regulate ROS and induce cell apoptosis. Apoptotic bodies originate from plasma membrane invagination and have a diameter ranging from 500 to 2000 nm and transport antigen, nuclear fractions, and cell organelles [23, 25, 26]. Although EVs are small in size, their surfaces are rich in lipids and proteins, including transmembrane/GPI-anchored extracellular protein and cytosolic/periplasmic protein with lipid or membrane protein-binding ability. Moreover, EVs carry functional molecules including deoxyribonucleic acid, ribonucleic acid, lipids, metabolites, cytoplasmic substances, and soluble extracellular proteins that are functionally active (such as cytokines, growth factors, and extracellular stroma) [21].

Several studies have explored the important roles of EVs. Previous studies report that EVs play key roles in immune response [27–29]. In addition to carrying proteins such as growth factors and cytokines, EVs can induce different signaling pathways, such as the Wnt and Notch pathways, through their surface ligands [30, 31], which are related to immune inflammation. Further, EVs can transfer and present antigen peptides. Therefore, EVs have high potential in vaccine preparation and use as diagnostic markers owing to their immunogenicity.

EVs are involved in both long and short distance intercellular communication. After being secreted from the cell, a small portion of the EVs membrane ruptures to release its contents, such as growth factors, which are then used in adjacent cells [32]. In addition, EVs can travel between cells, moving to areas adjacent to tissues to function in paracrine way and also to distant body fluids, such as serum, lymph and cerebrospinal fluid, to intercellular communicate [33]. EVs can deliver cargo into the cytoplasm of target cells to perform intercellular communication through membrane fusion [34]. EVs can induce signaling by binding to many differentially exposed receptors on the surface of target cells [35–38]. Alternatively, EVs are transferred to the cytoplasm by endocytosis [39–41] and then discharge its cargo when it fuses with the endocytic membrane [36, 38]. By means of the above, EVs can transmit signal and transport substance to function as intercellular communicator (Figure 2).

Ability of EVs to encapsulate contents and transport them between cells has been widely explored [42–45]. Potential of EVs as drug carriers, known as "natural delivery systems, " has received considerable attention. EVs are structures produced by the body naturally; thus, they are not easily attacked by the immune system and can circulate in the body for a long time. In addition, they can effectively cross natural barriers to transport drugs to the target site.

3. Characteristics and Functions of MSCs

MSCs are pluripotent nonhematopoietic stem cells derived from bone marrow (BM), umbilical cord (UC), placenta, amniotic fluid, fat, dental pulp, and induced pluripotent stem cells (IPSCs) or human embryonic stem cells (ESCs) [46, 47]. Primary BMSCs are plastic-adherent stromal cells with self-renewing ability, which have immunophenotypic strongly positive surface markers such as CD105, CD73, and CD90, but lack markers such as CD45, CD34, CD14, CD11b, and CD19. MSCs are characterized by multidirectional differentiation ability [48, 49], including chondrogenic ability which can be applied in intervertebral disc therapy.

MSCs have high regenerative ability and high immunomodulatory properties. Moreover, they can repair tissue damage and regulate cellular immunity by secreting bioactive substances including exosomes [50, 51]. Previous studies reported that MSCs promote development of immune cells mainly through cellular interactions. However, recent studies report that BMSCs also mediate their therapeutic function through the paracrine system [52, 53]. MSC transplantation has a positive effect on IVD regeneration. Hypoxia promotes differentiation of BMSCs into nucleus pulposus- (NP-) like cells. Notably, the structure of IVD has a unique microenvironment that is highly harsh compared with that of any other tissue. Acidic and high osmotic pressure environment of IVD can affect the function of transplanted cells and promote death of cells [2, 13, 54, 55].

Improved immune compatibility of MSCs has high potential in the field of disc therapy owing to the reduced risk of rejection. However, immunogenicity of BMSCs can be increased by exposure to inflammation and oxidative stress. This reduces their viability and differentiation ability, ultimately affecting the therapeutic application of BMSCs in the nucleus pulposus tissues which are already inflamed [56]. Nucleus pulposus is surrounded by a solid AF envelope. Therefore, it is difficult to transport a large number of MSCs into the NP without causing severe injury to the IVD, which significantly limits its therapeutic effect [15]. Therefore, MSC EVs have high potential as effective delivery vehicles in the intervertebral disc owing to their small size, low immunogenicity, and easy availability.

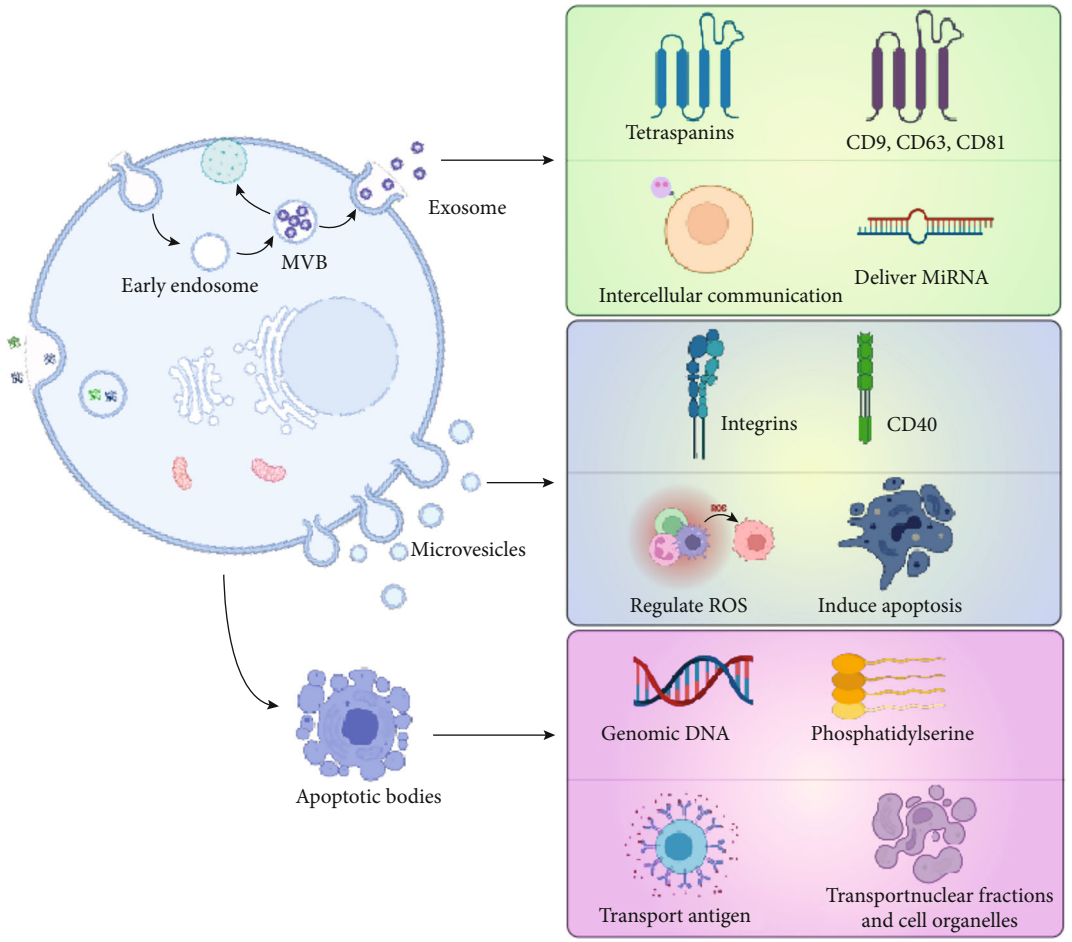

Figure 1: The origin, characteristic, and function of three main types of extracellular vesicles, including exosomes, microvesicles, and apoptotic bodies.

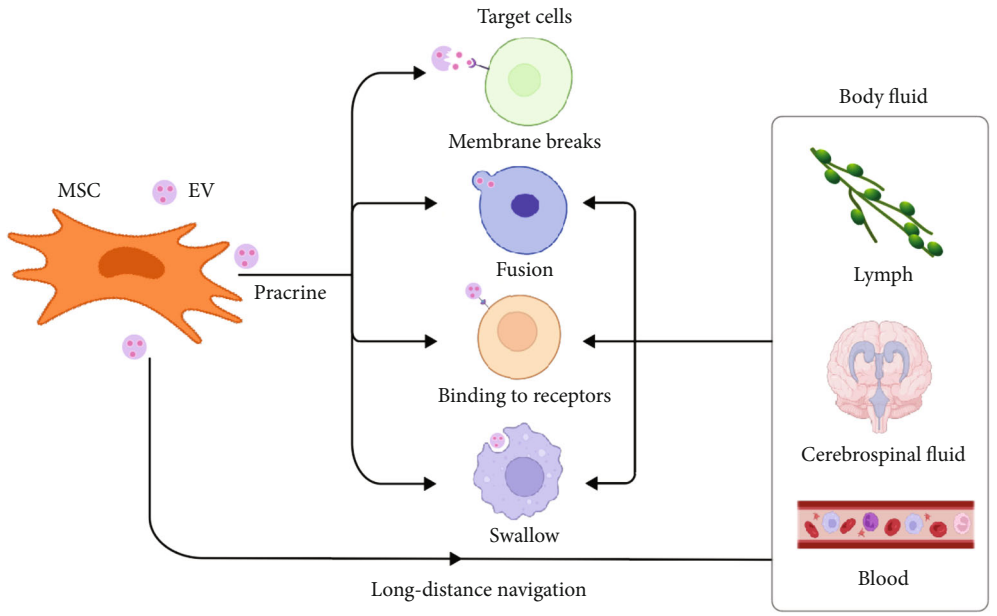

Figure 2: MSC EVs can carry out material transport and transmit signal to adjacent target cells by means of paracrine secretion. Alternatively, they can enter the blood, cerebrospinal fluid, lymph, and other body fluids for long-distance intercellular communication with target cells in other parts of the body.

4. General Characteristics and Functions of MSC EVs

MSC EVs are EVs produced by the paracrine pathway of MSCs. MSCs secrete higher amounts of EVs compared with other types of cells [57]. Several experimental and clinical studies indicate that the therapeutic effect of bone marrow MSCs (BMSCs) is mainly mediated through their paracrine role, especially through EVs [17, 18, 58, 59]. MSCs EVs play immunomodulatory roles through paracrine effects thus transporting small biological molecules. MSC EVs carry complex cargoes similar to EVs, including proteins, nucleic acids and lipids [57]. However, MSC EVs can express tetraspanins such as common exosomal surface markers (CD81, CD63, and CD9) and adhesion molecules (such as CD29, CD44, and CD73) [57, 60]. As a result, MSC EVs play an indispensable role in cell communication, signal transduction, and cytokine delivery. Several growth factors and cytokines expressed by MSCs are transported by EVs as signal peptides; thus, they can be recognized by target cells. This makes MSC EVs an essential part of maintaining vitality and stability of their microenvironment [61].

MSC exosomes are cell-derived but have a very different composition from cell plasma. MSC exosomes are enriched in CD9, CD63, CD81, and HSP70, whereas GM130, calnexin, and cytochrome-C, which are expressed in MSC cells, are not expressed or are under-expressed in exosomes [62]. Zhang et al. explored miRNA profiles of adipose-derived MSC (ADSC) EVs and reported that 148 known miRNAs were present in ADSC EVs [63]. In addition, proteomic analysis of ADSC EVs showed presence of 1466 proteins associated with various cell functions [64]. High expression levels of extracellular proteins in MSC EVs relative to the cytoplasm protect cells affected by inflammation. Studies in leukemia using next-generation sequencing technology indicate that different types of miRNAs are significantly upregulated and downregulated in AML-derived BMSC EVs, implying that MSCs actively package miRNAs into EVs thus playing an immune-related role in disease [65]. These findings indicate that MSC EVs is not passively involved in delivery of cargos, but rather actively transport proteins and RNA from the cytoplasm to exert effects, including anti-inflammatory.

And MSC EVs have a double membrane structure that effectively insulates the contents from the harsh external microenvironment. Therefore, MSC EVs are promising drug-delivery systems for treatment of IVDD.

5. Therapeutic Application of Stem Cell-Derived EVs in Different Tissues

Inflammation, degradation of extracellular matrix, inhibition of cell proliferation, and oxidative stress are key characteristics of IVDD [5, 6, 66]. Therefore, inhibition of overexpression of inflammation, degradation of extracellular matrix, oxidative stress, and cell apoptosis plays a significant role in the treatment of IVDD.

Several diseases exhibit similar immune characteristics to IVDD (Figure 3). High levels of inflammatory cytokines such as IL-1 β, TNF-α, and other inflammation-related factors affect insulin secretion and biosynthesis in diabetic patients [67]. Cord blood-derived MSC EVs and BMSCs EVs inhibit development of helper T1 (Th1) and Th17 cells and shift cytokine production from proinflammatory to anti-inflammatory cytokines. This shift restores the balance between Th1 and Th2 immune responses, thus improving therapy efficacy for type 1 diabetes [68, 69]. Moreover, EVs derived from human BMSCs alleviate type 2 diabetes by inhibiting inflammation [67].

MSC EVs can encapsulate mRNA and miRNAs, enabling MSCs to exert anti-inflammatory and immunomodulatory effects in a variety of tissues and organs [70]. EVs can change their miRNA profile according to the environment and participate in the recovery process of stroke by regulating inflammation by targeting the TGF-β signaling pathway [71–73]. MSC EVs carrying miRNAs can mediate immunity to slow disease progression by mediating oxidative stress in neurodegenerative diseases such as Alzheimer's disease and Parkinson's disease [74]. Liu et al. reported that human UCMSC EVs promote cell proliferation and migration by transferring miR-126 to promote fracture healing under hypoxic conditions [75]. Jing et al. reported that human UCMSCs incubated with kartogenin secrete miR-381-abanent EVs to target TAOK1 thus promoting chondrogenesis by upregulating expression of SOX9, aggrecan, and collagen II genes [76].

In summary, MSC EV agents have high potential in a wide range of diseases, and the therapeutic modalities for each disease may be different and specific, including inhibiting inflammation, inhibition of extracellular matrix decomposition, inhibition of oxidative stress, and promotion of cell proliferation. These phenotypic changes play a positive role in IVDD therapy.

6. Potential Applications of MSC EVs in IVDD

MSC EVs have high potential in treatment of IVDD. Bone marrow, cord blood, and adipose tissue are common sources of MSCs. MSCs from different sources have the ability to regenerate and secrete large amounts of EVs [75–85]. The microenvironment in degenerated IVD has low irrigation and high mechanical stress, low oxygen, high acid, and other factors [15]. Acidic environment can increase intake of EVs and further enhance the role of EVs in repairing original cells in the disc and promoting production of the extracellular matrix. These changes exert significant effect on maintaining the height of the disc and promoting restoration of the internal environment of the disc.

In addition, MSC EVs are natural components of the human body and have low immunogenicity. The lipid bilayer of MSC EVs enables them to overcome the harsh intervertebral disc microenvironment. The small size of MSC EVs allows them to enter the intervertebral disc in large quantities without eliciting an immune response. MSC EVs transport mRNAs, microRNAs, and proteins to regulate the changes in the IVD thus playing a role in maintaining microenvironment stability [86]. These features

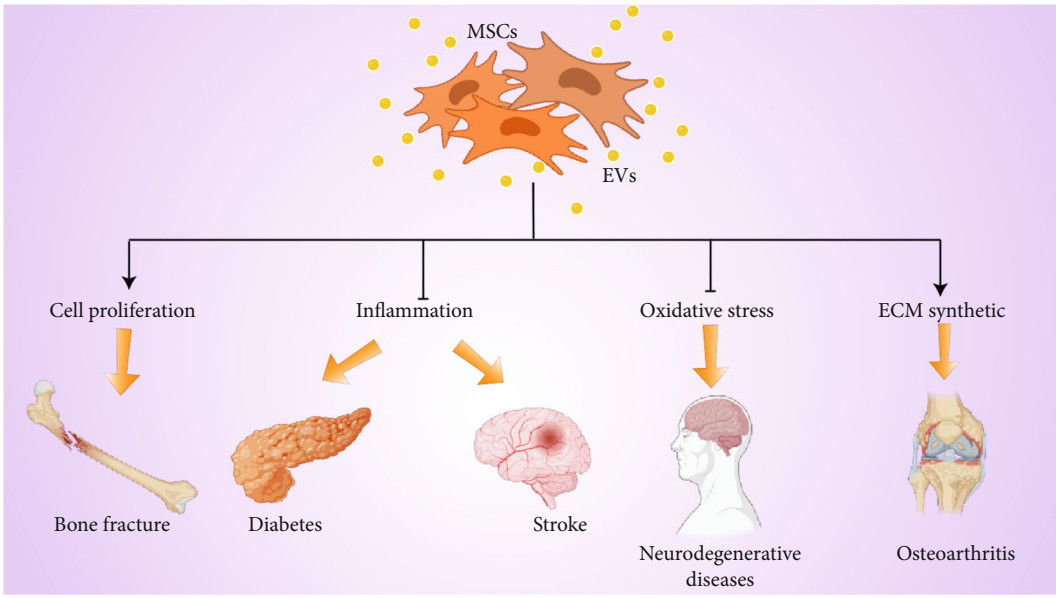

Figure 3: MSC EVs play a therapeutic role in a variety of diseases. MSC EVs repair fractures by promoting cellular cell proliferation, treat diabetes and stroke through anti-inflammatory therapy, treat degenerative neuropathy through antioxidative stress, and treat osteoarthritis by promoting extracellular matrix synthesis.

make EVs a good substitute to alleviate the limitations in IVDD treatment.

The main causes of IVDD include cell death, oxidative stress, loss of extracellular matrix, and accumulation of inflammatory cytokines. The mechanism of EVs in treatment of IVDD is described in the subsequent sections based on these aspects (Figure 4).

6.1. Antioxidative Stress. Overproduction of reactive oxygen species (ROS) is common in degenerative IVD. Oxidative stress promotes progression if IVD by regulating matrix metabolism, proinflammatory phenotype, apoptosis, autophagy, and disc cell senescence. Moreover, oxidative stress enhances matrix degradation and inflammation and reduces the number of viable and functional cells in the IVD microenvironment. In addition, ROS modifies matrix proteins in IVD, leading to oxidative damage of the extracellular matrix of the intervertebral disc and impairing of the mechanical structure and function of IVD [87]. Therefore, inhibition of oxidative stress is a potential mechanism of protecting the degenerated disc.

MSC EVs alleviate IVDD through exerting antioxidant and anti-inflammatory activities [88]. miRNA-31 found in MSC EVs play a significant role in inhibiting calcification in endplate chondrocytes (EPCs) under oxidative stress by targeting the ATF6-related ER-stress pathway. MSC EVs target ATF6-related oxidative stress pathway by delivering miR-31-5p in EPCs to inhibit apoptosis and calcification in EPCs under oxidative stress thus improving the symptoms of IVDD rat model [89]. And Hu has reported that BMSC EVs could reduce ROS and alleviate the inhibitory effect of compression on NP cells proliferation and viability by inhibiting oxidative stress [90].

6.2. Anti-Inflammatory. NP and annulus fibrosus cells, as well as immune system cells (such as macrophages, monocytes, dendritic cells, B lymphocytes, and NK cells), comprise several proinflammatory molecules, leading to changes in the microenvironment of IVD, thus indirectly causing degeneration. Cytokines trigger a series of pathogenic responses that lead to autophagy, senescence, and apoptosis in the IVD [91–94]. NF-κB pathway, MAPK pathway, and Notch pathway are closely related to expression levels of interleukin-1 (IL-1) and tumor necrosis factor-α (TNF-α), which are key factors implicated in IVDD [6]. Therefore, suppression of inflammation, regulation of immunity, and restoration of homeostasis is essential for treatment of IVDD.

Shim et al. reported that EVs secreted by MSCs downregulated expression of various proinflammatory cytokine genes which are associated with degeneration of NP in a coculture of MSCs from the vertebral body and NPCs [14]. Chen reported that NP cells take up BMSC EVs and suppress expression of H_2O_2-induced inflammatory markers such as iNOS and IL-6. Moreover, BMSC EVs suppress H_2O_2-induced NLRP3 inflammasome activation in NP cells and dampen activation of inflammatory factors such as caspase-1, IL-1β, TXNIP, and NLRP3 [88]. Human embryonic MSC EVs increase M2 macrophage infiltration and decrease infiltration of M1 macrophages and M1-associated cytokines, IL-1β, and TNF-α in cartilage tissues [95]. The effect of human embryonic MSC EVs on IVD may be similar to the effect on cartilage tissue owing to the similarity between IVD and cartilage tissue.

6.3. Extracellular Matrix Degradation and Synthesis. Extracellular matrix degradation plays an important role in etiology of IVDD. Inhibition of matrix degradation is an

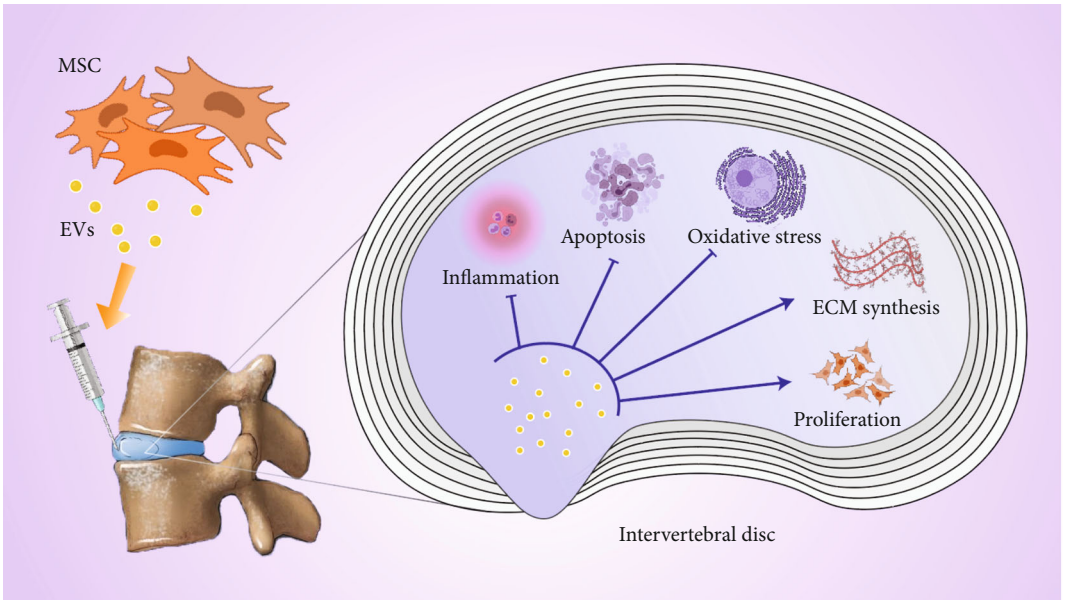

Figure 4: MSC EVs can play a role in anti-inflammatory, antiapoptotic, and antioxidative stress, extracellular matrix synthesis, and cell proliferation in degenerated IVD.

important approach for preventing matrix loss during cell degeneration and can be used to treat the diseased system to protect tissue engineering structures. Therefore, inhibition of matrix degradation and promotion of its synthesis has practical therapeutic implications.

MSCs can effectively promote expression of collagen II and chondroitin sulfate (CS) which are implicated in NP extracellular matrix synthesis [96]. Notably, treatment of NPCs with BMSC EVs upregulated expression of anabolic/matrix protective genes in NPCs such as aggrecan, collagen II, and sox-9. On the contrary, BMSC EVs downregulated expression of matrix-degrading genes (MMP-1 and MMP-3) [97]. These findings indicate that BMSC EVs maintain stability of the matrix in NP cells and protect it from dysregulated gene expression. IVD is characterized by several progenitor cells. BMSC EVs can recruit progenitor cells to the degenerated IVD and induce them into NP cells thus replacing the lost cells and promoting formation of extracellular matrix [97]. Human embryonic MSC EVs highly express CD73/Exto-5′-nucleotidase, which converts extracellular AMP to adenosine. Adenosine induces prosurvival AKT and ERK signaling through interaction with adenosine receptors to further promote cell proliferation, migration, and extracellular matrix secretion [95]. These findings indicate that MSC EVs can be used for treatment of IVDD by increasing the relative amount of extracellular matrix.

6.4. Antiapoptotic and Regenerative Activities of MSC EVs. Abnormal apoptosis-induced np cell death can lead to disorders in metabolism of extracellular matrix in the nucleus pulposus of the intervertebral disc. Therefore, interventions that target apoptosis of NP can inhibit progression of IVDD [98]. Moreover, supportive cell proliferation increases the relative volume of nucleus pulposus cells as a therapeutic strategy for IVDD [99]. Therefore, studies on NP cell apoptosis and regeneration can improve understanding of IVDD and provide a basis for development of potential therapeutic strategies.

Recent studies report that MSC EVs play an important role in inhibiting apoptosis of NP cells. The effect of BMSC EVs on H_2O_2-induced apoptosis of NP cells was previously explored. The levels of apoptotic proteins such as caspase-3 and caspase-9 increased after H_2O_2 treatment but the expression of these proteins was downregulated by BMSC EV treatment [88]. BMSC EVs increase the level of autophagy in NPCs and decrease apoptosis level by upregulating the miR-155 expression, which targets Bach1 in NPCs and promotes expression level of HO-1 thus abrogating IVDD [100].

Studies report that MSC EVs play a role in regeneration in IVDD. Previous findings indicated that PCNA+ cells were significantly increased, and CCP3+ cells were significantly decreased in cartilage tissue in the exosome-treated group after 12 weeks compared with the control group. This indicated that human embryonic stem cell-derived MSC EVs promoted proliferation of chondrocytes. MSC EVs can promote proliferation of NP cells and reduce apoptosis in IVDD owing to the similarity between IVD and cartilage tissue [95]. Notably, previous findings from CCK8 assay showed that the NPC proliferation rate increases with increase in the duration of interaction after treatment of BMSC EVs [97].

7. miRNA of MSC EVs Treating IVDD

MicroRNAs (miRNAs) is a class of short, endogenously initiated noncoding RNA. They are involved in regulation of gene expression at the posttranscriptional level through recognition of cognate sequences and interference of transcriptional, translational, or epigenetic processes [101, 102].

As components of EVs that play a major role in intercellular communication, miRNAs affect cell survival by altering the levels of components essential to life [103]. Katsuda and Ochiya reported that MSC exosomal miRNAs are associated with several MSC EV-mediated cellular activities, such as antiangiogenesis, antiapoptosis, immunomodulation, and antifibrosis [104]. This indicates that MSC EVs can be used as vehicles for gene transmission, thus exerting a positive effect on IVDD by delivering miRNA.

7.1. MiR-23. A previous study showed that high expression level of miR-23a-3p in human BMSCs EVs can promote cartilage regeneration and heal cartilage defects in vivo by increasing PTEN levels and upregulating AKT expression [105]. Moreover, Mir-23a-3p carried passively by MSC EVs can promote migration, proliferation, and differentiation of chondrocytes.

7.2. MiR-140. EVs derived from miR-140-5p-overexpressing synovial mesenchymal stem cells induce chondrocyte proliferation and migration without reducing ECM secretion. This implies that EVs can exert a similar effect on NPCs as that observed in articular cartilage. Furthermore, miR-140-5p promotes matrix synthesis by upregulating SOX9 and aggrecan expression through targeted inhibition of RALA [106]. Notably, miR-140 (miR-140-3p) inhibits apoptosis by regulating the regenerative role of KLF5/N-cadherin/MDM2/Slug axis in IVDD [107]. Studies report that miR-140 exerts beneficial effect on chondrocytes and cartilage matrix. MSC EVs are promising cargo carriers for miR-140 delivery for treatment of osteoarthritis by remodeling cartilage matrix without any unwanted immune responses [108].

7.3. MiR-25. Recent studies indicate that miR-25-3p-overexpressing BMSCs secrete miR-25-3p through EVs [109]. Notably, miRNA-25-3p delays progression of IVDD by inhibiting IL-1β-induced inflammation effects [110]. In addition, miR-25-3p regulates cartilage homeostasis by targeting ECM degradation and is thus a potential therapy for IVDD [111]. MiR-25 protects NPCs against apoptosis in IVDD by targeting SUMO2 [112]. These findings indicate that EVs derived from mir-25-3p-overexpressing BMSCs have high potential for development of IVDD therapy.

7.4. MiR-142. BMSC EVs actively packaged with miR-142-3p inhibit MAPK signaling by targeting MLK3 thus alleviating IL-1-mediated inflammatory injury of NPCs [113]. Furthermore, miR-142-3p promotes expression of HMGB1, induces proliferation and migration of cartilage endplate (CEP) cells, and inhibits apoptosis of CEP cells by promoting autophagy [114]. Moreover, miR-142-3p inhibits activation of NF-κB and JNK pathways thus inhibiting inflammation and apoptosis of NPCs in degenerated IVD [113, 115].

8. Discussion

8.1. Prospects. Several effective drugs for degenerative diseases have been developed in the recent past which makes treatment of degenerative diseases more diversified. However, most advanced drugs do not reach their targets owing to the harsh microenvironment. Thus, efficient drug vehicles should be developed to transport the drug through the microenvironment while maintaining its stability and efficient delivery to its target.

EVs can be used to circumvent the limitations of traditional drugs, including poor water solubility, poor biocompatibility, low permeability to cells, unsatisfactory distribution, and effective elimination in vivo. EVs have a natural targeting ability and high biological barrier permeability; thus, they can efficiently deliver drugs to their targets.

Biocompatibility of MSC-EV plays a significant role in minimizing adverse manifestations including immune reactions [116–118]. They deliver cargo to target cells through a series of surface adhesion proteins and carrier ligands. Moreover, MSC EVs can effectively permeate cell membranes to deliver their contents to target cells in vivo. In addition, EVs can deliver a variety of bioactive substances and easy-to-deactivate or easily degradable ingredients through multiple pathways and sites. They safely transfer these substances to target cells thus modulating several processes such as tissue repair and immune response [119]. Nanotechnology has high potential as it is characterized by targeting of drugs to specific sites and controlled-release of drugs to minimize side effects. EVs combine the advantages of nanomaterials and biological delivery system thus improving drug delivery [120]. EVs show great therapeutic potential when used in combination with hydrogel, thus timely transport of cargos with short half-lives can be achieved in vivo. Long-term retention and controlled release of extracellular vesicles in vivo is a novel research approach for treatment of IVDD using combinations of EVs and hydrogels.

MSCs are characterized by several limitations when directly transplanted in vivo. Nongenetically modified bone marrow mesenchymal stem cells may exhibit chromosomal abnormalities during an early passage, resulting in formation of malignant tumors [121]. Notably, studies have not explored the tumorigenesis potential of MSC-EVs [122]. Acquisition and amplification of MSCs result in mixing with other cells, resulting in low purity and cellular senescence during amplification process. Transplanted MSCs decrease with decrease in metabolic level, and their repairability is weakened over time [123]. In vitro ability of MSCs to differentiate and proliferate decreases gradually in culture [124, 125]. These limitations affect survival and differentiation of MSCs. Moreover, the actual number of NPCs differentiated from MSC in the IVD after MSC transplantation is not high. Recent studies report that MSC transplantation may not secrete products that inhibit inflammatory responses during MSC transplantation in IVD [126].

MSC EV therapy is an effective alternative for traditional MSC therapy for repair of IVDD. Paracrine activity of MSCs plays a major role in therapeutic effect compared with use of MSCs s [127]. EVs are significantly relative to MSCs in volume and are suitable for use in narrow IVD environments, implying that transplanting EVs into IVD potentially causes less damage compared with implanting MSCs [128]. In addition, MSCs can produce continuously abundant EVs when

making immortal cell lines. This implies that MSCs can consistently and repeatedly produce EVs for experimental and clinical applications. Furthermore, MSCs can be modified to upregulate expression of specific miRNAs in the EVs, this abrogating progression of IVDD [129]. Moreover, EVs have potential ability for tissue regeneration. Studies report that MSC EVs present high potential for treatment of osteoarthritis [130]. Notably, MSC EVs enhance periodontal ligament cell function and stimulate periodontal regeneration [131]. MSC EVs promote proliferation, migration, and tenogenic differentiation of tendon stem or progenitor cells [132]. Therefore, further studies should explore the regenerative capacity of MSC-EV on intervertebral disc tissue.

8.2. Limitations of Application of MSC EVs. MSC EVs have been used clinically in some fields. MSC EVs can be used as early prediction tools for preclinical trials. Further, they are used to effectively detect drug effects in humans [133]. However, application of MSC EVs is associated with a few limitations; thus, they are not widely used in clinical trials.

Firstly, a unified standard should be formulated when extracting and storing EVs. A major challenge in converting MSC-EV formulations into experimental therapeutic products is determining the specific ability or capability of a product to achieve a particular biological effect which is referred as the potency metrics [134]. Development of quantifiable, robust, and reproducible parameters to predict the therapeutic efficacy of MSC-EVS can help address this issue in analysis of MSC-EVs [135]. Studies have found that the biological activity and the morphology of EVs will still be impacted in 4 weeks when stored in a comprehensive storage way. Standardized procedures for isolating and storing EVs still need to be developed customized for EV matrix and application technologies, reagents and storage containers, and storage times [136]. Therefore, developing the storage stability of EVs from multiple perspectives, especially the long-term stability, is significant.

Secondly, the reported efficacy of MSC-EVs formulations for multiple diseases is complex and varied. Thus, to develop potency analyses, it is important to identify and quantify the most relevant EV properties expected to be biologically active in EV-mediated therapy [137]. Some studies have found that EVs rely on their miRNA for therapeutic effects, and since EVs carry many different types of miRNAs, the role of miRNAs of various EV sources in the intervertebral disc should be explored further.

Thirdly, in vivo safety of MSC EVs should be determined in preclinical trials. Further, clinical use of MSC EVs should be explored further.

9. Conclusion

Cell therapy is widely used in treatment of IVDD. Previous studies reported that MSCs alleviated IVDD through differentiation of MSC cells into NPC cells, which promoted regeneration of IVD. However, recent studies report that paracrine activity of MSCs plays a major role in alleviating IVDD. MSC EVs are products of MSC secretion that can perfectly replace MSC in development of IVDD therapy. MSC EVs are promising products in acellular therapy. They can secrete several factors thus promoting cell proliferation and antiapoptosis, regulating the microenvironment, and thus reducing the impact of factors such as inflammatory cues in IVDD. MSC EVs can adapt to the harsh microenvironment of IVDs, overcoming in the limitations of MSC transplantation. Further, MSC EVs can be used in drug delivery to maintain the stability of the drug in the harsh microenvironment of IVD. In summary, MSC EVs play a significant role in treatment of IVDD.

Data Availability

Data sharing is not applicable to this article as no new data was created or analyzed in this study.

Consent

All authors provided consent to the publication of this work.

Conflicts of Interest

The authors declare that they have no competing interests.

Authors' Contributions

Shaojun Hu and Hongyuan Xing contributed equally to this work. All authors reviewed the manuscript and approved the final manuscript. Ning Zhang and Yiying Qi conceived the hypothesis and contributed to the preparation of the final version of the manuscript.

Acknowledgments

This work was supported by the National Natural Science Foundation of China (grant Nos. 81603126 and 81972514).

References

[1] T. Vos, C. Allen, M. Arora et al., "Global, regional, and national incidence, prevalence, and years lived with disability for 310 diseases and injuries, 1990-2015: a systematic analysis for the Global Burden of Disease Study 2015," *The Lancet*, vol. 388, no. 10053, pp. 1545–1602, 2016.

[2] D. Sakai and G. B. Andersson, "Stem cell therapy for intervertebral disc regeneration: obstacles and solutions," *Nature Reviews Rheumatology*, vol. 11, no. 4, pp. 243–256, 2015.

[3] M. Adams and P. Dolan, "Could sudden increases in physical activity cause degeneration of intervertebral discs?," *The Lancet*, vol. 350, no. 9079, pp. 734-735, 1997.

[4] F. Williams, A. Bansal, J. van Meurs et al., "Novel genetic variants associated with lumbar disc degeneration in northern Europeans: a meta-analysis of 4600 subjects," *Annals of the Rheumatic Diseases*, vol. 72, no. 7, pp. 1141–1148, 2013.

[5] J. A. Hoyland, C. Le Maitre, and A. J. Freemont, "Investigation of the role of IL-1 and TNF in matrix degradation in the intervertebral disc," *Rheumatology*, vol. 47, no. 6, pp. 809–814, 2008.

[6] M. V. Risbud and I. M. Shapiro, "Role of cytokines in intervertebral disc degeneration: pain and disc content," *Nature Reviews Rheumatology*, vol. 10, no. 1, pp. 44–56, 2014.

[7] D. Sakai, Y. Nakamura, T. Nakai et al., "Exhaustion of nucleus pulposus progenitor cells with ageing and degeneration of the intervertebral disc," *Nature Communications*, vol. 3, article 1264, 2012.

[8] T. Tsai, B. Nelson, P. Anderson, T. Zdeblick, and W. Li, "Intervertebral disc and stem cells cocultured in biomimetic extracellular matrix stimulated by cyclic compression in perfusion bioreactor," *The Spine Journal*, vol. 14, no. 9, pp. 2127–2140, 2014.

[9] W. Chen, W. Lo, J. Lee et al., "Tissue-engineered intervertebral disc and chondrogenesis using human nucleus pulposus regulated through TGF-beta1 in platelet-rich plasma," *Journal of Cellular Physiology*, vol. 209, no. 3, pp. 744–754, 2006.

[10] C. L. Korecki, J. M. Taboas, R. S. Tuan, and J. C. Iatridis, "Notochordal cell conditioned medium stimulates mesenchymal stem cell differentiation toward a young nucleus pulposus phenotype," *Stem Cell Research & Therapy*, vol. 1, no. 2, p. 18, 2010.

[11] C. Centeno, J. Markle, E. Dodson et al., "Treatment of lumbar degenerative disc disease-associated radicular pain with culture-expanded autologous mesenchymal stem cells: a pilot study on safety and efficacy," *Journal of Translational Medicine*, vol. 15, no. 1, p. 197, 2017.

[12] C. Han, C. Jiang, C. Yu, and H. Shen, "Differentiation of transforming growth factor β1-induced mesenchymal stem cells into nucleus pulposus-like cells under simulated microgravity conditions," *Cellular and Molecular Biology*, vol. 61, no. 2, pp. 50–55, 2015.

[13] J. V. Stoyanov, B. Gantenbein-Ritter, A. Bertolo et al., "Role of hypoxia and growth and differentiation factor-5 on differentiation of human mesenchymal stem cells towards intervertebral nucleus pulposus-like cells," *European Cells & Materials*, vol. 21, pp. 533–547, 2011.

[14] E. Shim, J. Lee, D. Kim et al., "Autogenous mesenchymal stem cells from the vertebral body enhance intervertebral disc regeneration via paracrine interaction: an in vitro pilot study," *Cell Transplantation*, vol. 25, no. 10, pp. 1819–1832, 2016.

[15] V. Leung, D. Chan, and K. Cheung, "Regeneration of intervertebral disc by mesenchymal stem cells: potentials, limitations, and future direction," *European Spine Journal*, vol. 15, no. S3, Supplement 3, pp. S406–S413, 2006.

[16] S. Al-Khawaga and E. M. Abdelalim, "Potential application of mesenchymal stem cells and their exosomes in lung injury: an emerging therapeutic option for COVID-19 patients," *Stem Cell Research & Therapy*, vol. 11, no. 1, p. 437, 2020.

[17] J. L. Spees, R. H. Lee, and C. A. Gregory, "Mechanisms of mesenchymal stem/stromal cell function," *Stem Cell Research & Therapy*, vol. 7, no. 1, p. 125, 2016.

[18] S. Keshtkar, N. Azarpira, and M. H. Ghahremani, "Mesenchymal stem cell-derived extracellular vesicles: novel frontiers in regenerative medicine," *Stem Cell Research & Therapy*, vol. 9, no. 1, p. 63, 2018.

[19] C. Le Maitre, A. Binch, A. Thorpe, and S. Hughes, "Degeneration of the intervertebral disc with new approaches for treating low back pain," *Journal of Neurosurgical Sciences*, vol. 59, no. 1, pp. 47–61, 2015.

[20] H. F. Heijnen, A. E. Schiel, R. Fijnheer, H. J. Geuze, and J. J. Sixma, "Activated platelets release two types of membrane vesicles: microvesicles by surface shedding and exosomes derived from exocytosis of multivesicular bodies and alpha-granules," *Blood*, vol. 94, no. 11, pp. 3791–3799, 1999.

[21] C. Thery, K. W. Witwer, E. Aikawa et al., "Minimal information for studies of extracellular vesicles 2018 (MISEV2018): a position statement of the International Society for Extracellular Vesicles and update of the MISEV2014 guidelines," *Journal of Extracellular Vesicles*, vol. 7, no. 1, article 1535750, 2018.

[22] D. K. Jeppesen, A. M. Fenix, J. L. Franklin et al., "Reassessment of exosome composition," *Cell*, vol. 177, no. 2, pp. 428–445.e18, 2019.

[23] H. Shao, H. Im, C. Castro, X. Breakefield, R. Weissleder, and H. Lee, "New technologies for analysis of extracellular vesicles," *Chemical Reviews*, vol. 118, no. 4, pp. 1917–1950, 2018.

[24] H. Deng, C. Sun, Y. Sun et al., "Lipid, protein, and MicroRNA composition within mesenchymal stem cell-derived exosomes," *Cellular Reprogramming*, vol. 20, no. 3, pp. 178–186, 2018.

[25] L. Mashouri, H. Yousefi, A. Aref, A. Ahadi, F. Molaei, and S. Alahari, "Exosomes: composition, biogenesis, and mechanisms in cancer metastasis and drug resistance," *Molecular Cancer*, vol. 18, no. 1, p. 75, 2019.

[26] J. Akers, D. Gonda, R. Kim, B. Carter, and C. Chen, "Biogenesis of extracellular vesicles (EV): exosomes, microvesicles, retrovirus-like vesicles, and apoptotic bodies," *Journal of Neuro-Oncology*, vol. 113, no. 1, pp. 1–11, 2013.

[27] U. Gehrmann, T. Näslund, S. Hiltbrunner, P. Larssen, and S. Gabrielsson, "Harnessing the exosome-induced immune response for cancer immunotherapy," *Seminars in Cancer Biology*, vol. 28, pp. 58–67, 2014.

[28] P. Kurywchak, J. Tavormina, and R. Kalluri, "The emerging roles of exosomes in the modulation of immune responses in cancer," *Genome Medicine*, vol. 10, no. 1, p. 23, 2018.

[29] P. Robbins and A. Morelli, "Regulation of immune responses by extracellular vesicles," *Nature reviews Immunology*, vol. 14, no. 3, pp. 195–208, 2014.

[30] R. Johnstone, "Maturation of reticulocytes: formation of exosomes as a mechanism for shedding membrane proteins," *Biochimie et biologie cellulaire*, vol. 70, no. 3-4, pp. 179–190, 1992.

[31] A. Zomer, T. Vendrig, E. Hopmans, M. van Eijndhoven, J. Middeldorp, and D. Pegtel, "Exosomes: fit to deliver small RNA," *Communicative & integrative Biology*, vol. 3, no. 5, pp. 447–450, 2010.

[32] G. Schiera, P. Proia, C. Alberti, M. Mineo, G. Savettieri, and I. Di Liegro, "Neurons produce FGF2 and VEGF and secrete them at least in part by shedding extracellular vesicles," *Journal of Cellular and Molecular Medicine*, vol. 11, no. 6, pp. 1384–1394, 2007.

[33] M. Jakubec, J. Maple-Grodem, S. Akbari, S. Nesse, O. Halskau, and A. E. Mork-Jansson, "Plasma-derived exosome-like vesicles are enriched in lyso-phospholipids and pass the blood-brain barrier," *PLoS One*, vol. 15, no. 9, article e0232442, 2020.

[34] M. Gabrielli, N. Battista, L. Riganti et al., "Active endocannabinoids are secreted on extracellular membrane vesicles," *EMBO Reports*, vol. 16, no. 2, pp. 213–220, 2015.

[35] L. Chen and D. R. Brigstock, "Integrins and heparan sulfate proteoglycans on hepatic stellate cells (HSC) are novel receptors for HSC-derived exosomes," *FEBS Letters*, vol. 590, no. 23, pp. 4263–4274, 2016.

[36] K. C. French, M. A. Antonyak, and R. A. Cerione, "Extracellular vesicle docking at the cellular port: extracellular vesicle

binding and uptake," *Seminars in Cell & Developmental Biology*, vol. 67, pp. 48–55, 2017.

[37] L. A. Mulcahy, R. C. Pink, and D. R. Carter, "Routes and mechanisms of extracellular vesicle uptake," *Journal of Extracellular Vesicles*, vol. 3, no. 1, 2014.

[38] I. Prada, L. Amin, R. Furlan, G. Legname, C. Verderio, and D. Cojoc, "A new approach to follow a single extracellular vesicle-cell interaction using optical tweezers," *BioTechniques*, vol. 60, no. 1, pp. 35–41, 2016.

[39] J. P. Lim and P. A. Gleeson, "Macropinocytosis: an endocytic pathway for internalising large gulps," *Immunology and Cell Biology*, vol. 89, no. 8, pp. 836–843, 2011.

[40] I. Prada and J. Meldolesi, "Binding and fusion of extracellular vesicles to the plasma membrane of their cell targets," *International Journal of Molecular Sciences*, vol. 17, no. 8, p. 1296, 2016.

[41] T. Tian, Y. L. Zhu, Y. Y. Zhou et al., "Exosome uptake through clathrin-mediated endocytosis and macropinocytosis and mediating miR-21 delivery," *The Journal of Biological Chemistry*, vol. 289, no. 32, pp. 22258–22267, 2014.

[42] S. el Andaloussi, S. Lakhal, I. Mäger, and M. Wood, "Exosomes for targeted siRNA delivery across biological barriers," *Advanced Drug Delivery Reviews*, vol. 65, no. 3, pp. 391–397, 2013.

[43] C. Lai and X. Breakefield, "Role of exosomes/microvesicles in the nervous system and use in emerging therapies," *Frontiers in Physiology*, vol. 3, p. 228, 2012.

[44] R. Lai, R. Yeo, K. Tan, and S. Lim, "Exosomes for drug delivery – a novel application for the mesenchymal stem cell," *Biotechnology Advances*, vol. 31, no. 5, pp. 543–551, 2013.

[45] L. Alvarez-Erviti, Y. Seow, H. Yin, C. Betts, S. Lakhal, and M. Wood, "Delivery of siRNA to the mouse brain by systemic injection of targeted exosomes," *Nature Biotechnology*, vol. 29, no. 4, pp. 341–345, 2011.

[46] T. Zhou, Z. Yuan, J. Weng et al., "Challenges and advances in clinical applications of mesenchymal stromal cells," *Journal of Hematology & Oncology*, vol. 14, no. 1, p. 24, 2021.

[47] M. Xu, G. Shaw, M. Murphy, and F. Barry, "Induced pluripotent stem cell-derived mesenchymal stromal cells are functionally and genetically different from bone marrow-derived mesenchymal stromal cells," *Stem Cells*, vol. 37, no. 6, pp. 754–765, 2019.

[48] F. J. Vizoso, N. Eiro, L. Costa et al., "Mesenchymal stem cells in homeostasis and systemic diseases: hypothesis, evidences, and therapeutic opportunities," *International Journal of Molecular Sciences*, vol. 20, no. 15, p. 3738, 2019.

[49] D. Mushahary, A. Spittler, C. Kasper, V. Weber, and V. Charwat, "Isolation, cultivation, and characterization of human mesenchymal stem cells," *Cytometry Part A*, vol. 93, no. 1, pp. 19–31, 2018.

[50] O. Andrukhov, C. Behm, A. Blufstein, and X. Rausch-Fan, "Immunomodulatory properties of dental tissue-derived mesenchymal stem cells: implication in disease and tissue regeneration," *World Journal of Stem Cells*, vol. 11, no. 9, pp. 604–617, 2019.

[51] Y. Shi, Y. Wang, Q. Li et al., "Immunoregulatory mechanisms of mesenchymal stem and stromal cells in inflammatory diseases," *Nature Reviews Nephrology*, vol. 14, no. 8, pp. 493–507, 2018.

[52] R. H. Lee, A. A. Pulin, M. J. Seo et al., "Intravenous hMSCs improve myocardial infarction in mice because cells embolized in lung are activated to secrete the anti-inflammatory protein TSG-6," *Cell Stem Cell*, vol. 5, no. 1, pp. 54–63, 2009.

[53] A. I. Caplan and D. Correa, "The MSC: an injury drugstore," *Cell Stem Cell*, vol. 9, no. 1, pp. 11–15, 2011.

[54] C. Liang, H. Li, Y. Tao et al., "Responses of human adipose-derived mesenchymal stem cells to chemical microenvironment of the intervertebral disc," *Journal of Translational Medicine*, vol. 10, no. 1, p. 49, 2012.

[55] K. Wuertz, K. Godburn, C. Neidlinger-Wilke, J. Urban, and J. C. Iatridis, "Behavior of mesenchymal stem cells in the chemical microenvironment of the intervertebral disc," *Spine*, vol. 33, no. 17, pp. 1843–1849, 2008.

[56] L. Barrachina, A. R. Remacha, A. Romero et al., "Priming equine bone marrow-derived mesenchymal stem cells with Proinflammatory cytokines: implications in immunomodulation-immunogenicity balance, cell viability, and differentiation potential," *Stem Cells and Development*, vol. 26, no. 1, pp. 15–24, 2017.

[57] B. Yu, X. Zhang, and X. Li, "Exosomes derived from mesenchymal stem cells," *International Journal of Molecular Sciences*, vol. 15, no. 3, pp. 4142–4157, 2014.

[58] A. Andrzejewska, S. Dabrowska, B. Lukomska, and M. Janowski, "Mesenchymal stem cells for neurological disorders," *Advanced Science*, vol. 8, no. 7, article 2002944, 2021.

[59] I. L. Colao, R. Corteling, D. Bracewell, and I. Wall, "Manufacturing exosomes: a promising therapeutic platform," *Trends in Molecular Medicine*, vol. 24, no. 3, pp. 242–256, 2018.

[60] M. Colombo, G. Raposo, and C. Thery, "Biogenesis, secretion, and intercellular interactions of exosomes and other extracellular vesicles," *Annual Review of Cell and Developmental Biology*, vol. 30, pp. 255–289, 2014.

[61] R. Lai, R. Yeo, and S. Lim, "Mesenchymal stem cell exosomes," *Seminars in Cell & Developmental Biology*, vol. 40, pp. 82–88, 2015.

[62] R. Samaeekia, B. Rabiee, I. Putra et al., "Effect of human corneal mesenchymal stromal cell-derived exosomes on corneal epithelial wound healing," *Investigative Ophthalmology & Visual Science*, vol. 59, no. 12, pp. 5194–5200, 2018.

[63] Y. Zhang, M. Yu, M. Dai et al., "miR-450a-5p within rat adipose tissue exosome-like vesicles promotes adipogenic differentiation by targeting WISP2," *Journal of Cell Science*, vol. 130, no. 6, pp. 1158–1168, 2017.

[64] J. Ni, H. Li, Y. Zhou et al., "Therapeutic potential of human adipose-derived stem cell exosomes in stress urinary incontinence-an in vitro and in vivo study," *Cellular Physiology and Biochemistry*, vol. 48, no. 4, pp. 1710–1722, 2018.

[65] J. Barrera-Ramirez, J. R. Lavoie, H. B. Maganti et al., "MicroRNA profiling of exosomes from marrow-derived mesenchymal stromal cells in patients with acute myeloid leukemia: implications in leukemogenesis," *Stem Cell Reviews and Reports*, vol. 13, no. 6, pp. 817–825, 2017.

[66] C. Ruiz-Fernández, V. Francisco, J. Pino et al., "Molecular relationships among obesity, inflammation and intervertebral disc degeneration: are adipokines the common link?," *International Journal of Molecular Sciences*, vol. 20, no. 8, p. 2030, 2019.

[67] M. Y. Donath, C. A. Dinarello, and T. Mandrup-Poulsen, "Targeting innate immune mediators in type 1 and type 2 diabetes," *Nature Reviews Immunology*, vol. 19, no. 12, pp. 734–746, 2019.

[68] F. Ezquer, M. Ezquer, D. Contador, M. Ricca, V. Simon, and P. Conget, "The antidiabetic effect of mesenchymal stem cells is unrelated to their transdifferentiation potential but to their capability to restore Th1/Th2 balance and to modify the pancreatic microenvironment," *Stem Cells*, vol. 30, no. 8, pp. 1664–1674, 2012.

[69] Y. Zhao, Z. Jiang, T. Zhao et al., "Reversal of type 1 diabetes via islet β cell regeneration following immune modulation by cord blood-derived multipotent stem cells," *BMC Medicine*, vol. 10, no. 1, p. 3, 2012.

[70] D. Phinney and M. Pittenger, "Concise review: MSC-derived exosomes for cell-free therapy," *Stem Cells*, vol. 35, no. 4, pp. 851–858, 2017.

[71] K. Jeyaseelan, K. Lim, and A. Armugam, "MicroRNA expression in the blood and brain of rats subjected to transient focal ischemia by middle cerebral artery occlusion," *Stroke*, vol. 39, no. 3, pp. 959–966, 2008.

[72] T. Lusardi, S. Murphy, J. Phillips et al., "MicroRNA responses to focal cerebral ischemia in male and female mouse brain," *Frontiers in Molecular Neuroscience*, vol. 7, p. 11, 2014.

[73] F. Liu, K. Lim, P. Kaur et al., "microRNAs involved in regulating spontaneous recovery in embolic stroke model," *PLoS One*, vol. 8, no. 6, article e66393, 2013.

[74] X. Wang, Y. Zhou, Q. Gao et al., "The role of Exosomal microRNAs and oxidative stress in neurodegenerative diseases," *Oxidative Medicine and Cellular Longevity*, vol. 2020, Article ID 3232869, 17 pages, 2020.

[75] W. Liu, L. Li, Y. Rong et al., "Hypoxic mesenchymal stem cell-derived exosomes promote bone fracture healing by the transfer of miR-126," *Acta Biomaterialia*, vol. 103, pp. 196–212, 2020.

[76] H. Jing, X. Zhang, K. Luo et al., "miR-381-abundant small extracellular vesicles derived from kartogenin- preconditioned mesenchymal stem cells promote chondrogenesis of MSCs by targeting TAOK1," *Biomaterials*, vol. 231, article 119682, 2020.

[77] B. Gyorgy, T. G. Szabo, M. Pasztoi et al., "Membrane vesicles, current state-of-the-art: emerging role of extracellular vesicles," *Cellular and Molecular Life Sciences*, vol. 68, no. 16, pp. 2667–2688, 2011.

[78] R. Lai, F. Arslan, M. Lee et al., "Exosome secreted by MSC reduces myocardial ischemia/reperfusion injury," *Stem Cell Research*, vol. 4, no. 3, pp. 214–222, 2010.

[79] F. Arslan, R. Lai, M. Smeets et al., "Mesenchymal stem cell-derived exosomes increase ATP levels, decrease oxidative stress and activate PI3K/Akt pathway to enhance myocardial viability and prevent adverse remodeling after myocardial ischemia/reperfusion injury," *Stem Cell Research*, vol. 10, no. 3, pp. 301–312, 2013.

[80] C. Lee, S. Mitsialis, M. Aslam et al., "Exosomes mediate the cytoprotective action of mesenchymal stromal cells on hypoxia-induced pulmonary hypertension," *Circulation*, vol. 126, no. 22, pp. 2601–2611, 2012.

[81] T. Katsuda, R. Tsuchiya, N. Kosaka et al., "Human adipose tissue-derived mesenchymal stem cells secrete functional neprilysin-bound exosomes," *Scientific Reports*, vol. 3, no. 1, p. 1197, 2013.

[82] H. Xin, Y. Li, and M. Chopp, "Exosomes/miRNAs as mediating cell-based therapy of stroke," *Frontiers in Cellular Neuroscience*, vol. 8, p. 377, 2014.

[83] M. Ilmer, J. Vykoukal, A. R. Boiles, M. Coleman, and E. Alt, "Two sides of the same coin: stem cells in cancer and regenerative medicine," *FASEB Journal*, vol. 28, no. 7, pp. 2748–2761, 2014.

[84] C. Emanueli, A. Shearn, G. Angelini, and S. Sahoo, "Exosomes and exosomal miRNAs in cardiovascular protection and repair," *Vascular Pharmacology*, vol. 71, pp. 24–30, 2015.

[85] L. Huang, W. Ma, Y. Ma, D. Feng, H. Chen, and B. Cai, "Exosomes in mesenchymal stem cells, a new therapeutic strategy for cardiovascular diseases?," *International Journal of Biological Sciences*, vol. 11, no. 2, pp. 238–245, 2015.

[86] J. Yamamoto, K. Maeno, T. Takada et al., "Fas ligand plays an important role for the production of pro-inflammatory cytokines in intervertebral disc nucleus pulposus cells," *Journal of Orthopaedic Research*, vol. 31, no. 4, pp. 608–615, 2013.

[87] C. Feng, M. Yang, M. Lan et al., "ROS: crucial intermediators in the pathogenesis of intervertebral disc degeneration," *Oxidative Medicine and Cellular Longevity*, vol. 2017, Article ID 5601593, 12 pages, 2017.

[88] C. Xia, Z. Zeng, B. Fang et al., "Mesenchymal stem cell-derived exosomes ameliorate intervertebral disc degeneration via anti-oxidant and anti-inflammatory effects," *Free Radical Biology & Medicine*, vol. 143, pp. 1–15, 2019.

[89] L. Xie, Z. Chen, M. Liu et al., "MSC-derived exosomes protect vertebral endplate chondrocytes against apoptosis and calcification via the miR-31-5p/ATF6 Axis," *Molecular Therapy-Nucleic Acids*, vol. 22, pp. 601–614, 2020.

[90] Y. Hu, R. Tao, L. Wang et al., "Exosomes Derived from Bone Mesenchymal Stem Cells Alleviate Compression- Induced Nucleus Pulposus Cell Apoptosis by Inhibiting Oxidative Stress," *Oxidative Medicine and Cellular Longevity*, vol. 2021, Article ID 2310025, 12 pages, 2021.

[91] N. Rand, F. Reichert, Y. Floman, and S. Rotshenker, "Murine nucleus pulposus-derived cells secrete interleukins-1-beta, -6, and -10 and granulocyte-macrophage colony-stimulating factor in cell culture," *Spine*, vol. 22, no. 22, pp. 2598–2601, 1997.

[92] C. Kepler, D. Markova, A. Hilibrand et al., "Substance P stimulates production of inflammatory cytokines in human disc cells," *Spine*, vol. 38, no. 21, pp. E1291–E1299, 2013.

[93] D. Purmessur, B. Walter, P. Roughley, D. Laudier, A. Hecht, and J. Iatridis, "A role for TNFα in intervertebral disc degeneration: a non-recoverable catabolic shift," *Biochemical and Biophysical Research Communications*, vol. 433, no. 1, pp. 151–156, 2013.

[94] C. Shen, J. Yan, L. Jiang, and L. Dai, "Autophagy in rat annulus fibrosus cells: evidence and possible implications," *Arthritis Research & Therapy*, vol. 13, no. 4, p. R132, 2011.

[95] S. Zhang, S. J. Chuah, R. C. Lai, J. H. P. Hui, S. K. Lim, and W. S. Toh, "MSC exosomes mediate cartilage repair by enhancing proliferation, attenuating apoptosis and modulating immune reactivity," *Biomaterials*, vol. 156, pp. 16–27, 2018.

[96] S. Nakashima, Y. Matsuyama, K. Takahashi et al., "Regeneration of intervertebral disc by the intradiscal application of cross-linked hyaluronate hydrogel and cross-linked chondroitin sulfate hydrogel in a rabbit model of intervertebral disc injury," *Bio-Medical Materials and Engineering*, vol. 19, no. 6, pp. 421–429, 2009.

[97] K. Lu, H. Li, K. Yang et al., "Exosomes as potential alternatives to stem cell therapy for intervertebral disc degeneration:

in-vitro study on exosomes in interaction of nucleus pulposus cells and bone marrow mesenchymal stem cells," *Stem Cell Research & Therapy*, vol. 8, no. 1, p. 108, 2017.

[98] S. Yang, F. Zhang, J. Ma, and W. Ding, "Intervertebral disc ageing and degeneration: the antiapoptotic effect of oestrogen," *Ageing Research Reviews*, vol. 57, article 100978, 2020.

[99] T. J. DiStefano, K. Vaso, G. Danias, H. N. Chionuma, J. R. Weiser, and J. C. Iatridis, "Extracellular vesicles as an emerging treatment option for intervertebral disc degeneration: therapeutic potential, translational pathways, and regulatory considerations," *Advanced Healthcare Materials*, no. article 2100596, 2021.

[100] M. Shi, Y. Zhao, Y. Sun, D. Xin, W. Xu, and B. Zhou, "Therapeutic effect of co-culture of rat bone marrow mesenchymal stem cells and degenerated nucleus pulposus cells on intervertebral disc degeneration," *The Spine Journal*, vol. 29, no. 4, pp. 1567–1579, 2021.

[101] Y. Cai, X. Yu, S. Hu, and J. Yu, "A brief review on the mechanisms of miRNA regulation," *Genomics, Proteomics & Bioinformatics*, vol. 7, no. 4, pp. 147–154, 2009.

[102] L. Chen, L. Heikkinen, C. Wang, Y. Yang, H. Sun, and G. Wong, "Trends in the development of miRNA bioinformatics tools," *Briefings in Bioinformatics*, vol. 20, no. 5, pp. 1836–1852, 2019.

[103] M. J. Shurtleff, M. M. Temoche-Diaz, K. V. Karfilis, S. Ri, and R. Schekman, "Y-box protein 1 is required to sort microRNAs into exosomes in cells and in a cell-free reaction," *eLife*, vol. 5, 2016.

[104] T. Katsuda and T. Ochiya, "Molecular signatures of mesenchymal stem cell-derived extracellular vesicle-mediated tissue repair," *Stem Cell Research & Therapy*, vol. 6, p. 212, 2015.

[105] H. Hu, L. Dong, Z. Bu et al., "miR-23a-3p-abundant small extracellular vesicles released from Gelma/nanoclay hydrogel for cartilage regeneration," *Journal of Extracellular Vesicles*, vol. 9, no. 1, article 1778883, 2020.

[106] S. C. Tao, T. Yuan, Y. L. Zhang, W. J. Yin, S. C. Guo, and C. Q. Zhang, "Exosomes derived from miR-140-5p-overexpressing human synovial mesenchymal stem cells enhance cartilage tissue regeneration and prevent osteoarthritis of the knee in a rat model," *Theranostics*, vol. 7, no. 1, pp. 180–195, 2017.

[107] Z. Wang, S. Zhang, Y. Zhao et al., "MicroRNA-140-3p alleviates intervertebral disc degenerationviaKLF5/N-cadherin/MDM2/Slug axis," *RNA biology*, vol. 18, no. 12, pp. 2247–2260, 2021.

[108] L. Duan, Y. Liang, X. Xu, Y. Xiao, and D. Wang, "Recent progress on the role of miR-140 in cartilage matrix remodelling and its implications for osteoarthritis treatment," *Arthritis Research & Therapy*, vol. 22, no. 1, p. 194, 2020.

[109] L. Zhao, X. Jiang, J. Shi et al., "Exosomes derived from bone marrow mesenchymal stem cells overexpressing microRNA-25 protect spinal cords against transient ischemia," *The Journal of Thoracic and Cardiovascular Surgery*, vol. 157, no. 2, pp. 508–517, 2019.

[110] Y. Huang, L. Huang, L. Li et al., "MicroRNA-25-3p therapy for intervertebral disc degeneration by targeting the IL-1β/ZIP8/MTF1 signaling pathway with a novel thermoresponsive vector," *Annals of Translational Medicine*, vol. 8, no. 22, p. 1500, 2020.

[111] S. H. Li and Q. F. Wu, "MicroRNAs target on cartilage extracellular matrix degradation of knee osteoarthritis," *European Review for Medical and Pharmacological Sciences*, vol. 25, no. 3, pp. 1185–1197, 2021.

[112] C. Lei, J. Li, G. Tang, and J. Wang, "MicroRNA-25 protects nucleus pulposus cells against apoptosis via targeting SUMO2 in intervertebral disc degeneration," *Molecular Medicine Reports*, vol. 24, no. 4, 2021.

[113] L. Zhu, Y. Shi, L. Liu, H. Wang, P. Shen, and H. Yang, "Mesenchymal stem cells-derived exosomes ameliorate nucleus pulposus cells apoptosis via delivering miR-142-3p: therapeutic potential for intervertebral disc degenerative diseases," *Cell Cycle*, vol. 19, no. 14, pp. 1727–1739, 2020.

[114] B. Wang, D. Ji, W. Xing et al., "miR-142-3p and HMGB1 are negatively regulated in proliferation, apoptosis, migration, and autophagy of cartilage endplate cells," *Cartilage*, vol. 13, Supplement 2, pp. 592S–603S, 2021.

[115] P. Yang, R. Gao, W. Zhou, and A. Han, "Protective impacts of circular RNA VMA21 on lipopolysaccharide-engendered WI-38 cells injury via mediating microRNA-142-3p," *BioFactors*, vol. 46, no. 3, pp. 381–390, 2020.

[116] J. Beckman, R. Minor, C. White, J. Repine, G. Rosen, and B. Freeman, "Superoxide dismutase and catalase conjugated to polyethylene glycol increases endothelial enzyme activity and oxidant resistance.," *The Journal of Biological Chemistry*, vol. 263, no. 14, pp. 6884–6892, 1988.

[117] K. Yoshida, G. F. Burton, H. Young, and E. F. Ellis, "Brain levels of polyethylene glycol-conjugated superoxide dismutase following fluid percussion brain injury in rats," *Journal of Neurotrauma*, vol. 9, no. 2, pp. 85–92, 1992.

[118] F. Veronese, P. Caliceti, O. Schiavon, and M. Sergi, "Polyethylene glycol-superoxide dismutase, a conjugate in search of exploitation," *Advanced Drug Delivery Reviews*, vol. 54, no. 4, pp. 587–606, 2002.

[119] Y. Zhang, J. Bi, J. Huang, Y. Tang, S. Du, and P. Li, "Exosome: a review of its classification, isolation techniques, storage, diagnostic and targeted therapy applications," *International Journal of Nanomedicine*, vol. 15, pp. 6917–6934, 2020.

[120] E. Batrakova and M. Kim, "Using exosomes, naturally-equipped nanocarriers, for drug delivery," *Journal of Controlled Release*, vol. 219, pp. 396–405, 2015.

[121] J. Jeong, J. Han, J. Kim et al., "Malignant tumor formation after transplantation of short-term cultured bone marrow mesenchymal stem cells in experimental myocardial infarction and diabetic neuropathy," *Circulation Research*, vol. 108, no. 11, pp. 1340–1347, 2011.

[122] S. Bruno, G. Chiabotto, and G. Camussi, "Extracellular vesicles: a therapeutic option for liver fibrosis," *International Journal of Molecular Sciences*, vol. 21, no. 12, p. 4255, 2020.

[123] A. Hiyama, J. Mochida, and D. Sakai, "Stem cell applications in intervertebral disc repair," *Cellular and Molecular Biology*, vol. 54, no. 1, pp. 24–32, 2008.

[124] S. M. Churchman, S. A. Boxall, D. McGonagle, and E. A. Jones, "Predicting the remaining lifespan and cultivation-related loss of osteogenic capacity of bone marrow multipotential stromal cells applicable across a broad donor age range," *Stem Cells International*, vol. 2017, Article ID 6129596, 10 pages, 2017.

[125] A. Stolzing, E. Jones, D. McGonagle, and A. Scutt, "Age-related changes in human bone marrow-derived mesenchymal stem cells: consequences for cell therapies," *Mechanisms of ageing and development.*, vol. 129, no. 3, pp. 163–173, 2008.

[126] H. Xin, Y. Li, Y. Cui, J. Yang, Z. Zhang, and M. Chopp, "Systemic administration of exosomes released from mesenchymal stromal cells promote functional recovery and neurovascular plasticity after stroke in rats," *Journal of cerebral blood flow and metabolism: official journal of the International Society of Cerebral Blood Flow and Metabolism.*, vol. 33, no. 11, pp. 1711–1715, 2013.

[127] W. S. Park, S. Y. Ahn, S. I. Sung, J. Y. Ahn, and Y. S. Chang, "Strategies to enhance paracrine potency of transplanted mesenchymal stem cells in intractable neonatal disorders," *Pediatric Research*, vol. 83, no. 1-2, pp. 214–222, 2018.

[128] K. Park, E. Bandeira, G. Shelke, C. Lässer, and J. Lötvall, "Enhancement of therapeutic potential of mesenchymal stem cell-derived extracellular vesicles," *Stem Cell Research & Therapy*, vol. 10, no. 1, p. 288, 2019.

[129] M. Loibl, K. Wuertz-Kozak, G. Vadala, S. Lang, J. Fairbank, and J. Urban, "Controversies in regenerative medicine: should intervertebral disc degeneration be treated with mesenchymal stem cells?," *JOR Spine*, vol. 2, no. 1, article e1043, 2019.

[130] S. Cosenza, M. Ruiz, K. Toupet, C. Jorgensen, and D. Noël, "Mesenchymal stem cells derived exosomes and microparticles protect cartilage and bone from degradation in osteoarthritis," *Scientific Reports*, vol. 7, no. 1, p. 16214, 2017.

[131] J. Chew, S. Chuah, K. Teo et al., "Mesenchymal stem cell exosomes enhance periodontal ligament cell functions and promote periodontal regeneration," *Acta Biomaterialia*, vol. 89, pp. 252–264, 2019.

[132] H. Yu, J. Cheng, W. Shi et al., "Bone marrow mesenchymal stem cell-derived exosomes promote tendon regeneration by facilitating the proliferation and migration of endogenous tendon stem/progenitor cells," *Acta Biomaterialia*, vol. 106, pp. 328–341, 2020.

[133] L. Bagno, K. Hatzistergos, W. Balkan, and J. Hare, "Mesenchymal stem cell-based therapy for cardiovascular disease: progress and challenges," *Molecular Therapy*, vol. 26, no. 7, pp. 1610–1623, 2018.

[134] Y. Chen and L. Tang, "Stem cell senescence: the obstacle of the treatment of degenerative disk disease," *Current Stem Cell Research & Therapy*, vol. 14, no. 8, pp. 654–668, 2019.

[135] K. W. Witwer, B. W. M. Van Balkom, S. Bruno et al., "Defining mesenchymal stromal cell (MSC)-derived small extracellular vesicles for therapeutic applications," *Journal of Extracellular Vesicles*, vol. 8, no. 1, article 1609206, 2019.

[136] T. Lener, M. Gimona, L. Aigner et al., "Applying extracellular vesicles based therapeutics in clinical trials - an ISEV position paper," *Journal of Extracellular Vesicles*, vol. 4, no. 1, article 30087, 2015.

[137] M. Gimona, M. F. Brizzi, A. B. H. Choo et al., "Critical considerations for the development of potency tests for therapeutic applications of mesenchymal stromal cell-derived small extracellular vesicles," *Cytotherapy*, vol. 23, no. 5, pp. 373–380, 2021.

Hindawi
Stem Cells International
Volume 2022, Article ID 4363632, 13 pages
https://doi.org/10.1155/2022/4363632

Research Article

Schwann Cells Accelerate Osteogenesis via the Mif/CD74/FOXO1 Signaling Pathway In Vitro

Jun-Qin Li,[1,2,3] Hui-Jie Jiang,[1] Xiu-Yun Su,[2] Li Feng,[3] Na-Zhi Zhan,[3] Shan-Shan Li,[3] Zi-Jie Chen,[3] Bo-Han Chang,[3] Peng-Zhen Cheng,[1] Liu Yang,[1] and Guo-Xian Pei[1,2,3]

[1]*Department of Orthopaedics, Xijing Hospital, Air Force Medical University, Xi'an 710032, China*
[2]*Southern University of Science and Technology Hospital, No. 6019 Liuxian Street, Xili Avenue, Nanshan District, Shenzhen 518055, China*
[3]*School of Medicine, Southern University of Science and Technology, Shenzhen 518055, China*

Correspondence should be addressed to Liu Yang; yangliu@fmmu.edu.cn and Guo-Xian Pei; nfperry@163.com

Received 17 August 2021; Revised 13 November 2021; Accepted 21 December 2021; Published 13 January 2022

Academic Editor: Yi Zhang

Schwann cells have been found to promote osteogenesis by an unclear molecular mechanism. To better understand how Schwann cells accelerate osteogenesis, RNA-Seq and LC-MS/MS were utilized to explore the transcriptomic and metabolic response of MC3T3-E1 to Schwann cells. Osteogenic differentiation was determined by ALP staining. Lentiviruses were constructed to alter the expression of Mif (macrophage migration inhibitory factor) in Schwann cells. Western blot (WB) analysis was employed to detect the protein expression. The results of this study show that Mif is essential for Schwann cells to promote osteogenesis, and its downstream CD74/FOXO1 is also involved in the promotion of Schwann cells on osteogenesis. Further, Schwann cells regulate amino acid metabolism and lipid metabolism in preosteoblasts. These findings unveil the mechanism for Schwann cells to promote osteogenesis where Mif is a key factor.

1. Introduction

Schwann cells have been found to have an important role in osteogenesis. During development, the presence of nerve and Schwann cells in the niche supports osteogenic differentiation of osteoprogenitor cells leading to new bone formation [1]. During bone repair, several studies have found that Schwann cells can be utilized to promote osteogenesis in TEB (tissue-engineered bone) [2, 3]. Besides, Schwann cell precursors have been found to contribute to skeletal formation during embryonic development in mice and zebrafish [4]. Schwann cells were also found to promote osteogenesis in vitro [5]. However, the mechanism of how Schwann cells promote osteogenesis is unclear.

Mif is an important inflammatory cytokine involved in tissue protection and regeneration, such as nerve and muscle [6–8]. It can be synthesized with a variety of cells; stored in the cytoplasm, such as Schwann cells; and released with a specific stimulus, such as bacteria-derived metabolites and hypoxia [9]. Mif has been found to play an important role in the development and repair of bones; however, its role in osteogenesis remains controversial. Discrepancies in the findings may result from stimuli coming from different cells [5, 10].

Above all, this study intends to study the role of Mif in Schwann cells promoting osteogenesis. Besides, the transcriptomic and metabolic response of preosteoblast cells and the correlation between metabolomics and transcriptomics were analyzed, to understand the mechanisms of Schwann cells and its Mif in promoting osteogenesis.

2. Materials and Methods

2.1. Cell Culture. Schwann cells were harvested from the mouse sciatic nerve with the method previously published [11]. 24 hours after initial plating and incubation for 2–3

days to remove fibroblasts, the arabinoside (10^{-5} mol/L) was added to the culture medium. The coculture system was established with six-well Transwell clear polyester membrane inserts with 0.4 μm pore size (Costar Corning, USA). $5 * 10^4$ Schwann cells were plated on the transwell inserts; $1 * 10^5$ MC3T3-E1 cells were plated on the tissue culture plates. MC3T3-E1 was harvested for RNA-Seq and LC-MC/MS after 3 days of coculture.

2.2. Lentiviral Vectors. The Mif overexpression lentivirus and knockdown lentivirus were constructed by Shanghai Genechem Co., Ltd. For the Mif overexpression lentivirus (lv-Mif), the Mif sequence was cloned into the Ubi-MCS-Cherry-SV40-puromycin. For the Mif knockdown lentivirus (sh-Mif), the siRNA sequence of Mif, CCTGCACAGCA TCGGCAAGAT, was cloned into the U6-MCS-Ubiquitin-Cherry-IRES-puromycin lentivirus.

2.3. ALP Staining and Activity. To test the differentiation of osteoblast, after 12 days of coculture in commercial kit MC3T3-E1 cell osteogenic differentiation medium (Cyagen, MUXMT-90021), MC3T3-E1 were washed with PBS and stained with the commercial kit according to the manufacturer's instruction (Sigma, USA). ALP activity was detected by an ALP activity kit (P0321S, Beyotime). Briefly, cells were lysed and incubated with chromogenic substrate and detection buffer at 37°C for 6 mins; the incubation was stopped by stop solution; then, the ALP activity was measured at 405 nm.

2.4. RNA-Seq. RNA-Seq and RNA-Seq analysis were performed as previously reported [12]. To remove the adaptors and low-quality reads, raw reads were firstly trimmed and then mapped to mouse genome with Hisat2 v2.0.5, and gene expression levels were quantified as read counts generated with featureCounts v1.5.0-p3. With DESeq2 R package (1.16.1), differential gene expression was then analyzed.

2.5. Untargeted LC-MS/MS. Untargeted LC-MS/MS analyses were performed with an UHPLC system (Vanquish, Thermo Fisher Scientific) with a UPLC BEH Amide column (2.1 mm × 100 mm, 1.7 μm) coupled to the Q Exactive HFX mass spectrometer (Orbitrap MS, Thermo). The mobile phase consisted of 25 mmol/L ammonium acetate and 25 ammonia hydroxide in water (pH = 9.75) (A) and acetonitrile (B). The autosampler temperature was 4°C with an injection volume of 3 μL.

The QE HFX mass spectrometer was utilized for its ability to acquire MS/MS spectra on an information-dependent acquisition (IDA) mode in the control of the acquisition software (Xcalibur, Thermo). The acquisition software in this mode continuously evaluates the full scan MS spectrum. The ESI source conditions were set as the following: 30 Arb for sheath gas flow rate, 25 Arb for Aux gas flow rate, 350°C for capillary temperature, 60000 for full MS resolution, 7500 for MS/MS resolution, 10/30/60 in NCE mode for collision energy, and 3.6 kV (positive) for spray voltage or -3.2 kV (negative), respectively.

The raw data were converted to the mzXML format with ProteoWizard and processed with an in-house program, which was developed with R and based on XCMS for peak detection, extraction, alignment, and integration. Then, an in-house MS2 database (BiotreeDB) was applied in metabolite annotation. The cutoff for annotation was set at 0.3.

2.6. Quantitative Real-Time RT-PCR (qPCR). Total RNA was purified from cells using TRIzol (Invitrogen, 15596026), reverse-transcribed using Prime Script™ RT Master Mix (TaKaRa, Japan), and subjected to qPCR using Taq SYBR Green Power PCR Master Mix (Invitrogen, A25777) on a CFX96™ real-time system (Bio-Rad). Gapdh was used as an internal control. The primer sequences were the following: Alp forward: CACGTTGACTGTGGTTACT GCTGA and reverse: CCTTGTAACCAGGCCCGTTG; Col1a1 forward: GACATGTTCAGCTTTGTGGACCTC and reverse: GGGACCCTTAGGCCATTGTGTA; Osx forward: TGACTGCCTGCCTAGTGTCTACA and reverse: TGGATGCCCGCCTTGT; Runx2 forward: CATGGCCGG GAATGATGAG and reverse: TGTGAAGACCGTTATG GTCAAAGTG; and Gapdh forward: ATGTGTCCGTC GTGGATCTGA and reverse: ATGCCTGCTTCACCAC CTTCTT.

2.7. Western Blot. Pretreated cells were gathered on ice and lysed with RIPA lysis buffer. Proteins were separated on 4%–12% Bis-Tris polyacrylamide gels and transferred to the PVDF membrane. The blots were incubated with primary antibodies overnight at 4°C and then with secondary antibodies. The following primary antibodies were adopted: Actin (Servicebio, GB12001; 1 : 1000); Aldoc (Proteintech, 14884-1-AP, 1 : 5000); CD74 (Bioss, bs-2518R, 1 : 2000); CYP51 (Proteintech, 13431-1-AP, 1 : 5000); EBP (Proteintech, 15518-1-AP, 1 : 1000); ENO2 (Servicebio, GB11376, 1 : 1000); FDFT1 (Proteintech, 13128-1-AP, 1 : 1000); FOXO1 (Servicebio, GB11286; 1: 2000); Gapdh (Proteintech, 60004-1-Ig, 1 : 20000); Gpi1 (Proteintech, 15171-1-AP, 1 : 1000); Hif-1a (Servicebio, GB111339, 1 : 1000); Mif (Proteintech, 26992-1-AP, 1 : 1000); NSDHL (Proteintech, 15111-1-AP, 1 : 1000); PFKL (abcam, ab181064, 1 : 5000); Pgk1 (abcam, ab199438, 1 : 2000); PKM (abcam, ab150377, 1 : 5000); p53 (Proteintech, 10442-1-AP, 1 : 1000); Tpi1 (abcam, ab196618, 1 : 1000).

2.8. Statistical Analysis. GraphPad Prism 8.0.1 (GraphPad Software, LLC.) was utilized for the statistical analysis to quantify ALP activity. The mean ± standard deviation was recorded for all the experiments. Statistical significance between two groups was assessed with Student's *t*-test. *P* values < 0.05 were regarded to be of statistical significance. The content of differential genes and differential metabolites was used to provide transcriptome and metabolome correlations. Spearman correlation analyses were used where *P* values < 0.05 were regarded to be of statistical significance.

3. Results

3.1. The Transcriptomic Response of Preosteoblast to Schwann Cells. To study the effect of Schwann cells on osteogenesis, we cocultured Schwann cells and MC3T3-E1. Schwann cells were identified and characterized by

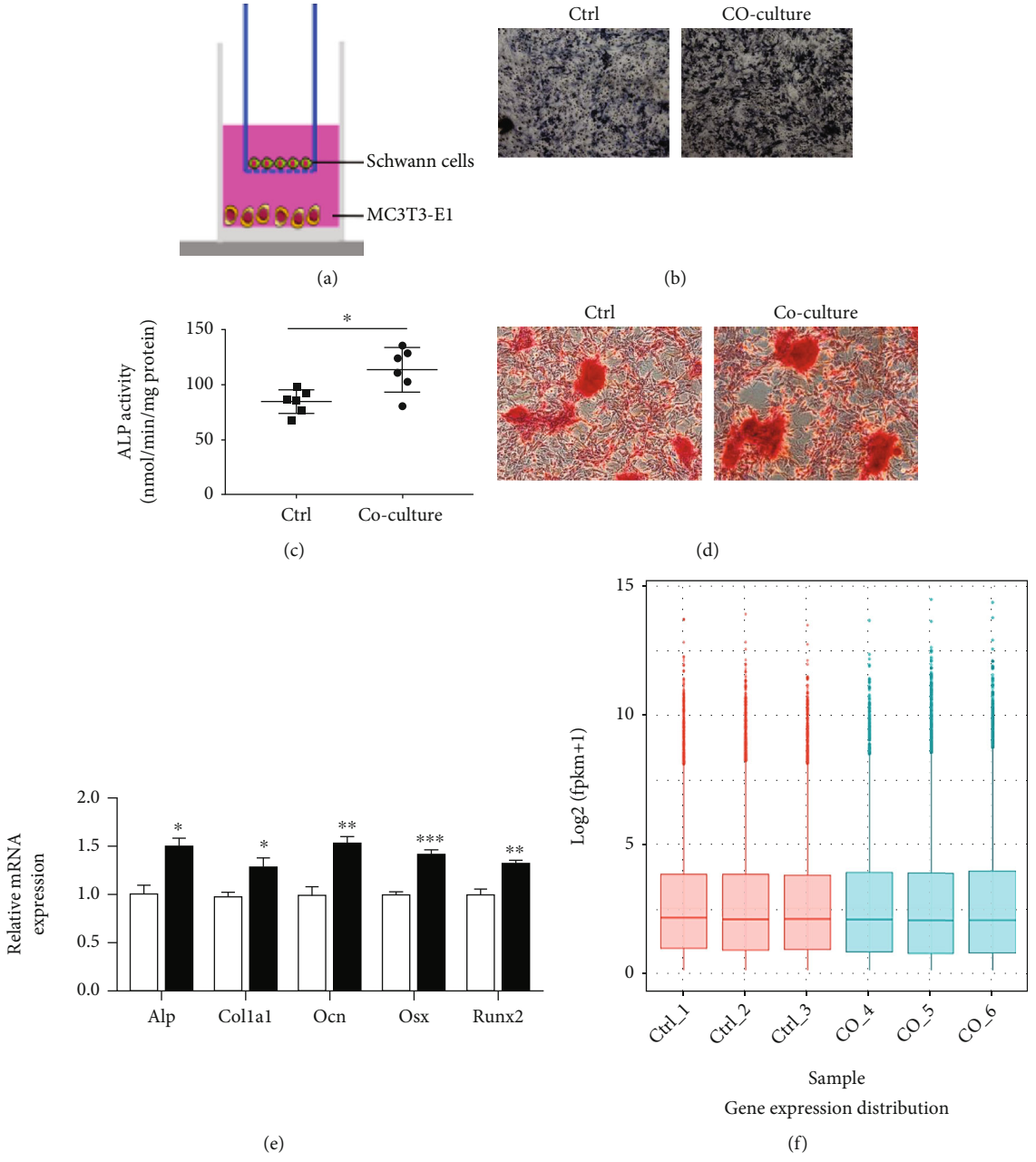

Figure 1: Continued.

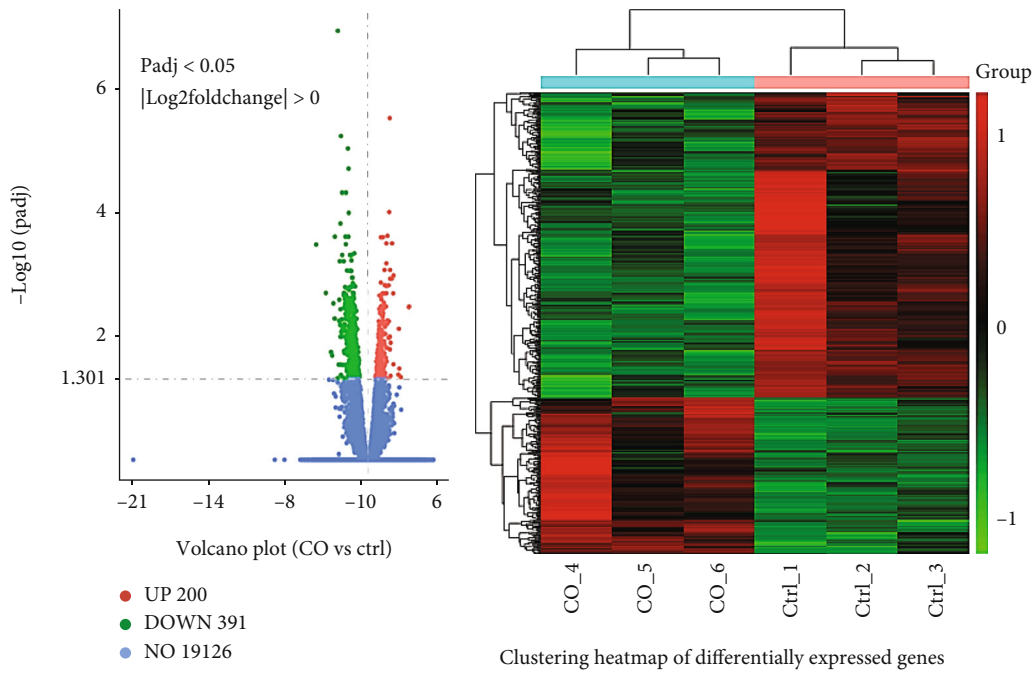

(g) (h)

Figure 1: Continued.

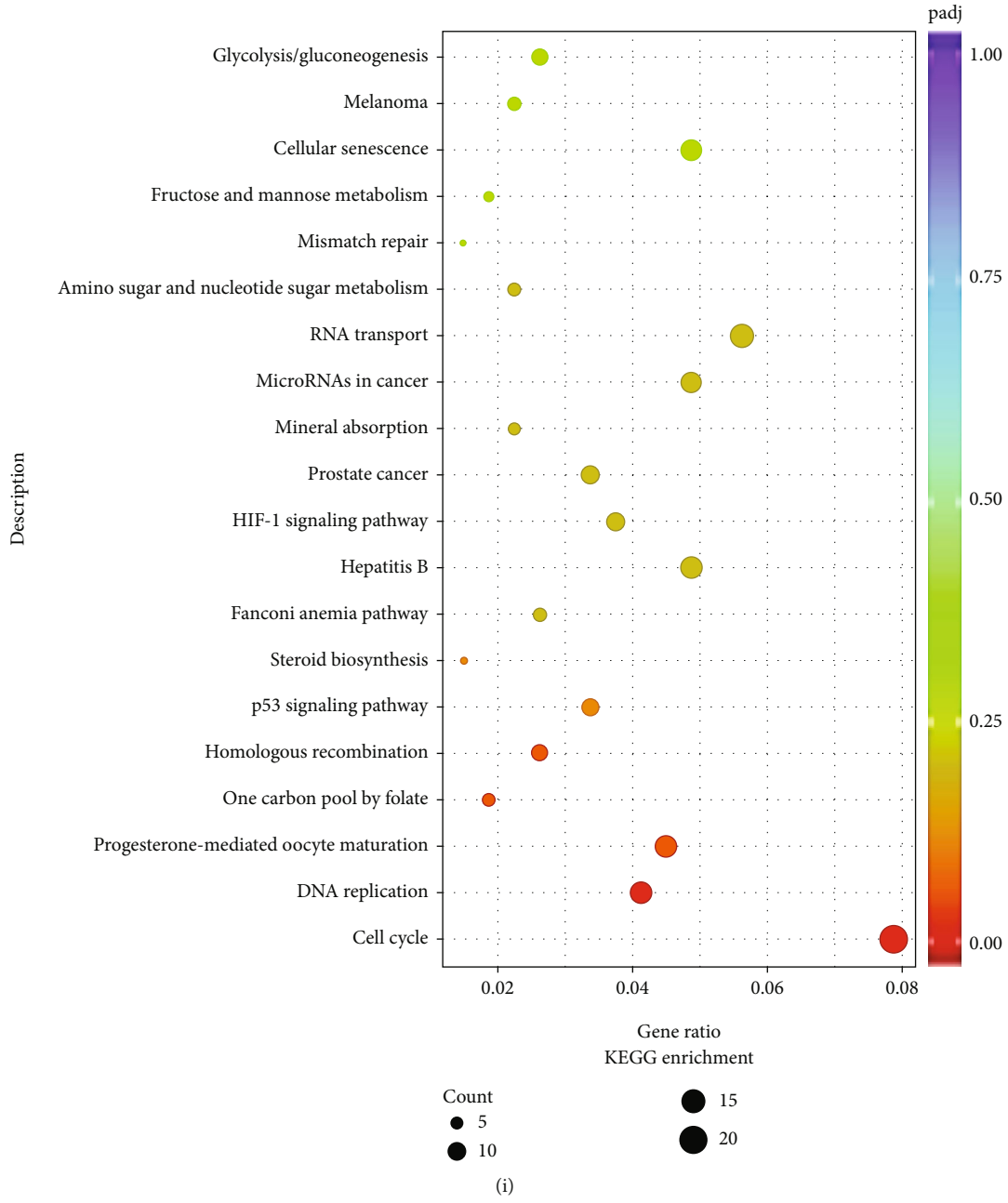

Figure 1: (a) Diagram of the Schwann cells and MC3T3-E1 cell coculture model; (b) representative images showing ALP staining; (c) ALP activity was measured with an ALP assay kit, $n = 6$, $p = 0.0108$; l; (d) representative images showing Alizarin red staining; l; (e) real-time RT-PCR (qPCR) analyses. $^{*}P < 0.05$, Student's t-test. $N = 4$; (f–i) transcriptome differences between the coculture group and the control group in MC3T3-E1 cells; (f) the boxplots represent the distribution of expression levels; the ordinate is gene expression level; (g) volcano plot of differential gene expression analysis; the dotted blue line indicates the threshold of the differential genes selected; (h) cluster heatmap of differentially expressed genes; (i) the KEGG enrichment scatter plot. The size of the black spots represents the gene number; the gradual color represents the P value.

immunofluorescent staining target its marker S100 and GFAP (Supplementary Figure S1a). As previously published [13, 14], Schwann cells promote osteoblastic differentiation (Figures 1(a)–1(e)). RNA-Seq showed that Schwann cells can regulate the expression of multiple genes in MC3T3-E1 (Figure 1(f)), with 200 transcripts upregulated and 391 transcripts downregulated (Figure 1(g)). Differential gene cluster analysis for all the treatments was conducted (Figure 1(h)). KEGG pathway analysis showed 20 most significantly enriched pathways (Figure 1(i)), including mineral absorption, mainly conducted by osteoclasts. It indicated that Schwann cells could regulate osteoblast/osteoclast coupling and mineralization. Besides, the most enriched pathways also included cell cycle, cell stemness, and signal pathways including p53 and HIF-1 and metabolism such as

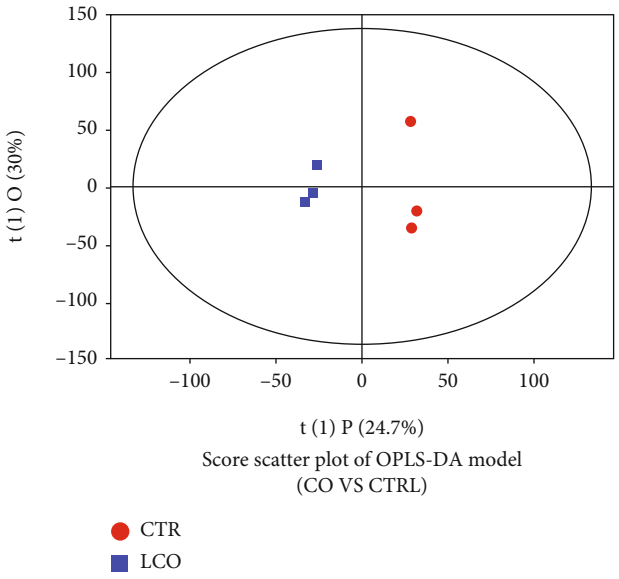

(a)

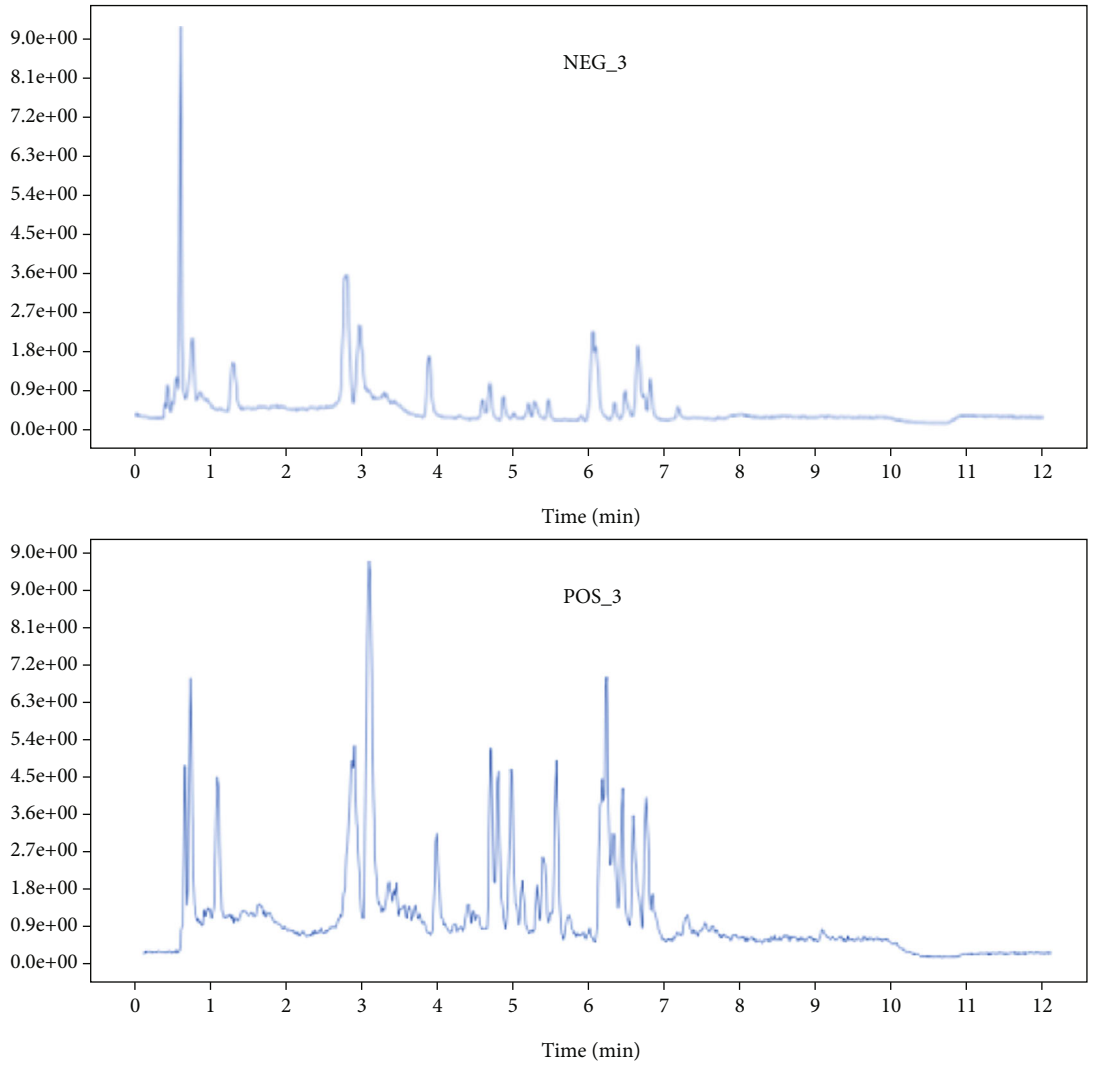

(b)

Figure 2: Continued.

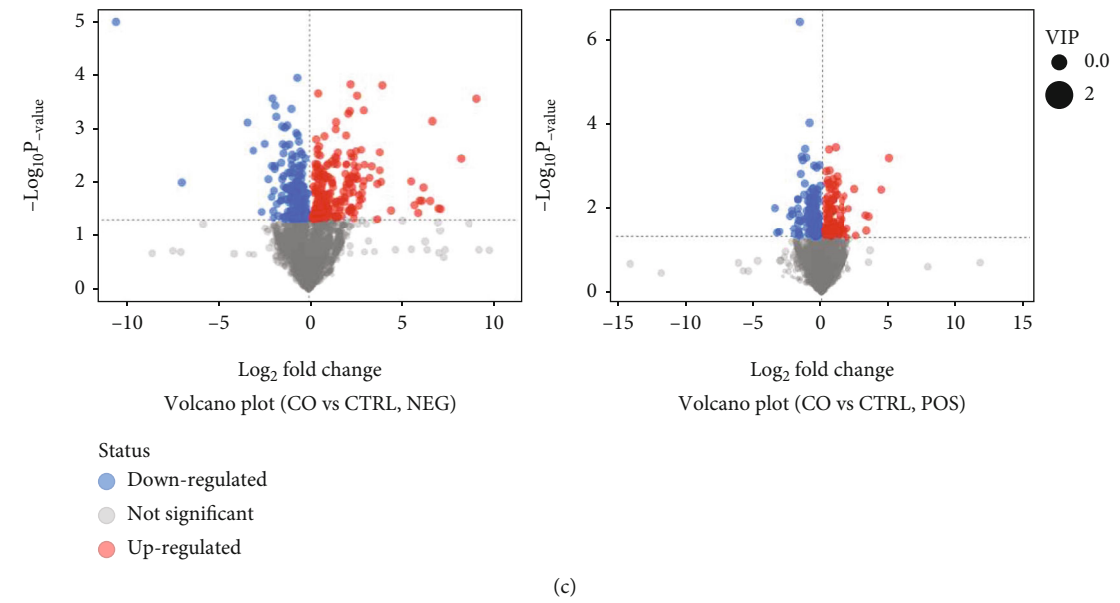

(c)

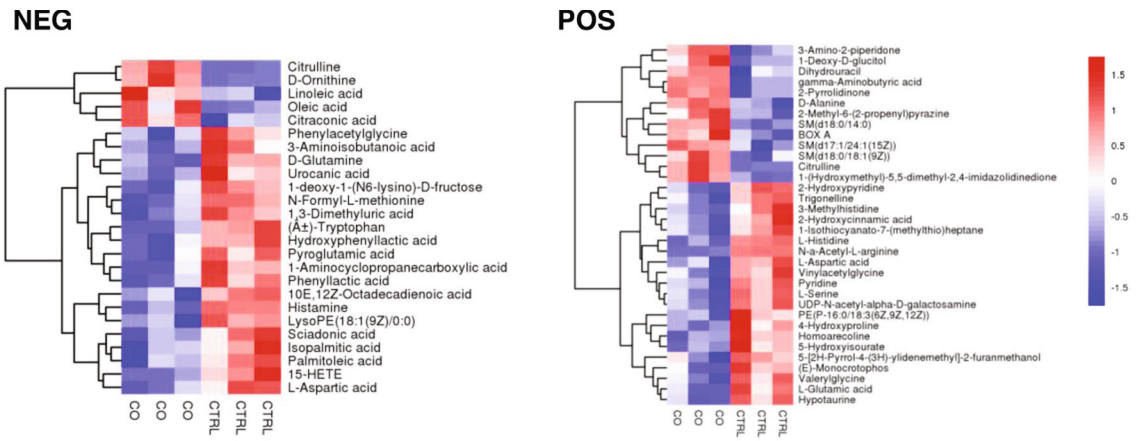

(d)

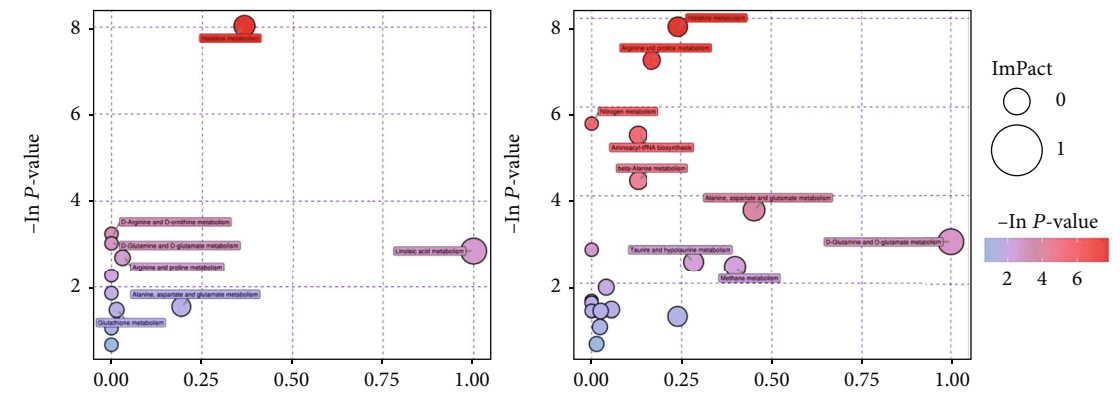

(e)

Figure 2: (a) OPLS-DA score scatter plot. Each point represents a sample; (b) representative chromatograms in positive (POS) and negative (NEG) ion modes; (c) volcano plot of differential metabolite analysis. The dotted line indicates the threshold of the differential metabolites selected; (d) cluster analysis of differential metabolites; (e) pathway analysis.

Figure 3: KEGG pathway classification: metabolites detected and annotated; red/blue dots represent the differentially expressed compounds; color depth represents the *P* value.

glycolysis, steroid biosynthesis, amino sugar, and nucleotide sugar metabolism. Then, we studied the metabolic response of preosteoblast to Schwann cells.

3.2. The Metabolic Response of Preosteoblast to Schwann Cells. Untargeted LC-MS/MS were performed to study the metabolic response of preosteoblast to Schwann cells. After being cocultured with Schwann cells, metabolites in MC3T3-E1 have been altered to a great extent (Figure 2(a)). Data acquisition was performed in both positive (POS) and negative (NEG) ion modes (Figures 2(b)–2(d) and Supplemental Figure S2). Chromatograms of all samples in positive (POS) and negative (NEG) ion modes are shown in Figure 2(b) and Supplemental Figure S2. The results of the metabolic pathway analysis are shown via a bubble plot (Figure 2(e)), and the altered metabolites were mainly enriched in "amino acid metabolism"; linoleic acid metabolism (belonging to fatty acid metabolism) was also significantly elevated by Schwann cells. However, there was no significant change in glucose metabolism. After further functional annotation of the differentially accumulated metabolites with the KEGG database, significant metabolite changes were also enriched in amino acid metabolisms (Figure 3, zoom region), such as arginine biosynthesis (NEG, POS); cysteine and methionine metabolism (POS); glycine, serine, and threonine metabolism (POS); and valine, leucine, and isoleucine biosynthesis (NEG).

3.3. Correlations between the Metabolic and Transcriptomic Response of Preosteoblast to Schwann Cells. In further analysis, we studied the correlations between differential metabolites and genes. Differential transcripts were selected from the following pathways: glucose metabolism including glycolysis/gluconeogenesis and fructose and mannose metabolism; fatty acid metabolism including steroid biosynthesis; signaling pathways including p53, HIF-1, and FOXO signaling pathway; and mineral absorption (Supplemental Figure S3). Differential metabolites were taken from the top 16 metabolites with significant differences (Supplemental Figure S3). All differential transcripts and metabolites selected for correlation analysis are shown in Supplemental Figure S3. Correlation analysis

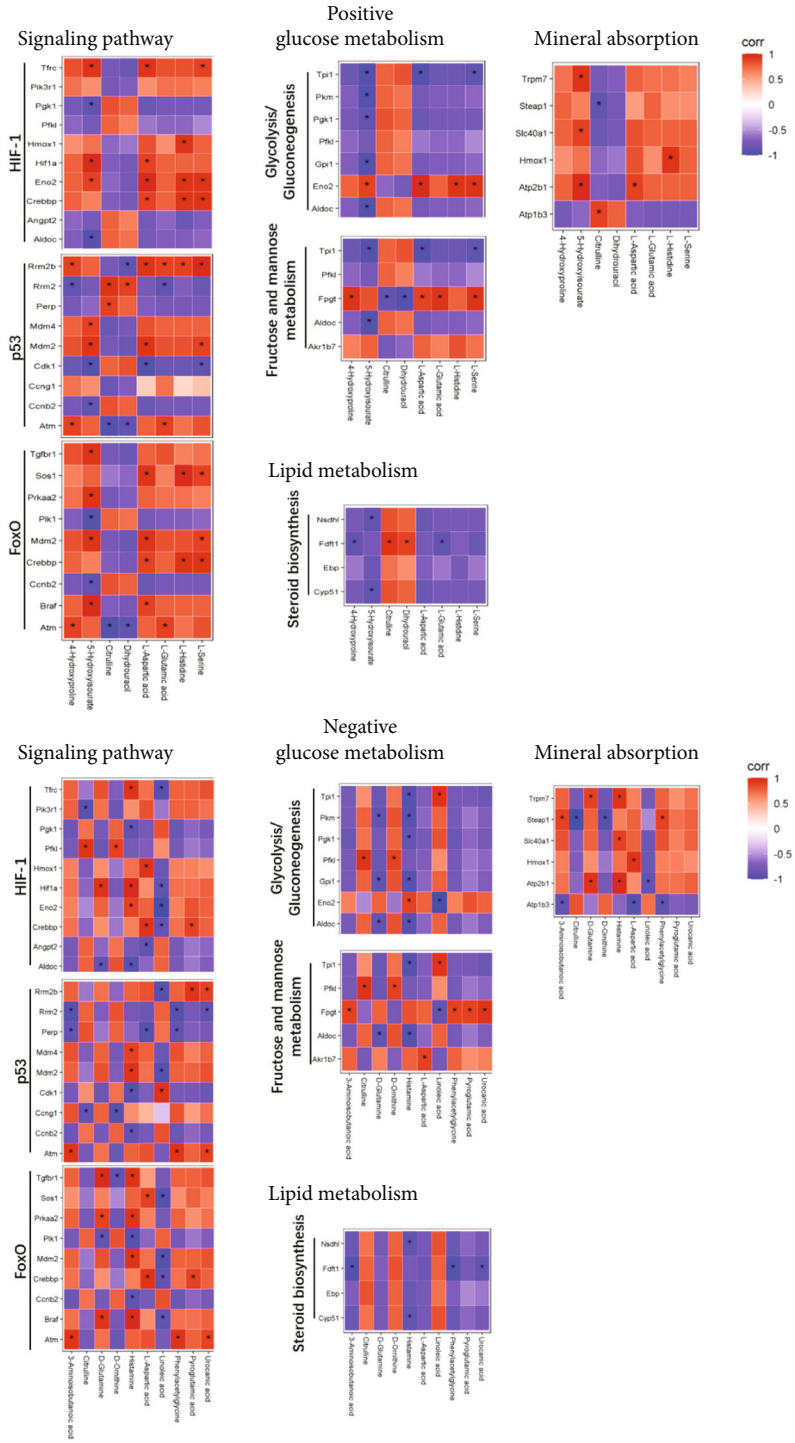

FIGURE 4: Heatmap indicating the correlation between the differential transcripts and metabolites. Red (corr = 1), blue (corr = −1), and white (corr = 0); $^{*}P < 0.05$ for Spearman correlation.

was based on the content of differential transcripts and metabolites (Figure 4). Differential metabolites are highly correlated with signaling pathways with the greatest number of significant correlations with the p53 signaling pathway in POS mode and the greatest number of significant correlations with the FOXO1 signaling pathway in NEG mode.

3.4. Schwann Cells Promote Osteogenesis by Mif. Mif is a critical chemokine in Schwann cells during nerve regeneration [15, 16]. Blocking Mif on the Schwann cell greatly reduced neurite outgrowth [17]. Mif has also been found to be promoted on osteoblast differentiation [5]. Then, we probed the role of Mif in Schwann cells promoting osteoblast differentiation. Firstly, to confirm whether Mif can be released

from the Schwann cells, we performed ELISA and found a dose-response curve of Mif in response to increasing numbers of SN (Figure 4(d)). These results therefore prove that Mif is a secreted factor from Schwann cells. We then studied the role of Mif in Schwann cells' promotion of osteogenesis; Mif were overexpressed/downregulated in Schwann cells by lentivirus (Supplemental Figure S4a), and the lentivirus vector did not affect Schwann cells' function on osteogenesis (Supplemental Figure S4b). We can find that overexpression of Mif could significantly enhance the ability of Schwann cells to promote osteogenesis, while the downregulation of Mif significantly attenuates the ability of Schwann cells to promote osteogenesis (Figures 5(b) and 5(c)).

CD74 is the main receptor for Mif [18]. WB results showed that CD74 expression has been increased in MC3T3-E1 cells by Schwann cells, and the expression of CD74 has been altered following Mif overexpression/downregulation (Figures 5(f) and 5(h)) with a consistent trend. In the RNA-Seq results, Hif-1a, p53, and FOXO1 signaling pathways were the most outstanding pathways involved for Schwann cells to promote osteogenesis. According to WB results, the expression of Hif-1a and p53 was downregulated by Schwann cells, but their expression was inconsistent with Schwann cells and its Mif promoting osteogenesis. The FOXO1 was upregulated by Schwann cells, and its expression changes were consistent with the changes of the Mif/CD74 signal axis when Schwann cells promote osteogenesis. Since the FOXO1 is a transcription factor, the FOXO1 level in the nucleus was also measured, and the factor expression changes were also consistent with the changes of the Mif/CD74 signal axis when Schwann cells promote osteogenesis (Figures 5(g) and 5(h)). Above all, Schwann cells promote osteogenesis through the signaling pathway of Mif/CD74/FOXO1.

According to the RNA-Seq results, there are differential transcripts in glucose metabolism (glycolysis/gluconeogenesis and gluctose and mannose metabolism) and fatty metabolism (steroid biosynthesis). Then, WB were performed to detect the expression response of differential factors in steroid biosynthesis (Figure 5(d)) and glycolysis/gluconeogenesis (Figure 5(e)) to Schwann cells and its Mif. It was found that CYP51, FDFT1, and NSDHL in lipid metabolism were all upregulated by Schwann cells, but only the NSDHL was regulated by Schwann cells-derived Mif. In sugar metabolism, the expression of ¨Pgk1 and Tpi1 was upregulated by Schwann cells; ENO2 and PKM were downregulated by Schwann cells; however, all the factors above in glucose metabolism were not regulated by Mif derived from Schwann cells.

4. Discussion

As one of the largest innervated organs [19], peripheral nerve fibers are widely distributed in the bone tissue and most frequently found in metabolically active bone [20]. Schwann cells are glial cells to form myelin in the peripheral nervous system [21]; here, we found that Schwann cells can promote osteogenesis by Mif. Studies undertaken so far provide conflicting evidence concerning the role of Mif in osteogenesis; Onodera et al. generated transgenic mice overexpressing Mif (Mif Tg) with a hybrid promoter composed of a cytomegalovirus (CMV) enhancer and a β-actin/β-globin promoter. They found that bone formation increase in several measures in Mif Tg mice [10]. However, Zheng et al. [5] found that 4-iodo-6-phenylpyrimidine (4-IPP), one of the Mif inhibitors, potentiated osteoblast differentiation and mineralization also through the inhibition of the p65/NF-κB signaling cascade, which implies a negative correlation between Mif and osteogenesis. Mif is a pluripotent protein with diverse functions [22]; with a factor synthesized and stored in the cytoplasm, it will be released and function after activation by diverse stimuli [23], such as bacteria-derived metabolites [24, 25], hypoxia [26, 27], and other inflammatory cytokines [28]. Previous studies have failed to demonstrate a consistent connection between Mif and bone, and the bias of response may result from different sources of Mif.

Further, we found that Schwann cells promote osteogenesis Mif. CD74 is a type II transmembrane protein and a putative Mif receptor that plays a role in Mif-regulated responses [29, 30]. Mun et al. found that the bone phenotype of CD74 KO mice is similar to that of Mif KO mice [31]. We found that CD74 were regulated by Schwann cells and its Mif in MC3T3-E1 cells. FOXO1 belongs to the FOXO family of transcription factors (FoxOs), which can translate environmental signaling into gene expression [32], regulating many cellular processes, including cell survival, proliferation, differentiation, apoptosis, oxidative stress resistance, metabolism, inflammation, and aging [33–36]. FOXO1 promotes osteogenesis; overexpression/depletion of FoxO1 in MC3T3-E1 cells could contribute to promoting/attenuating osteoblast differentiation [37]. The underlying mechanisms are that FOXO1 interacts with Runx2 and ALP gene promoter [38]. Here, we found that FOXO1 is involved in the Schwann cells promoting osteogenesis and regulated by Mif/CD74. FOXO1 is generally involved in lipid metabolism and plays a critical role in the development of lipid-related diseases [39].

We found that Schwann cells could elevate linoleic acid in preosteoblast cells. Further, we found that NSDHL, the enzyme which participated in the steroid synthesis, was elevated by Schwann cells and its Mif. Mif can regulate metabolism in many metabolic diseases, such as glucose metabolism in diabetes; however, its role in bone metabolism has never been thoroughly studied before. NSDHL plays important roles in bone development; defects of the NSDHL gene are the cause of male-lethal mutations bare patches (Bpa) and striated (Str) phenotypes; heterozygous Bpa females are dwarfed and demonstrate abnormal deposits of calcium in tail vertebrae [40, 41]. Linoleic acid is important for the human body to maintain many physiological functions such as the synthesis of phospholipids and other lipid metabolisms. Linoleic acid was found to have the capacity to prevent age-induced bone loss [42] in mice through decreasing adipocyte and increasing osteoblastogenesis [43]. In conclusion, Schwann cells and their Mif can regulate fatty acid

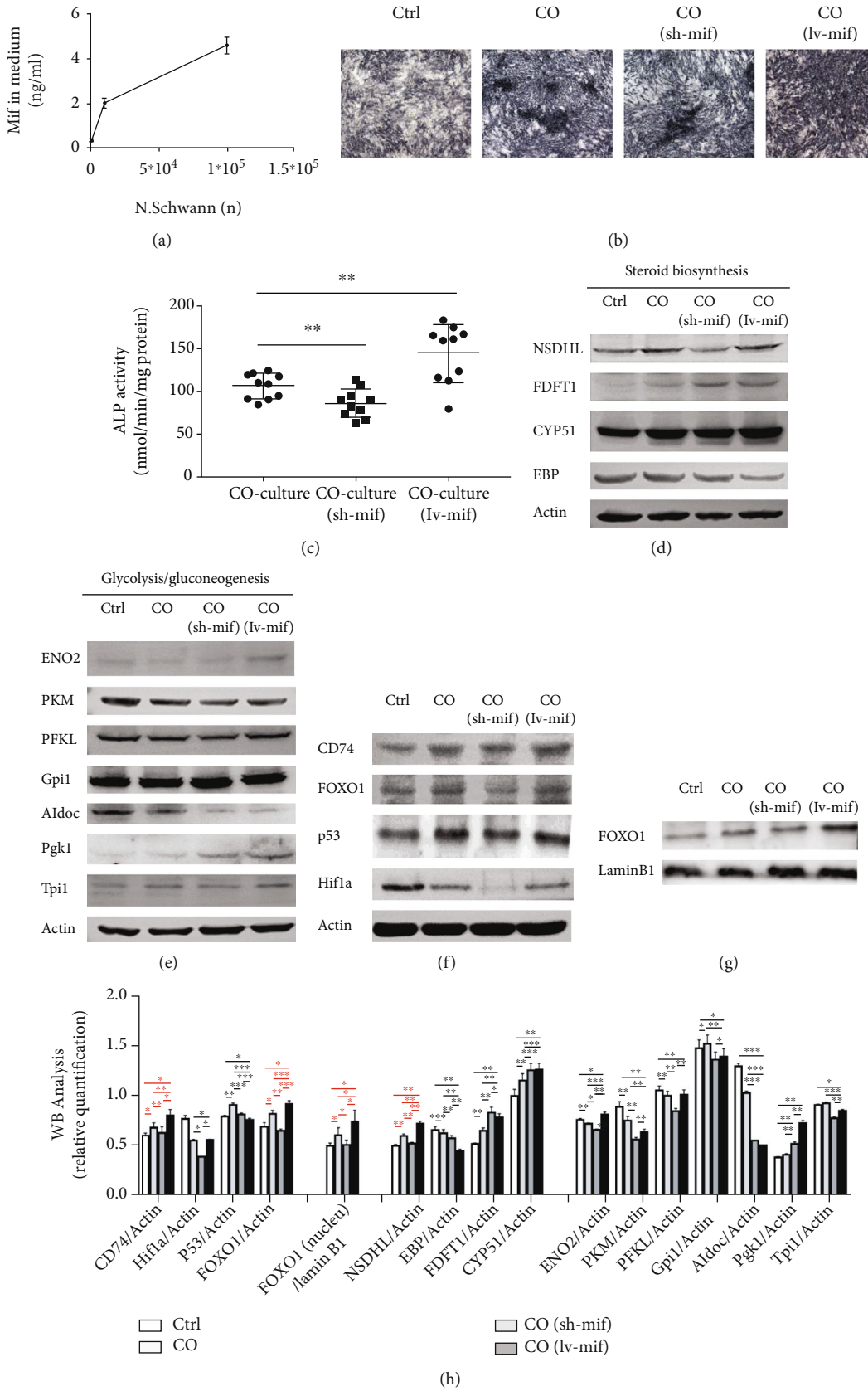

FIGURE 5: Schwann cells promote osteogenesis by Mif/CD74/FOXO1 signaling. (a) Mif concentration in the medium released from Schwann cells; (b) representative images showing ALP staining; (c) ALP activity was measured with an ALP assay kit, $n = 6$; (d–h) representative WB images for steroid biosynthesis (d), glycolysis/gluconeogenesis (e), and signaling pathway (f, g). WB analysis was also quantified by ImageJ.

metabolism in promoting osteogenesis. The metabolites regulated by Schwann cells were mainly enriched in "amino acid metabolism." Amino acids are critical precursors for several metabolic pathways, just as aspartate and glutamine are essential for pyrimidine and purine synthesis while providing α-ketoglutarate for the TCA cycle [44]. Through complex transition and inter- and intra-interactions, metabolites form complex networks which still need further study to elucidate.

5. Conclusions

These findings unveil the mechanism for Schwann cells to promote osteogenesis where Schwann cells accelerate osteogenesis via the Mif, and its downstream CD74/FOXO1 is also involved in the promotion of Schwann cells on osteogenesis. Schwann cells and their Mif can regulate amino acid metabolism and fatty acid metabolism in preosteoblasts.

Data Availability

All data needed to evaluate the conclusions in the paper are present in the paper and/or Supplementary Materials. Additional data related to this paper may be requested from the authors.

Conflicts of Interest

The authors declare no competing interests.

Authors' Contributions

Jun-Qin Li and Hui-Jie Jiang designed and performed the main study experiments, analyzed the data, and wrote the manuscript; Li Feng purified Schwann cells and modified Schwann cells; Na-Zhi Zhan and Shan-Shan Li performed western blotting experiments; Zi-Jie Chen and Bo-Han Chang performed ALP staining; Xiu-Yun Su and Peng-Zhen Cheng commented on and approved the final manuscript; Guo-Xian Pei and Liu Yang conceived and supervised the research.

Acknowledgments

We thank the staff of the Orthopaedic Research Institute of PLA at the Xijing Hospital. This work was supported by the Supporting funds for scientific research of Southern University of Science and Technology (Y01416214) and the NSFC's Youth Program of National Natural Science Foundation of China (Grant No. 81902202).

Supplementary Materials

Supplementary Figure S1: representative chromatograms in positive (POS) and negative (NEG) ion modes. Supplementary Figure S2: differential transcripts and metabolites selected for correlation analysis. Supplementary Figure S3: (a) representative WB images to detect infection efficiency; (b) ALP activity, $n = 6$. *(Supplementary Materials)*

References

[1] A. Salhotra, H. N. Shah, B. Levi, and M. T. Longaker, "Mechanisms of bone development and repair," *Nature Reviews. Molecular Cell Biology*, vol. 21, no. 11, pp. 696–711, 2020.

[2] Z. Wu, P. Pu, Z. Su, X. Zhang, L. Nie, and Y. Chang, "Schwann cell-derived exosomes promote bone regeneration and repair by enhancing the biological activity of porous Ti6Al4V scaffolds," *Biochemical and Biophysical Research Communications*, vol. 531, no. 4, pp. 559–565, 2020.

[3] X. Zhang, X. Jiang, S. Jiang, X. Cai, S. Yu, and G. Pei, "Schwann cells promote prevascularization and osteogenesis of tissue-engineered bone via bone marrow mesenchymal stem cell-derived endothelial cells," *Stem Cell Research & Therapy*, vol. 12, no. 1, 2021.

[4] M. Xie, D. Kamenev, M. Kaucka et al., "Schwann cell precursors contribute to skeletal formation during embryonic development in mice and zebrafish," *Proceedings of the National Academy of Sciences of the United States of America*, vol. 116, no. 30, pp. 15068–15073, 2019.

[5] L. Zheng, J. Gao, K. Jin et al., "Macrophage migration inhibitory factor (MIF) inhibitor 4-IPP suppresses osteoclast formation and promotes osteoblast differentiation through the inhibition of the NF-κB signaling pathway," *The FASEB Journal*, vol. 33, no. 6, pp. 7667–7683, 2019.

[6] F. Wang, S. Xu, X. Shen, X. Guo, Y. Peng, and J. Yang, "Spinal macrophage migration inhibitory factor is a major contributor to rodent neuropathic pain-like hypersensitivity," *Anesthesiology*, vol. 114, no. 3, pp. 643–659, 2011.

[7] I. Kang and R. Bucala, "The immunobiology of MIF: function, genetics and prospects for precision medicine," *Nature Reviews Rheumatology*, vol. 15, no. 7, pp. 427–437, 2019.

[8] R. M. García Hernández, P. Martín Calvo, R. Blumer, R. de la Cruz RM, and Á. M. Pastor Loro, "Functional diversity of motoneurons in the oculomotor system," *Proceedings of the National Academy of Sciences of the United States of America*, vol. 116, no. 9, pp. 3837–3846, 2019.

[9] J. B. Bilsborrow, E. Doherty, P. V. Tilstam, and R. Bucala, "Macrophage migration inhibitory factor (MIF) as a therapeutic target for rheumatoid arthritis and systemic lupus erythematosus," *Expert Opinion on Therapeutic Targets*, vol. 23, no. 9, pp. 733–744, 2019.

[10] S. Onodera, S. Sasaki, S. Ohshima et al., "Transgenic mice overexpressing macrophage migration inhibitory factor (MIF) exhibit high-turnover osteoporosis," *Journal of Bone and Mineral Research*, vol. 21, no. 6, pp. 876–885, 2006.

[11] J. P. Brockes, G. E. Lemke, and D. R. Balzer Jr., "Purification and preliminary characterization of a glial growth factor from the bovine pituitary.," *The Journal of Biological Chemistry*, vol. 255, no. 18, pp. 8374–8377, 1980.

[12] G. Hu, X. Dong, S. Gong, Y. Song, A. P. Hutchins, and H. Yao, "Systematic screening of CTCF binding partners identifies that BHLHE40 regulates CTCF genome-wide distribution and long-range chromatin interactions," *Nucleic Acids Research*, vol. 48, no. 17, pp. 9606–9620, 2020.

[13] A. Ozaki, A. Nagai, Y. B. Lee, N. H. Myong, and S. U. Kim, "Expression of cytokines and cytokine receptors in human Schwann cells," *Neuroreport*, vol. 19, no. 1, pp. 31–35, 2008.

[14] E. A. Horner, J. Kirkham, D. Wood et al., "Long bone defect models for tissue engineering applications: criteria for choice," *Tissue Engineering. Part B, Reviews*, vol. 16, no. 2, pp. 263–271, 2010.

[15] T. Huang, J. Q. Qin, X. K. Huo et al., "Changes in content of macrophage migration inhibitory factor secreted by Schwann cells after peripheral nerve injury," *Di Yi Jun Yi Da Xue Xue Bao*, vol. 22, no. 6, pp. 493–495, 2002.

[16] T. Huang, J. Qin, S. Xiong et al., "Expression of macrophage migration inhibitory factor mRNA in Schwann cells," *Zhonghua Wai Ke Za Zhi*, vol. 40, no. 9, pp. 699–701, 2002.

[17] P. Ramamurthy, J. B. White, J. Yull Park et al., "Concomitant differentiation of a population of mouse embryonic stem cells into neuron-like cells and Schwann cell-like cells in a slow-flow microfluidic device," *Developmental Dynamics*, vol. 246, no. 1, pp. 7–27, 2017.

[18] C. R. Figueiredo, R. A. Azevedo, S. Mousdell et al., "Blockade of MIF-CD74 signalling on macrophages and dendritic cells restores the antitumour immune response against metastatic melanoma," *Frontiers in Immunology*, vol. 9, p. 1132, 2018.

[19] H. Chen, B. Hu, X. Lv et al., "Prostaglandin E2 mediates sensory nerve regulation of bone homeostasis," *Nature Communications*, vol. 10, no. 1, 2019.

[20] J. M. García-Castellano, P. Díaz-Herrera, and J. A. Morcuende, "Is bone a target-tissue for the nervous system? New advances on the understanding of their interactions," *The Iowa Orthopaedic Journal*, vol. 20, pp. 49–58, 2000.

[21] S. Nishimoto, H. Tanaka, M. Okamoto, K. Okada, T. Murase, and H. Yoshikawa, "Methylcobalamin promotes the differentiation of Schwann cells and remyelination in lysophosphatidylcholine-induced demyelination of the rat sciatic nerve," *Frontiers in Cellular Neuroscience*, vol. 9, 2015.

[22] S. S. Jankauskas, D. W. L. Wong, R. Bucala, S. Djudjaj, and P. Boor, "Evolving complexity of MIF signaling," *Cellular Signalling*, vol. 57, pp. 76–88, 2019.

[23] J. Harris, N. Deen, S. Zamani, and M. A. Hasnat, "Mitophagy and the release of inflammatory cytokines," *Mitochondrion*, vol. 41, pp. 2–8, 2018.

[24] J. Oteo, G. Bou, F. Chaves, and A. Oliver, "Microbiological methods for surveillance of carrier status of multiresistant bacteria," *Enfermedades Infecciosas y Microbiología Clínica*, vol. 35, no. 10, pp. 667–675, 2017.

[25] Z. Baharoglu and D. Mazel, "SOS, the formidable strategy of bacteria against aggressions," *FEMS Microbiology Reviews*, vol. 38, no. 6, pp. 1126–1145, 2014.

[26] O. Zis, S. Zhang, K. Dorovini-Zis, L. Wang, and W. Song, "Hypoxia signaling regulates macrophage migration inhibitory factor (MIF) expression in stroke," *Molecular Neurobiology*, vol. 51, no. 1, pp. 155–167, 2015.

[27] S. Zhang, O. Zis, P. T. Ly et al., "Down-regulation of MIF by NFκB under hypoxia accelerated neuronal loss during stroke," *The FASEB Journal*, vol. 28, no. 10, pp. 4394–4407, 2014.

[28] S. Ghosh, N. Jiang, L. Farr, R. Ngobeni, and S. Moonah, "Parasite-produced MIF cytokine: role in immune evasion, invasion, and pathogenesis," *Frontiers in Immunology*, vol. 10, 2019.

[29] H. Su, N. Na, X. Zhang, and Y. Zhao, "The biological function and significance of CD74 in immune diseases," *Inflammation Research*, vol. 66, no. 3, pp. 209–216, 2017.

[30] L. Leng, C. N. Metz, Y. Fang et al., "MIF signal transduction initiated by binding to CD74," *The Journal of Experimental Medicine*, vol. 197, no. 11, pp. 1467–1476, 2003.

[31] S. H. Mun, H. Y. Won, P. Hernandez, H. L. Aguila, and S. K. Lee, "Deletion of CD74, a putative MIF receptor, in mice enhances osteoclastogenesis and decreases bone mass," *Journal of Bone and Mineral Research*, vol. 28, no. 4, pp. 948–959, 2013.

[32] A. Ávila-Flores, J. Arranz-Nicolás, and I. Mérida, "Transcriptional activity of FOXO transcription factors measured by luciferase assays," in *FOXO Transcription Factors*, pp. 91–102, Springer, 2019.

[33] E. C. Genin, N. Caron, R. Vandenbosch, L. Nguyen, and B. Malgrange, "Concise review: forkhead pathway in the control of adult neurogenesis," *Stem Cells*, vol. 32, no. 6, pp. 1398–1407, 2014.

[34] G. Tuteja and K. H. Kaestner, "SnapShot:Forkhead Transcription Factors I," *Cell*, vol. 130, no. 6, pp. 1160.e1–1160.e2, 2007.

[35] S. T. Henderson and T. E. Johnson, "*daf-16* integrates developmental and environmental inputs to mediate aging in the nematode *Caenorhabditis elegans*," *Current Biology*, vol. 11, no. 24, pp. 1975–1980, 2001.

[36] A. E. Webb and A. Brunet, "FOXO transcription factors: key regulators of cellular quality control," *Trends in Biochemical Sciences*, vol. 39, no. 4, pp. 159–169, 2014.

[37] M. F. Siqueira, S. Flowers, R. Bhattacharya et al., "FOXO1 modulates osteoblast differentiation," *Bone*, vol. 48, no. 5, pp. 1043–1051, 2011.

[38] A. van der Horst and B. M. Burgering, "Stressing the role of FoxO proteins in lifespan and disease," *Nature Reviews. Molecular Cell Biology*, vol. 8, no. 6, pp. 440–450, 2007.

[39] Y. Li, Z. Ma, S. Jiang et al., "A global perspective on FOXO1 in lipid metabolism and lipid-related diseases," *Progress in Lipid Research*, vol. 66, pp. 42–49, 2017.

[40] M. E. Lucas, Q. Ma, D. Cunningham et al., "Identification of two novel mutations in the murine _Nsdhl_ sterol dehydrogenase gene and development of a functional complementation assay in yeast," *Molecular Genetics and Metabolism*, vol. 80, no. 1-2, pp. 227–233, 2003.

[41] X. Y. Liu, A. W. Dangel, R. I. Kelley et al., "The gene mutated in bare patches and striated mice encodes a novel 3β-hydroxysteroid dehydrogenase," *Nature Genetics*, vol. 22, no. 2, pp. 182–187, 1999.

[42] G. Lin, H. Wang, J. Dai et al., "Conjugated linoleic acid prevents age-induced bone loss in mice by regulating both osteoblastogenesis and adipogenesis," *Biochemical and Biophysical Research Communications*, vol. 490, no. 3, pp. 813–820, 2017.

[43] Y. Kim, O. J. Kelly, and J. Z. Ilich, "Synergism of α-linolenic acid, conjugated linoleic acid and calcium in decreasing adipocyte and increasing osteoblast cell growth," *Lipids*, vol. 48, no. 8, pp. 787–802, 2013.

[44] J. R. Oates, M. C. McKell, M. E. Moreno-Fernandez et al., "Macrophage function in the pathogenesis of non-alcoholic fatty liver disease: the mac attack," *Frontiers in Immunology*, vol. 10, 2019.